

The Effects of Fluid Composition on the One-Dimensional Consolidation Behaviour of Clay-Based Sealing Materials

NWMO TR-2008-20

November 2008

D.G. Priyanto¹

J.A. Blatz²

G.A. Siemens³

R.B. Offman²

J.S. Powell³

D.A. Dixon¹

¹Atomic Energy of Canada Limited

²University of Manitoba

³Royal Military College of Canada

nwmo

NUCLEAR WASTE
MANAGEMENT
ORGANIZATION

SOCIÉTÉ DE GESTION
DES DÉCHETS
NUCLÉAIRES

Nuclear Waste Management Organization
22 St. Clair Avenue East, 6th Floor
Toronto, Ontario
M4T 2S3
Canada

Tel: 416-934-9814
Web: www.nwmo.ca

**The Effects of Fluid Composition on the One-Dimensional Consolidation
Behaviour of Clay-Based Sealing Materials**

NWMO TR-2008-20

November 2008

D.G. Priyanto¹
J.A. Blatz²
G.A. Siemens³
R.B. Offman²
J.S. Powell³
D.A. Dixon¹

¹Atomic Energy of Canada Limited

²University of Manitoba

³Royal Military College of Canada

Disclaimer:

This report does not necessarily reflect the views or position of the Nuclear Waste Management Organization, its directors, officers, employees and agents (the "NWMO") and unless otherwise specifically stated, is made available to the public by the NWMO for information only. The contents of this report reflect the views of the author(s) who are solely responsible for the text and its conclusions as well as the accuracy of any data used in its creation. The NWMO does not make any warranty, express or implied, or assume any legal liability or responsibility for the accuracy, completeness, or usefulness of any information disclosed, or represent that the use of any information would not infringe privately owned rights. Any reference to a specific commercial product, process or service by trade name, trademark, manufacturer, or otherwise, does not constitute or imply its endorsement, recommendation, or preference by NWMO.

ABSTRACT

Title: The Effects of Fluid Composition on the One-Dimensional Consolidation Behaviour of Clay-Based Sealing Materials
Report No.: NWMO TR-2008-20
Author(s): D.G. Priyanto¹, J.A. Blatz², G.A. Siemens³, R.B. Offman², J.S. Powell³, and D.A. Dixon¹
Company: ¹Atomic Energy of Canada Limited, ²University of Manitoba, ³Royal Military College of Canada
Date: November 2008

Abstract

Groundwaters at proposed repository depths of 500 to 1000 m can contain significant quantities of soluble salts. These salts have the potential to affect the hydraulic-mechanical behaviour of clay-based sealing materials installed in a Deep Geologic Repository (DGR). As a result of the potential influence of salinity on material behaviour, one of the design decisions for the engineering of a sealing system is whether to prepare the sealing materials with fresh or saline fluid and to determine if this will affect the performance of the barrier materials. One-dimensional (1D) consolidation tests can be used as a tool in characterizing the hydraulic-mechanical behaviour of clay-based sealing materials.

This report summarizes the results of the 1D consolidation tests of three clay-based sealing materials: Highly Compacted Bentonite (HCB), Dense Backfill (DBF), and Light Backfill (LBF) that have been completed to the end of 2008. The testing program includes the use of three types of fluid either as the reservoir fluid or in specimen preparation: Distilled Water (DW), CaCl₂ and NaCl solutions having salinity as high as 250 g/L. In order to examine the effect of the boundary condition during initial saturation on the material performance, two different boundary conditions were applied during initial saturation: constant volume (CV) or constant vertical stress (CS).

Mechanical parameters including 1D-Modulus, Compression Index (Cc), and Swelling Index (Cs) have been interpreted from the results of these tests. Cc and Cs are found to decrease with an increase in concentration of solution in pore fluid, independent of the type of salt solution (i.e., CaCl₂ or NaCl). This report presents the relationship of Cc and Cs to the pore fluid concentration for use in defining the mechanical behaviour of clay-based sealing materials in THM numerical modelling.

Hydraulic conductivities (k) have also been interpreted from the results of these tests. Within each individual test, k decreases with increasing density. However, when all tests are combined, this trend is not clearly apparent indicating the difficulty in making accurate determination of k from 1D consolidation tests data.

TABLE OF CONTENTS

	<u>Page</u>
ABSTRACT	v
1. INTRODUCTION.....	1
1.1 BACKGROUND.....	3
2. OBJECTIVES AND SCOPE.....	4
2.1 PREVIOUS WORK (2006 TO 2007)	4
2.2 WORK IN 2008.....	4
2.3 TESTING LOCATIONS	8
3. MATERIALS	8
4. EQUIPMENT.....	8
5. SUMMARY OF THE RESULTS	10
5.1 CALCULATION OF VOID RATIO (e), DRY DENSITY AND EFFECTIVE MONTMORILLONITE DRY DENSITY (EMDD)	10
5.1.1 Correction Due to Salt Content	10
5.1.2 Calculation of Effective Montmorillonite Dry Density (EMDD).....	11
5.2 MECHANICAL CONSTITUTIVE MODEL PARAMETERS	12
5.3 HYDRAULIC CONSTITUTIVE MODELS	18
6. DISCUSSION.....	19
6.1 EMDD, HYDRAULIC CONDUCTIVITY AND 1D-MODULUS	19
6.2 COMPRESSION AND SWELLING INDICES	26
6.3 SWELLING PRESSURE UNDER CONSTANT VOLUME (CV) OF HCB.....	30
7. CONCLUDING REMARKS AND RECOMMENDATIONS.....	33
7.1 CONCLUDING REMARKS.....	33
7.2 RECOMMENDATIONS.....	33
ACKNOWLEDGEMENTS	34
REFERENCES	35
APPENDIX A: DETAILED DESCRIPTION: TESTING OF HIGHLY COMPACTED BENTONITE (HCB)	37

continued...

TABLE OF CONTENTS (Concluded)

	<u>Page</u>
APPENDIX B: DETAILED DESCRIPTION: TESTING OF DENSE BACKFILL (DBF)	53
APPENDIX C: DETAILED DESCRIPTION OF TESTS: LIGHT BACKFILL (LBF)	73
APPENDIX D: DATA	89

LIST OF TABLES

	<u>Page</u>
Table 1: Physical Characteristics of Engineering Barriers System Components (after Russell and Simmons 2003).....	1
Table 2: 1D-Consolidation Tests of Highly Compacted Bentonite (HCB) (2006-2008).....	5
Table 3: 1D-Consolidation Tests of Dense Backfill (DBF) (2006-2008).....	6
Table 4: 1D-Consolidation Tests of Light Backfill (LBF) (2006-2008).....	7
Table 5: Clay-Based Sealing Material Composition	12
Table 6: Coefficients to Calculate EMDD.....	12
Table 7: Swelling Stress of HCB Specimens During Initial Saturation.....	31

LIST OF FIGURES

	<u>Page</u>
Figure 1: RWE NUKEM's In-floor Borehole Placement Method Design (NUKEM 2003)	2
Figure 2: Deep Geological Repository – Generic Used Fuel Container Placement Designs for Vertical In-floor Borehole and Horizontal In-room (NUKEM 2003).....	2
Figure 3: Definition of Parameters C_c and C_s	14
Figure 4: Definition of 1D-Modulus.....	14
Figure 5: Vertical Stress versus Void Ratio of HCB	15
Figure 6: Vertical Stress versus Void Ratio of DBF	16
Figure 7: Vertical Stress versus Void Ratio of LBF	17
Figure 8: Vertical Stress versus Void Ratio of HCB, DBF, and LBF	18
Figure 9: Dry Density versus Hydraulic Conductivity of HCB, DBF and LBF	20
Figure 10: EMDD versus Hydraulic Conductivity of HCB, DBF and LBF	21
Figure 11: 1D-Modulus versus Void Ratio	21
Figure 12: 1D-Modulus versus Dry Density	22
Figure 13: 1D-Modulus versus EMDD	22
Figure 14: EMDD versus Hydraulic Conductivity of HCB.....	23
Figure 15: EMDD versus Hydraulic Conductivity of DBF	24
Figure 16: EMDD versus Hydraulic Conductivity of LBF.....	25
Figure 17: The Effect of CaCl_2 and NaCl Solution to the Compression Index (C_c) and Swelling Index (C_s) of HCB	27
Figure 18: The Effect of CaCl_2 and NaCl Solution to the Compression Index (C_c) and Swelling Index (C_s) of DBF	28
Figure 19: The Effect of CaCl_2 and NaCl Solution to the Compression Index (C_c) and Swelling Index (C_s) of LBF	29
Figure 20: Relationship of Compression Index (C_c) and Swelling Index (C_s) and TDS of Solution	30
Figure 21: Swelling Stress for Specimens HCB9 and HCB10	31
Figure 22: Swelling Stress for Specimens HCB12 and HCB14A.....	32

1. INTRODUCTION

Several sealing-system components are proposed for use in a placement-room sealing system (e.g., RWE NUKEM's in-floor borehole placement method shown in Figure 1) in a Canadian Deep Geologic Repository (DGR). Figure 2 shows the DGR of generic used fuel container placement designs for vertical in-floor borehole and horizontal in-room. For the clay-based portions of the repository sealing system, four sealing-system components are being considered.

1. Highly Compacted Bentonite (HCB) – 100% bentonite clay either installed at high dry density by in-situ compaction or prefabricated as blocks (shown in Figure 1 as “bentonite buffer blocks” and “bentonite buffer rings”).
2. Dense Backfill (DBF) – a mixture of lake clay, crushed host rock and bentonite clay, either installed at high dry density by in-situ compaction or prefabrication as blocks.
3. Light Backfill (LBF) – a mixture of bentonite clay and silica sand, likely installed in the form of dense pellets and installed at low-to-medium dry density.
4. Gapfill (GF) – either bentonite clay, possibly fabricated in the form of dense pellets, silica sand or some combination of the two, which are likely to be installed at low-to-medium average dry density (shown in Figure 1 as “buffer pellets”).

Some suggested compositions and fundamental physical characteristics of these candidate sealing-system components are presented in Table 1.

Table 1: Physical Characteristics of Engineering Barriers System Components
(after Russell and Simmons 2003)

Property	HCB	GF	DBF	LBF
Composition (dry mass %)	100% bentonite	100% bentonite	5% bentonite 25% glacial lake clay 70% crushed granite	50% bentonite 50% sand
Initial Gravimetric Water Content (%)	17	2	8.5	15
As-Placed Saturation (%)	65	6	80	33
Dry Density (Mg/m ³)	1.61	1.40	2.12	1.24
EMDD (Mg/m ³)*	1.50	1.25	0.8	0.66

* Effective Montmorillonite Dry Density - assumes that all bentonites have a minimum 75% montmorillonite content

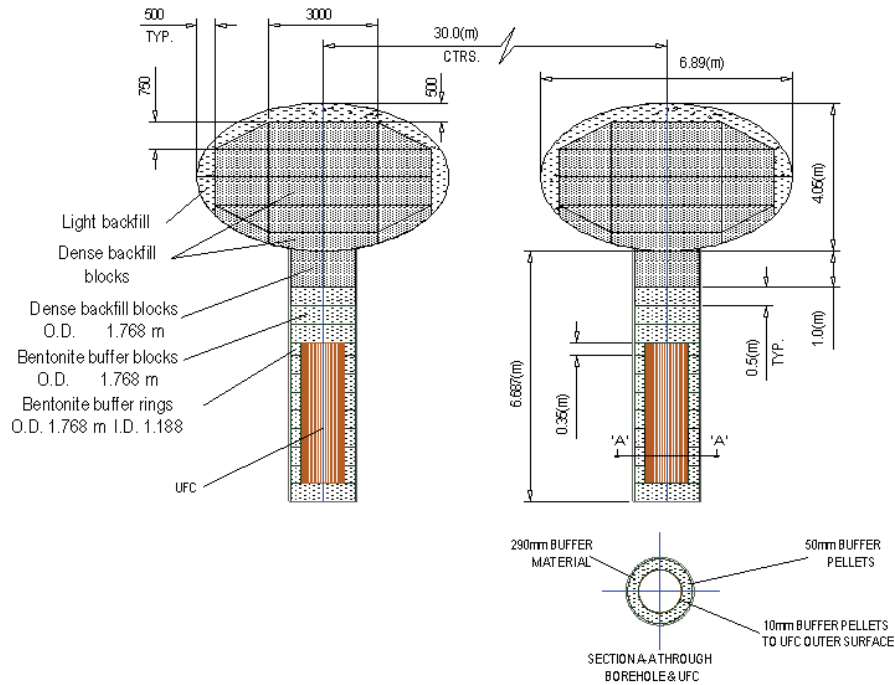


Figure 1: RWE NUKEM's In-floor Borehole Placement Method Design (NUKEM 2003)

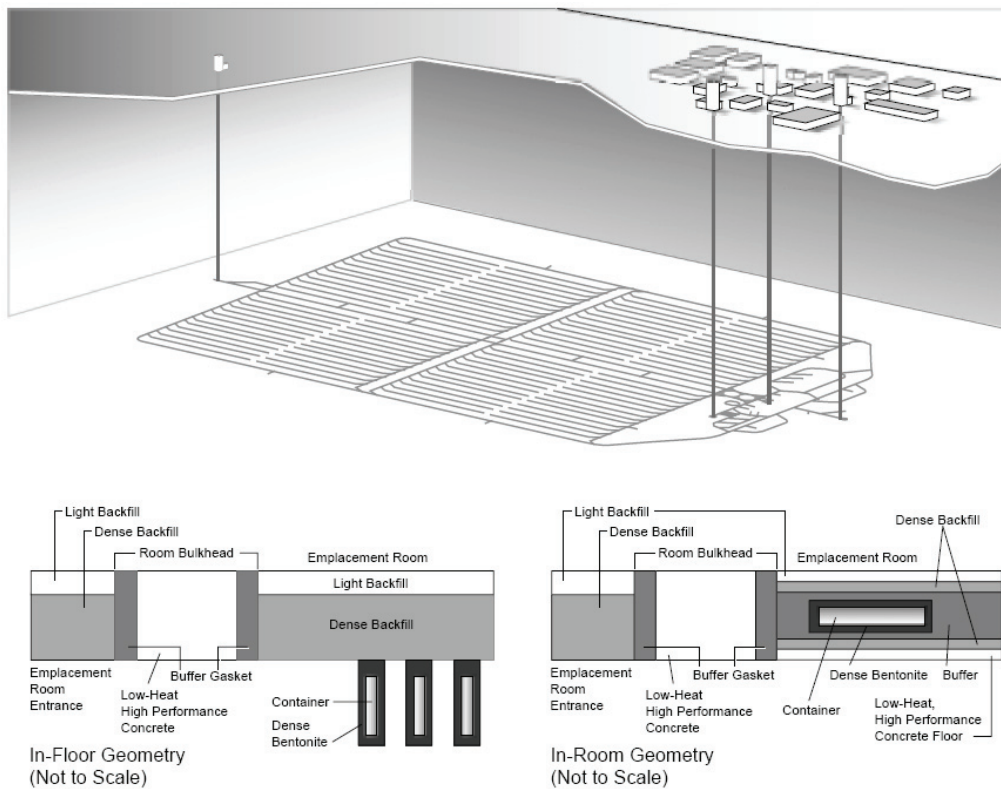


Figure 2: Deep Geological Repository – Generic Used Fuel Container Placement Designs for Vertical In-floor Borehole and Horizontal In-room (NUKEM 2003)

1.1 BACKGROUND

The chemistry of the pore fluid strongly affects the swelling potential and hydraulic conductivity of bentonite clay. Groundwaters at proposed repository depths of 500 to 1000 m can contain significant quantities of dissolved salts and an increase in salinity is known to decrease the swelling potential and increase the hydraulic conductivity (Dixon 2000) of barrier materials containing a swelling clay mineral component.

Gascoyne et al. (1987) and Mazurek (2004) have collated data from the crystalline rock of the Canadian Shield and the sedimentary rock in southern Ontario, respectively, and very high concentrations of dissolved salts can exist at depth. Salt concentrations also typically vary with depth, tending to be low near the surface and increasing with depth. Salt concentrations also vary considerably throughout the Canadian Shield. Salinities, in terms of Total Dissolved Solids (TDS) at proposed repository depths, can vary from 8 to >100 g/L in the Canadian Shield and can be greater than 200 g/L in Ordovician-age sediments. Salt speciation is often Na-Ca-Cl at shallow depth trending to Ca-Na-Cl at greater depth.

The presence of CaCl_2 and NaCl in groundwater makes testing of clay-based sealing materials with CaCl_2 and NaCl solutions of importance to confirm their behaviour. One-dimensional (1D) consolidation tests were completed for specimens using CaCl_2 solution at salinities up to 250 g/L (Baumgartner et al. 2008; Priyanto et al. 2008).

Baumgartner et al. (2008) completed 1D-consolidation tests using CaCl_2 solutions at salinities up to 100 g/L in order to start the process of increasing the behavioural database for sealing materials. Baumgartner et al. (2008) observed that specimen preparation affected the behaviour of the clay-based sealing materials. One of the design decisions for the engineering of a repository placement-room sealing system will be the choice for preparing the sealing materials with either fresh or saline water.

With identification of high salinity conditions (TDS > 200 g/L) in the crystalline rock of the Canadian Shield and the sedimentary rock in southern Ontario (Gascoyne et al. 1987; Mazurek 2004) the range of fluid concentrations examined by Baumgartner et al. (2008) needed to be extended. Priyanto et al. (2008) investigated the effect of salinities up to 250 g/L CaCl_2 on the behaviour of HCB, DBF and LBF using 1D consolidation tests. In response to potential effects of different methods of specimen preparation (mixing with saline solution (i.e., 250 g/L CaCl_2 solution) and mixing with Distilled Water (DW)), sample preparation with both fluids was examined.

The presence of NaCl solution in pore fluid of clay-based sealing materials may result in different 1D-consolidation behaviour. The observation of the role of NaCl solutions in the pore fluid of clay-based sealing material was only limited using constant-volume load cells (Dixon 2000). Several mechanical parameters cannot be interpreted from constant-volume load cells; consequently the 1D-consolidation tests using NaCl solutions are important.

This report discusses the results of 1D-consolidation tests of clay based sealing materials completed in 2006 to 2008. These tests include investigation of the effects of different type of salt solutions (NaCl versus CaCl_2) on the results of 1D-consolidation tests. The relationships of compression and swelling indices (C_c and C_s) from 1D-consolidation tests and the concentration of pore fluid for HCB, DBF, and LBF can be used to include the effect of pore fluid salinity on the mechanical behaviour of these materials using THM numerical models of

the DGR systems. The hydraulic conductivities (k) of these three materials with various pore fluids compositions have been determined from the results of 1D-consolidation tests and compared to investigate the effect of pore fluid compositions on the hydraulic behaviour of these materials.

2. OBJECTIVES AND SCOPE

The main objective of performing 1D-consolidation tests on potential sealing materials is to determine mechanical and hydraulic parameters for use in numerical modelling. A secondary objective is to assess the effect of pore fluid composition on these derived parameters.

2.1 PREVIOUS WORK (2006 TO 2007)

The results of the previous testing completed in 2006 and 2007 were presented in Baumgartner et al. (2008) and Priyanto et al. (2008), respectively. This document presents the results of 1D-consolidation tests completed in 2008. Tables 2, 3, and 4 show the 1D-consolidation tests of HCB, DBF, and LBF completed in 2006 to 2008.

The scope of the work in 2006 (Baumgartner et al. 2008) was to investigate the effect of pore fluid salinity on the results of 1D-consolidation behaviour of the HCB, DBF, and LBF specimens. The testing program included 1D-consolidation tests using distilled water and Calcium Chloride (CaCl_2) solution up to 100 g/L CaCl_2 for the LBF and DBF specimens and 75 g/L CaCl_2 solution for the HCB specimens. Except for the LBF specimens, the fluid used in specimen preparation was similar to that in the reservoir. Baumgartner et al. (2008) observed that specimen preparation affected the behaviour of the clay-based sealing materials for similar reservoir fluid. One of the design decisions for the engineering of a sealing system is the choice for preparing the sealing materials with either fresh or saline water. Consequently, specimens prepared with distilled water and salt solutions were included in the 1D-consolidation tests after 2006.

With identification of high salinity conditions ($\text{TDS} > 200$ g/L) in the crystalline rock of the Canadian Shield and the sedimentary rock in southern Ontario, the scope of the work in 2007 included the effects of higher pore fluid salinity (up to 250 g/L CaCl_2) and the effects of different mixing fluids used in specimen preparation and boundary conditions during initial saturation for HCB, DBF, and LBF specimens (Priyanto et al. 2008). The testing program included CaCl_2 solution with higher salinity (up to 250 g/L), two different specimen preparations: mixing with distilled water (DW) or 250 g/L CaCl_2 solution; and two different boundary conditions during initial saturation: Constant Volume (CV) and Constant vertical Stress (CS).

2.2 WORK IN 2008

Gascoyne et al. (1987) and Mazurek (2004) observed that salt speciation was often Na-Ca-Cl at shallow depth trending to Ca-Na-Cl at greater depth of the crystalline rock of the Canadian Shield and the sedimentary rock in southern Ontario. Thus, it was necessary to examine the effects of different type of salt (NaCl versus CaCl_2) on the 1D-consolidation behaviours of clay-based sealing materials. The current testing program (2008) presented in this document included NaCl solution with concentrations up to 250 g/L.

Table 2: 1D-Consolidation Tests of Highly Compacted Bentonite (HCB) (2006-2008)

Test No.	Sample No.	Mixing Fluid	Reservoir Fluid	Mixing Fluid TDS (g/L)	Reservoir Fluid TDS (g/L)	Boundary Condition During Saturation	Test Location	Reference
1	HCB1(06)	DW	DW	0	0	CS	AECL	
2	HCB2(06)	DW	DW	0	0	CS	AECL	
3	HCB3(06)	CaCl ₂	CaCl ₂	75	75	CS	AECL	Baumgartner et al. 2008
4	HCB4(06)	CaCl ₂	CaCl ₂	75	75	CS	AECL	
5	HCB5(06)	DW	DW	0	0	CS	AECL	
6	HCB6(06)	CaCl ₂	CaCl ₂	75	75	CS	AECL	
7	HCB7 (07)	DW	CaCl ₂	0	250	CS	AECL	Priyanto et al. 2008
8	HCB8 (07)	CaCl ₂	CaCl ₂	250	250	CS	AECL	
9	HCB9 (07)	DW	DW	0	0	CV	AECL	
10	HCB10 (07)	CaCl ₂	CaCl ₂	250	250	CV	AECL	
11	HCB11 (07)	DW	CaCl ₂	0	150	CS	AECL	
12	HCB12(08)	NaCl	NaCl	250	250	CV	AECL	This document
13	HCB13(08)	NaCl	NaCl	250	250	CS	AECL	
14	HCB14(08)	DW	NaCl	0	250	CV	AECL	
15	HCB14A (08)	DW	NaCl	0	250	CV	AECL	
16	HCB15 (08)	DW	NaCl	0	250	CS	AECL	

Note: CV: Constant Volume; CS: Constant Vertical Stress; DW: Distilled Water

Table 3: 1D-Consolidation Tests of Dense Backfill (DBF) (2006-2008)

Test No.	Sample No.	Mixing Fluid	Reservoir Fluid	Mixing Fluid TDS (g/L)	Reservoir Fluid TDS (g/L)	Boundary Condition During Saturation	Test Location	Reference
1	DBF1(06)	DW	DW	0	0	CS	UM	Baumgartner et al. 2008
2	DBF2(06)	DW	DW	0	0	CV	UM	
3	DBF3(06)	CaCl ₂	CaCl ₂	100	100	CS	UM	
4	DBF4(06)	CaCl ₂	CaCl ₂	100	100	CV	UM	
5	DBF5(06)	DW	DW	0	0	CS	UM	
6	DBF6(06)	CaCl ₂	CaCl ₂	100	100	CS	UM	
7	DBF1(08)	CaCl ₂	CaCl ₂	250	250	CS	UM	This Document
8	DBF2(08)	DW	CaCl ₂	0	250	CS	UM	
9	DBF3(08)	CaCl ₂	CaCl ₂	250	250	CV	UM	
10	DBF4(08)	DW	CaCl ₂	0	250	CV	UM	
11	DBF5(08)	NaCl	NaCl	250	250	CV	UM	
12	DBF6(08)	DW	NaCl	0	250	CV	UM	
13	DBFS1(08)	DW	NaCl	0	250	CS	AECL	
14	DBFS2(08)	NaCl	NaCl	0	250	CS	AECL	

Note: CV: Constant Volume; CS: Constant Vertical Stress; DW: Distilled Water; UM: University of Manitoba

Table 4: 1D-Consolidation Tests of Light Backfill (LBF) (2006-2008)

Test No.	Sample No.	Mixing Fluid	Reservoir Fluid	Mixing Fluid TDS (g/L)	Reservoir Fluid TDS (g/L)	Boundary Condition During Saturation	Test Location	Reference
1	HB2(06)	DW	DW	0	0	CV	LHU	Baumgartner et al. 2008
2	HB3(06)	DW	DW	0	0	CS	LHU	
3	HB4(06)	DW	DW	0	0	CV	LHU	
4	HB6(06)	DW	DW	0	0	CS	LHU	
5	HB7(06)	DW	DW	0	0	CV	LHU	
6	HB8(06)	DW	DW	0	0	CS	LHU	
7	HB9(06)	DW	DW	0	0	CV	LHU	
8	HB11(06)	DW	CaCl ₂	0	100	CS	LHU	
9	HB12(06)	DW	CaCl ₂	0	100	CS	LHU	
10	HB13(06)	CaCl ₂	CaCl ₂	100	100	CS	LHU	
11	HB14(06)	DW	CaCl ₂	0	100	CV	LHU	
12	HB15(06)	CaCl ₂	CaCl ₂	100	100	CS	LHU	
13	HB16(06)	DW	CaCl ₂	0	200	CS	LHU	
14	HB19(06)	DW	CaCl ₂	0	100	CS	LHU	
15	LBF_1(07)	CaCl ₂	CaCl ₂	227	227	CS	RMC	Priyanto et al. 2008
16	LBF_2(07)	DW	CaCl ₂	0	227	CS	RMC	
17	LBF_3(07)	CaCl ₂	CaCl ₂	227	227	CV	RMC	
18	LBF_4(07)	DW	CaCl ₂	0	227	CV	RMC	
19	LBF_5B(07)	CaCl ₂	CaCl ₂	91	91	CS	RMC	
20	LBF_6(07)	DW	CaCl ₂	0	91	CV	RMC	
21	LBF_1(08)	NaCl	NaCl	250	250	CV	RMC	This Document
22	LBF_2(08)	DW	NaCl	0	250	CV	RMC	
23	LBF_3(08)	DW	NaCl	0	100	CV	RMC	
24	LBF_4(08)	NaCl	NaCl	100	100	CV	RMC	
25	LBF_5(08)	DW	NaCl	0	50	CV	RMC	
26	LBF_6(08)	NaCl	NaCl	50	50	CV	RMC	

Note: CV: Constant Volume; CS: Constant Vertical Stress; DW: Distilled Water; LHU: Lakehead University; RMC: Royal Military College of Canada

2.3 TESTING LOCATIONS

The work done during 2006 consisted of a series of laboratory 1D consolidation tests on three clay-based sealing materials (i.e., HCB, DBF and LBF). Testing was divided between Atomic Energy of Canada Limited (AECL) geotechnical laboratory at the Underground Research Laboratory (URL), the Department of Civil Engineering at the University of Manitoba (U of M), and Department of Civil Engineering at Lakehead University (LHU). Each group was assigned a material-type to test. AECL tested the HCB, U of M tested the DBF, and LHU tested the LBF.

During 2007, AECL continued testing of HCB specimens and the U of M continued testing of DBF specimens. Due to resourcing issues at LHU in 2007, testing of LBF specimens was shifted to the Department of Civil Engineering at the Royal Military College of Canada (RMC).

In 2008, AECL continued testing of HCB specimens, the U of M continued testing of DBF specimens and the RMC continued testing of LBF specimens. AECL provided the material (i.e., DBF and LBF) and the specification of initial conditions, including target initial dry density, fluid used in specimen preparation and fluid added to the tests. Two (2) tests on DBF using smaller scale specimens were added to evaluate the behaviour of DBF under lower stress and to assess the effect of sample size. These tests were completed at AECL.

3. MATERIALS

The following three sealing-system components were tested in the series of consolidation tests.

- HCB, composed of 100% (by weight) Wyoming MX80 bentonite (montmorillonite content ~75%).
- LBF, composed of 50% (by weight) Avonlea (Saskatchewan) bentonite (montmorillonite content ~80%) and 50% (by weight) silica sand.
- DBF, composed of 75% (by weight) crushed granite, 18.75% crushed illite clay (Sealbond) and 6.25% (by weight) Avonlea bentonite (montmorillonite content ~80%).

This DBF composition differed from that provided in Table 1. This DBF composition using the Sealbond and Avonlea bentonite was a good representation of the DBF in Table 1 and a more consistent material than one prepared with glacial lake clay.

4. EQUIPMENT

Four different sizes of consolidation cells were required since each material had very different swelling and mechanical properties.

1. Conventional 50-mm-diameter consolidation cells that allowed 19-mm-thick specimens were used to test the LBF.
2. Larger 101-mm-diameter consolidation cells that allowed 101-mm-thick specimens were used to test the DBF to accommodate the large size of the aggregate (i.e., up to 35-mm granite chips).

3. Two 50-mm-diameter consolidation cells that allowed 40-mm-thick specimens were added to test the DBF in 2008.
4. Small 28.1-mm-diameter consolidation cells that allowed 10-mm-thick specimens were used to test the HCB. These cells permitted application of high stress (i.e., maximum 16 MPa).

All parts of the cells that had direct contact to salt solution were fabricated from non-corrosive material.

In cells 1 and 2, conventional dead-weight-type oedometers were used to test the LBF and DBF and data were collected by manually monitoring the deformation of these two materials using strain gauges.

In cells 3, prior to the compaction of the specimens, similar DBF material used in cells 2 was oven dried and crushed using a small rock-crusher to accommodate testing using smaller consolidation cells. Grinding the DBF mixture resulted in different grain size distribution, but it did not change the material composition. As this process did not affect the proportion of very fine (clay-sized) material present, it was not likely to cause a substantial change in the 1D-consolidation behaviour of the mixture. Conventional dead-weight-type oedometers were used in cells 3 to test the DBF. The displacement of the specimen was measured using a LVDT that was connected to a data logger.

The objectives of using smaller specimens to test the DBF were to: investigate scale effects, reduce the consolidation time, and investigate the DBF consolidation behaviour under lower stress. Using a conventional dead-weight-type oedometer, the minimum stress that could be achieved was equal to the weight of the top-cap consolidation cell. Since the top-cap weight of cells 3 was less than that of cells 2, so that lower minimum stress could be achieved using smaller cell (i.e., cell 3).

Small-diameter, thick-walled consolidation cells (i.e., cells 4) were used to test the HCB to accommodate the very high swelling capacity and associated high swelling pressure of the HCB. These cells used two different compression frames.

1. A loading frame using hydraulic rams that were actuated by high-pressure nitrogen-gas cylinders acting on a gas-over-oil accumulators had been used to test the HCB since the beginning of testing program in 2006.
2. A loading frame using a servo-hydraulic testing system manufactured by the MTS[®] (Materials Testing Services) was added in 2007 to test the HCB. This additional equipment enabled the application of different boundary conditions in the tests (i.e., constant volume or constant pressure).

LVDTs and a load cells, connected to a data logger, were used to monitor the displacement and vertical pressure of the HCB specimens in these loading frames.

5. SUMMARY OF THE RESULTS

5.1 CALCULATION OF VOID RATIO (e), DRY DENSITY AND EFFECTIVE MONTMORILLONITE DRY DENSITY (EMDD)

5.1.1 Correction Due to Salt Content

The measured dry density of a specimen mixed with salt solution is affected by the amount of salt remaining during the oven drying process (ASTM D2216-05, ASTM 2005). Dry density that is greater than actual dry density or void ratio that is lower than actual void ratio would be calculated without applying a correction factor.

The correction due to salt solution was applied in the calculation of the void ratio (e) and dry density in this report. The equations used for this correction are presented as follows.

The water content (w, %) measured in the laboratory is calculated as:

$$w = \frac{M - M_{\text{dry}}}{M_{\text{dry}}} \times 100\% \quad (1)$$

where M is the mass of wet soil. M_{dry} is mass of the soil after the oven-drying process according to ASTM D2216-05 (ASTM 2005), which is

$$M_{\text{dry}} = M_s + M_{\text{salt}} \quad (2)$$

where M_s is the mass of soil solids; and M_{salt} is the mass of salt remained after oven-drying process.

The fluid content (w_f) is the ratio of fluid mass (M_f) to the mass of soil solids (M_s). The relationship of the water content (w) to the fluid content (w_f) is as follows.

$$w_f = \frac{M_f}{M_s} \times 100\% = \frac{w}{1 - r(1 + w)} \quad (3)$$

where r is salinity expressed as the ratio of mass of salt (M_{salt}) to the mass of salt solution (M_f).

The salinity (r) can be calculated as:

$$r = \frac{M_{\text{salt}}}{M_f} = \frac{\text{TDS (g/L)}}{\rho_f(\text{Mg/m}^3) \times 1000} \quad (4)$$

where: TDS is total dissolved solid of the solution (g/L); and ρ_f is the density of the solution or fluid phase (Mg/m^3).

Bulk density (ρ) is calculated as:

$$\rho = \frac{M}{V} \quad (5)$$

where V is the total volume.

The dry density (ρ_{dry}) can be calculated as:

$$\rho_{dry} = \frac{\rho}{1 + w_l} \quad (6)$$

Finally void ratio (e) is calculated from:

$$e = \frac{G_s \cdot \rho_w}{\rho_{dry}} - 1 \quad (7)$$

where G_s is the specific gravity of soil solid and ρ_w is the water density.

These equations are similar as equations in ASTM D 4542-07 (ASTM 2007), but different notations were used with respect to different salt solutions in this document.

5.1.2 Calculation of Effective Montmorillonite Dry Density (EMDD)

The smectite minerals dominate the behaviour of the clay fraction in the bentonites and the smectite content in bentonite varies from different global sources. The term 'effective montmorillonite dry density' (EMDD) was derived (Baumgartner and Snider 2002; JNC 2000) to single out the role of montmorillonite in soil behaviour and is expressed as follows:

$$EMDD = \frac{M_m}{(V_m + V_v)} = \frac{f_m \cdot f_c \cdot \rho_d}{\left[1 - \left(\frac{(1 - f_c) \cdot \rho_d}{G_a \cdot \rho_w} \right) - \left(\frac{(1 - f_m) \cdot f_c \cdot \rho_d}{G_n \cdot \rho_w} \right) \right]} \quad (8)$$

where M_m = mass of montmorillonite component (kg);
 V_m = volume occupied by montmorillonite component (m^3);
 V_v = volume of void (m^3);
 f_m = mass fraction of montmorillonite in clay fraction f_c (e.g., > 75% in MX80);
 f_c = mass fraction of clay in dry solids (e.g., ~100% in bentonite clay);
 G_a = specific gravity of aggregate solid (e.g., quartz sand = 2.65);
 G_n = specific gravity of non-montmorillonite component in clay (e.g., 2.645);
 ρ_w = density of water (kg/m^3); and
 ρ_d = dry density of soil (kg/m^3).

The material compositions of three clay-based sealing materials (i.e., HCB, DBF, and LBF) are shown in Table 5. Table 6 shows the mass fractions and relative densities in Equation (7) determined from the material compositions in Table 5. These values are used in the calculation of the EMDD.

Table 5: Clay-Based Sealing Material Composition

Highly Compacted Bentonite (HCB)	
AGGREGATE	
Crushed granite =	0%
CLAY	
Sodium Bentonite (MX-80):	100%
100%	
Dense Backfill (DBF)	
AGGREGATE	
Crushed granite =	75%
CLAY	
Na-Bentonite (Avonlea) =	6.25%
Georgia Bay (Dundas) Shale ("Sealbond") =	18.75%
25%	
100%	
Light Backfill (LBF)	
AGGREGATE	
Quartz (sand)	50%
CLAY	
Na-Bentonite (Avonlea)	50%
100%	

Table 6: Coefficients to Calculate EMDD

		HCB	DBF	LBF
Specific gravity of solid	$G_s =$	2.745	2.643	2.702
Specific gravity of aggregate components	$G_a =$	1	2.620	2.650
Specific gravity of non-montmorillonite component in clay	$G_n =$	2.645	2.637	2.660
Mass fraction of clay in dry solids	$f_c =$	100%	25%	50%
Mass fraction of montmorillonite in clay fraction	$f_m =$	75%	19.75%	79%
Density of water (Mg/m^3)	$\rho_w =$	1	1	1

5.2 MECHANICAL CONSTITUTIVE MODEL PARAMETERS

Mechanical constitutive model parameters for the HCB, DBF and LBF are interpreted from the Log-linear relationships of the results of 1D consolidation tests. The parameters C_c and C_s are the slope in loading and reloading, respectively, obtained from the void ratio (e) versus vertical

stress (σ_v) (in log scale) plot as illustrated in Figure 3. Points A and B in Figure 3 can be used as a reference point to draw pre-consolidation line (Line A-B). Point A shows the pre-consolidation stress (σ_c) and void ratio corresponding to the pre-consolidation stress ($e(\sigma_c)$). Point B shows the stress before unloading (σ_u), and its corresponding void ratio ($e(\sigma_u)$).

Figure 5, Figure 6, and Figure 7 show the void ratio (e) versus vertical stress (σ_v) of the HCB, DBF and LBF, respectively. The configuration of the tests in Figures 5, 6, and 7 are shown in Tables 2, 3, and 4, respectively. Currently, a total of fifty-six (56) 1D consolidation tests have been completed: 16 tests on the HCB; 14 tests on the DBF; and 26 tests on the LBF. Figure 8 shows the comparison of the void ratio versus vertical stress of the HCB, DBF and LBF specimens.

C_c and C_s are interpreted from the results of 1D consolidation tests. The parameters C_c and C_s for the HCB, DBF and LBF are presented in Appendix D. The results of current testing program for the HCB, DBF and LBF are presented in Appendices A, B and C respectively.

Combined with the results of triaxial tests that define the behaviour of soil during shearing and the failure criteria, these parameters can be used to evaluate soil behaviour using a critical state model (e.g., modified cam-clay (MCC) (Roscoe and Burland 1968)).

Assuming the materials are elastic for small stress-strain increment, the 1D-modulus, which is sometimes called the constrained modulus, can be calculated from the slope of vertical stress-strain relationship. From the void ratio – log vertical stress relationship, the 1D-Modulus can be calculated as:

$$1D - Modulus = \frac{\sigma_{v1} - \sigma_{v2}}{(e_1 - e_2)/(1 + e_1)} \quad (9)$$

where: σ_{v1} and σ_{v2} are vertical stresses at points 1 and 2 respectively; e_1 and e_2 are void ratio at points 1 and 2 respectively (see Figure 4). The 1D-Modulus for each load increments of specimens HCB, DBF and LBF are calculated and summarized in Appendix D.

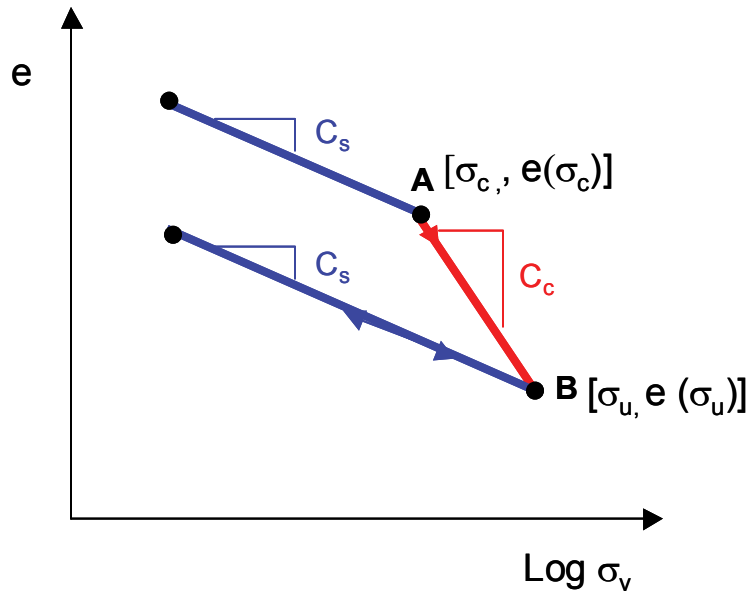


Figure 3: Definition of Parameters C_c and C_s

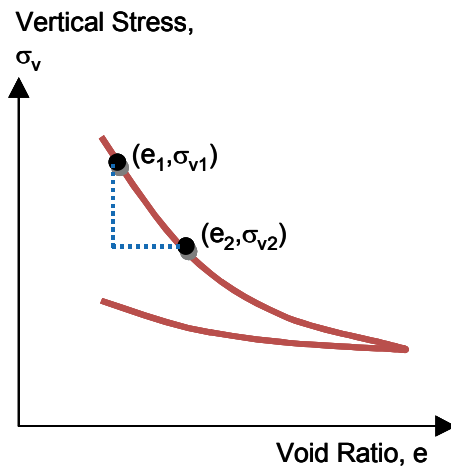


Figure 4: Definition of 1D-Modulus

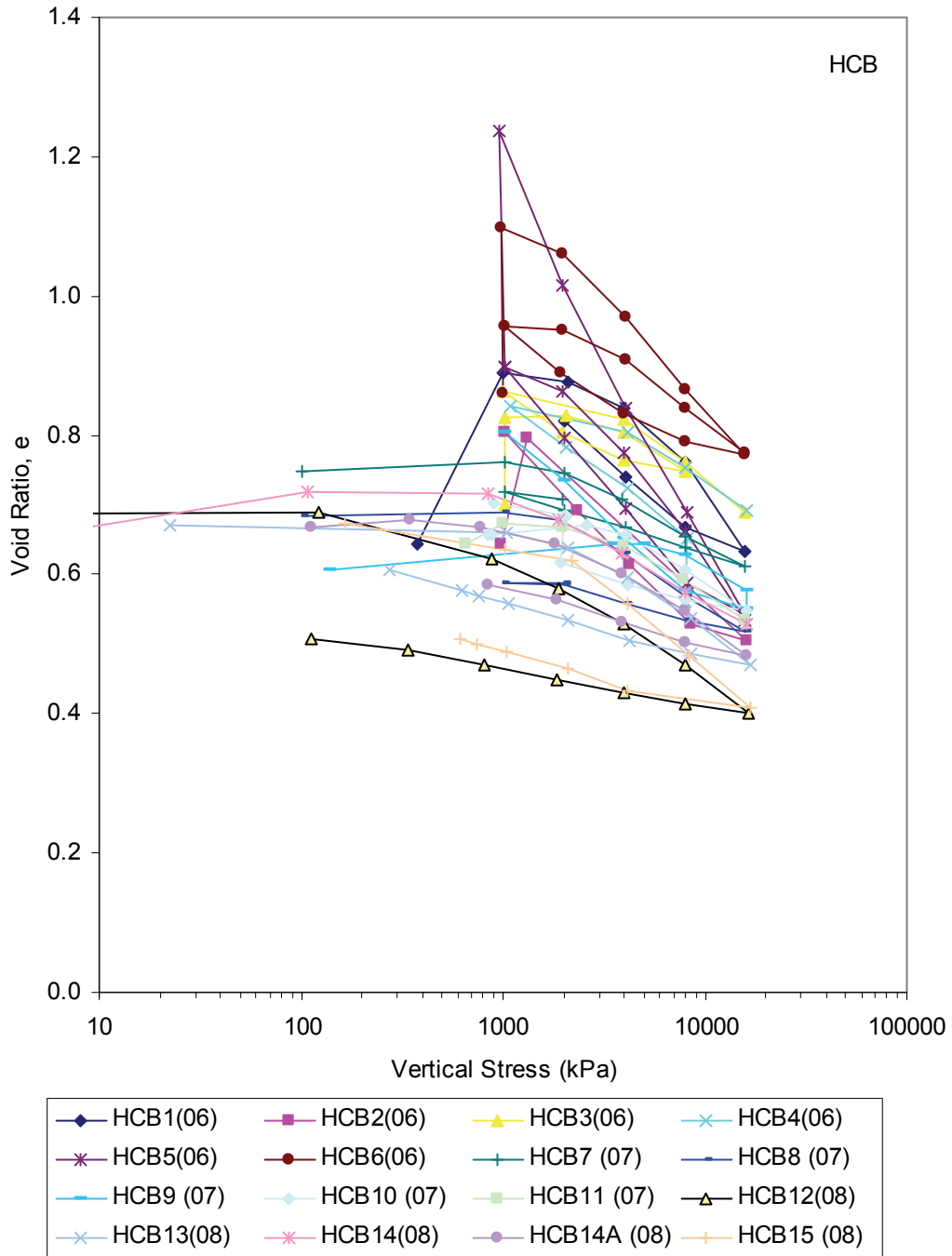


Figure 5: Vertical Stress versus Void Ratio of HCB (See Table 2 for Configuration of Each Test)

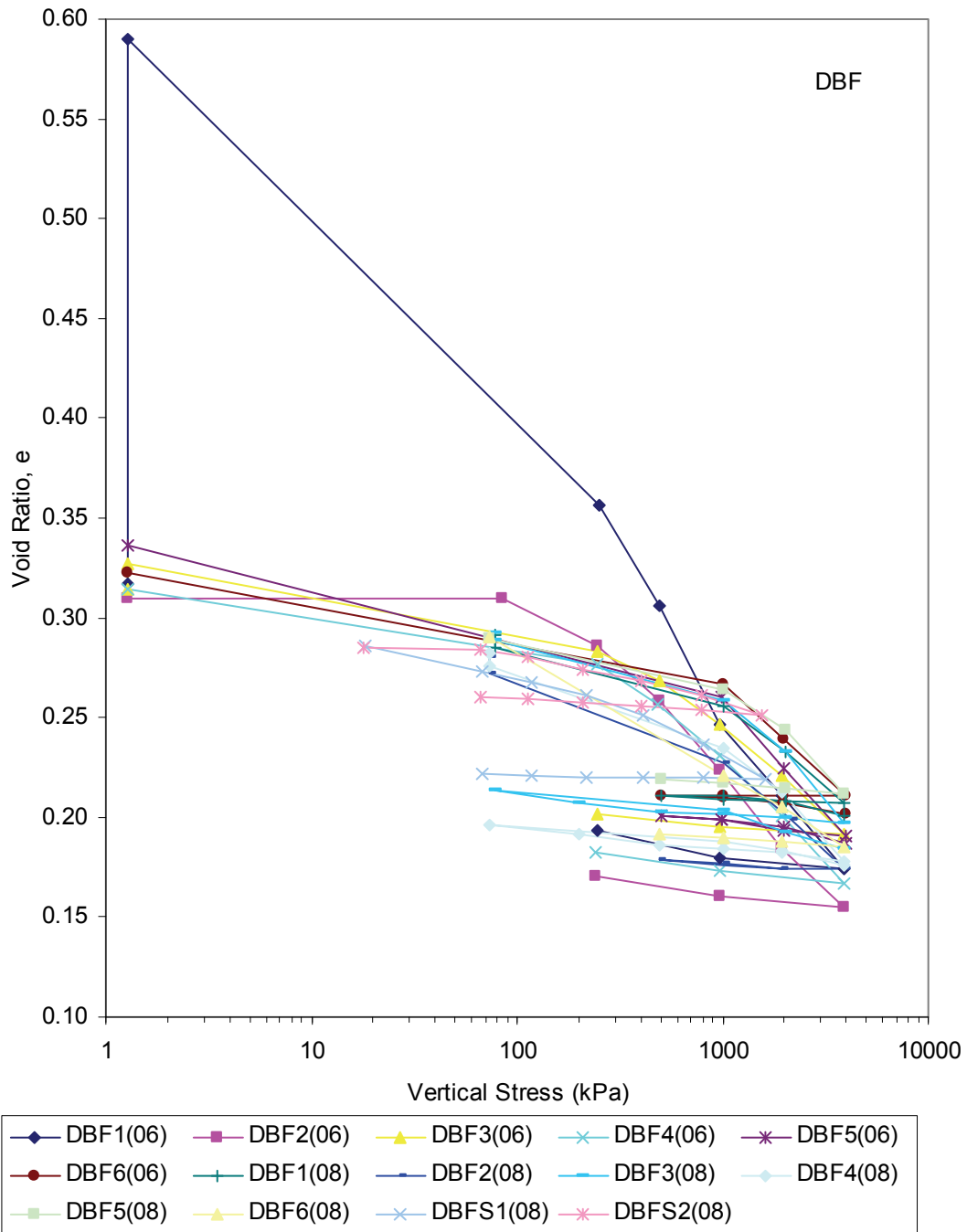


Figure 6: Vertical Stress versus Void Ratio of DBF (See Table 3 for Configuration of Each Test)

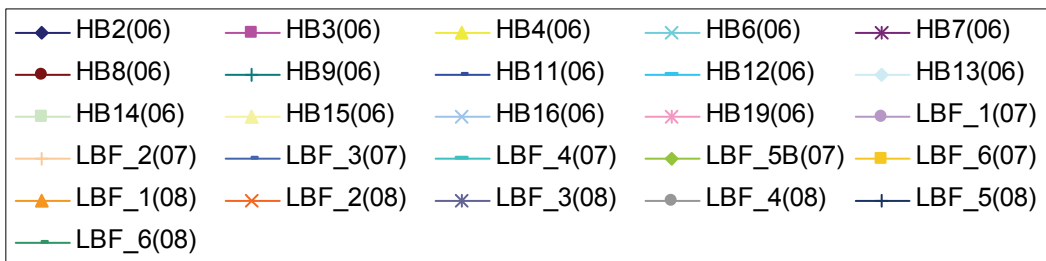
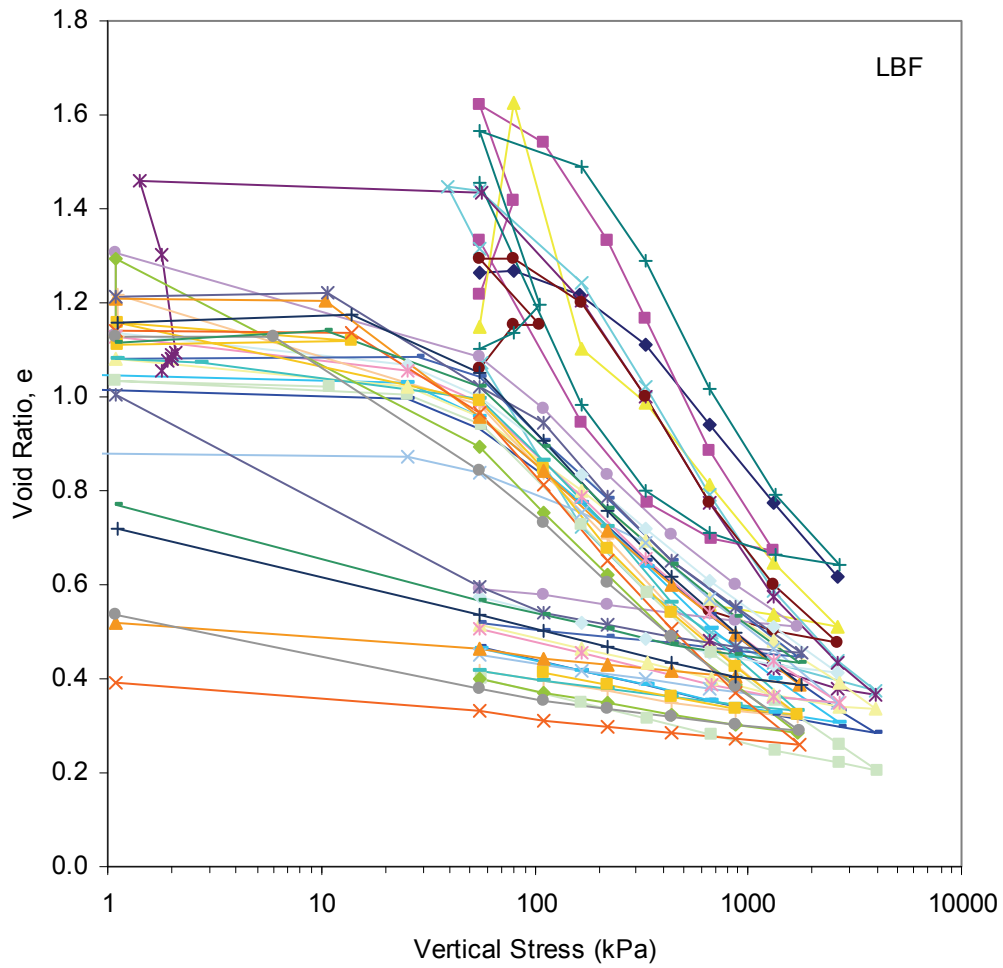


Figure 7: Vertical Stress versus Void Ratio of LBF (See Table 4 for Configuration of Each Test)

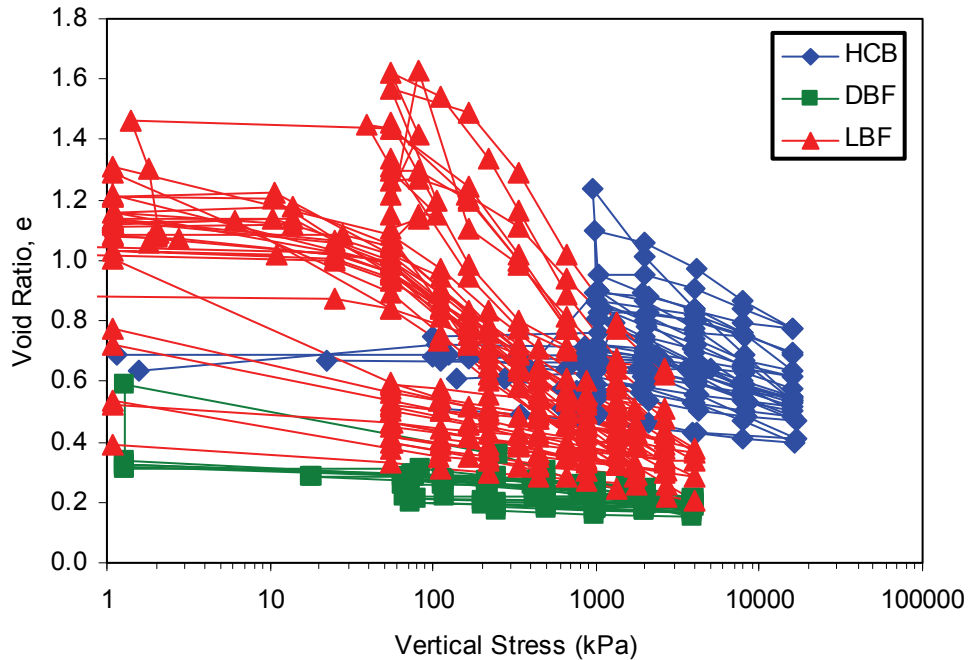


Figure 8: Vertical Stress versus Void Ratio of HCB, DBF, and LBF

5.3 HYDRAULIC CONSTITUTIVE MODELS

The coefficient of consolidation (c_v) for each load increment can be interpreted from the results of 1D-consolidation. The c_v is a parameter that couples hydraulic and mechanical behaviour of the soil. Assuming soil has linear-elastic behaviour for each load increment, the hydraulic conductivity (k) can be calculated from c_v using the relationships developed by Terzaghi (1943):

$$k = c_v \gamma_w \frac{\Delta e}{(1 + e_o) \Delta \sigma} = \frac{c_v \gamma_w}{1D - \text{Modulus}} \quad (10)$$

Although the material is non-linear (Figure 4), it is a reasonable assumption that within a single load increment (i.e. pt 1 to pt 2) that the relationship is approximately linear.

The c_v and k of HCB, DBF and LBF materials tested in this study have been interpreted from the 1D-consolidation test results. The data associated with these analyses are provided in Appendix D. Both square-root-time and log-time methods based on the ASTM 2435-04 (ASTM 2004) were used to determine the c_v . The c_v presented in this document is the average of c_v determined using these two methods.

The existing of secondary compression (e.g., in the HCB) that could add considerable uncertainty to the determination of t_{50} or t_{90} and, hence, to the determination of c_v and k . In this document, only primary compression portion were used to determine the c_v and k to reduce this uncertainty. A curve-fitting formulation based on the consolidation equations was also created using MS-Excel to improve consistency in determining the c_v and k .

It is recognized that the k determined from 1D-consolidation tests is not as reliable as the k from constant head permeability tests (e.g., Dixon et al. 1999; Dixon 2000), thus the actual k value should be obtained from the results of permeability tests (e.g., Dixon et al. 1999; Dixon 2000). Dixon and Gray (1985) observed that k determined using 1D-consolidation and constant head permeability tests were comparable (i.e., within one order of magnitude).

6. DISCUSSION

6.1 EMDD, HYDRAULIC CONDUCTIVITY AND 1D-MODULUS

The term 'effective montmorillonite dry density' (EMDD) was derived to single out the role of montmorillonite in soil behaviour (Baumgartner and Snider 2002; JNC 2000). The EMDD removed the mass and volume of the non-swelling components from the density calculation in order to better interpret the swelling and hydraulic behaviour that was mostly controlled by the montmorillonite.

Figure 9 and Figure 10 show the hydraulic conductivities (k) of HCB, DBF and LBF materials versus dry density and EMDD respectively. Without considering the types of fluid and loading paths of the specimens, the hydraulic conductivity of the HCB is the lowest (as compared to DBF and LBF). The hydraulic conductivity of the HCB ranges between 1×10^{-15} and 1×10^{-11} m/s for the dry density of 1.2 to 1.9 Mg/m³ and EMDD of 1.1 to 1.7 Mg/m³. The k of LBF is 1×10^{-13} to 5×10^{-9} m/s for the dry density range of 1.2 to 1.9 Mg/m³ (EMDD of 1.1 to 1.7 Mg/m³). The DBF has a k ranging from 5×10^{-15} to 5×10^{-10} m/s for the dry density of 2.0 to 2.5 Mg/m³ and EMDD of 0.3 to 1.0 Mg/m³.

In most cases, the increase in EMDD results in an decrease in k for the HCB, DBF and the LBF materials. Figures 9 and 10 do not show any clear relationship (increasing or decreasing) between k and density for a given material. It probably speaks to the uncertainty of determining k from consolidation data since these relationships have been clearly defined from permeability measurements.

Figure 11, Figure 12 and Figure 13 show the 1D-modulus versus void ratio, dry density and EMDD, respectively. Figures 12 and 13 show that 1D-modulus are only dependent upon material type (i.e. the modulus of LBF is less than the other two materials, and that there is no dependency on either EMDD or dry density). It is observed that the modulus of LBF (which contains 50% of sand) is consistently less than the modulus of HCB (which contains no sand) at the same void ratio. It can be related to the specimen preparation or the lateral response of these materials, where further investigations are still required.

Figure 14, Figure 15 and Figure 16 show the hydraulic conductivity (k) versus EMDD for the HCB, DBF and LBF, respectively. Figures 14a, 15a and 16a are classified based on the specimen name. The configurations of the specimens HCB, DBF, and LBF in these figures are

shown in Tables 2, 3, and 4, respectively. The data related to these figures are shown in Appendix D.

Figures 14b, 15b and 16b are classified based on the type of fluids used in the tests. Notation “(DW)” in the legends in Figures 14b, 15b and 16b indicates that the distilled water (DW) was used as the mixing fluid during specimen preparation. Notation “(s)” in the legend in Figure 14b indicates the smaller specimen used in the test.

The hydraulic conductivity of tests using distilled water for the LBF specimens (Figure 16b) is consistently less than those tests that used saline pore fluids at similar densities, but it is not the case for the HCB and DBF specimens. The hydraulic conductivity of tests using distilled water for the HCB and DBF specimens (Figure 14b and Figure 15b) is not clearly higher or lower than tests using saline pore fluids at similar densities. It is notable that within each individual test that k decreases with increasing density, although globally (all tests combined) that trend is not apparent. This trend for each individual test concurs with the permeability tests by Dixon (2000).

Comparison of specimens having similar salt solution in the reservoir with different type of fluid in specimen preparation shows that specimens prepared with distilled water (DW) has lower hydraulic conductivity than specimens prepared with salt solutions (Figure 14b). For similar EMDD's, the HCB specimens using 250 g/L NaCl have higher hydraulic conductivity than specimens using 250 g/L CaCl_2 (Figure 14b). A similar relationship is also observed for the DBF and LBF specimens (Figure 15b and Figure 16b).

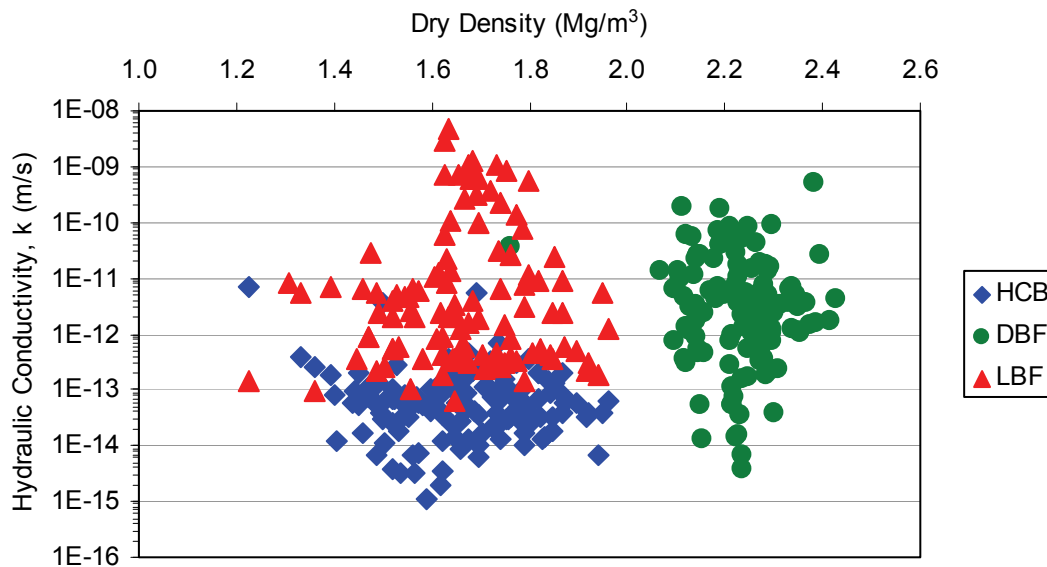


Figure 9: Dry Density versus Hydraulic Conductivity of HCB, DBF and LBF

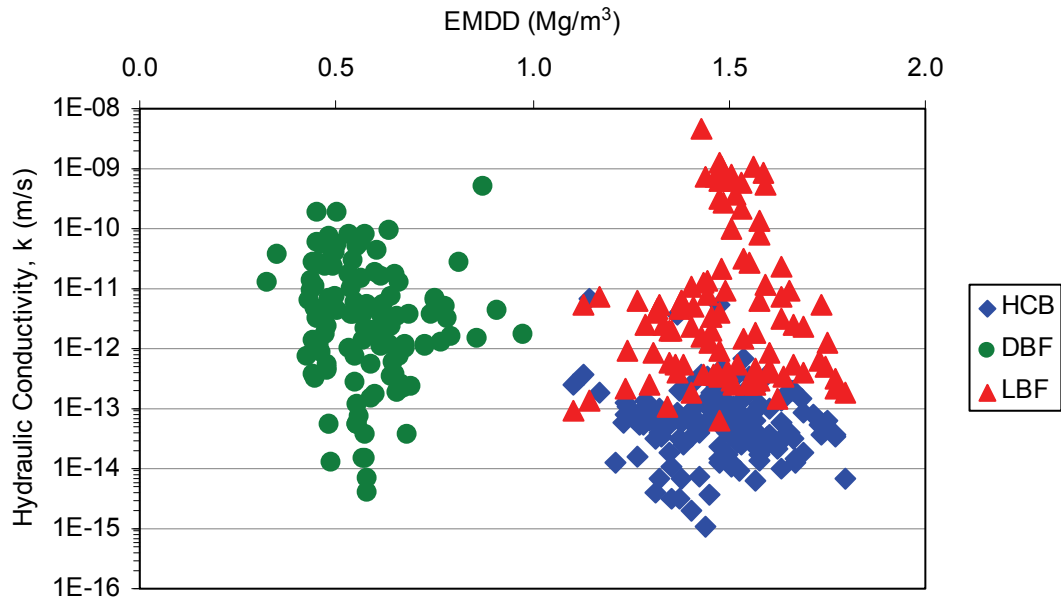


Figure 10: EMDD versus Hydraulic Conductivity of HCB, DBF and LBF

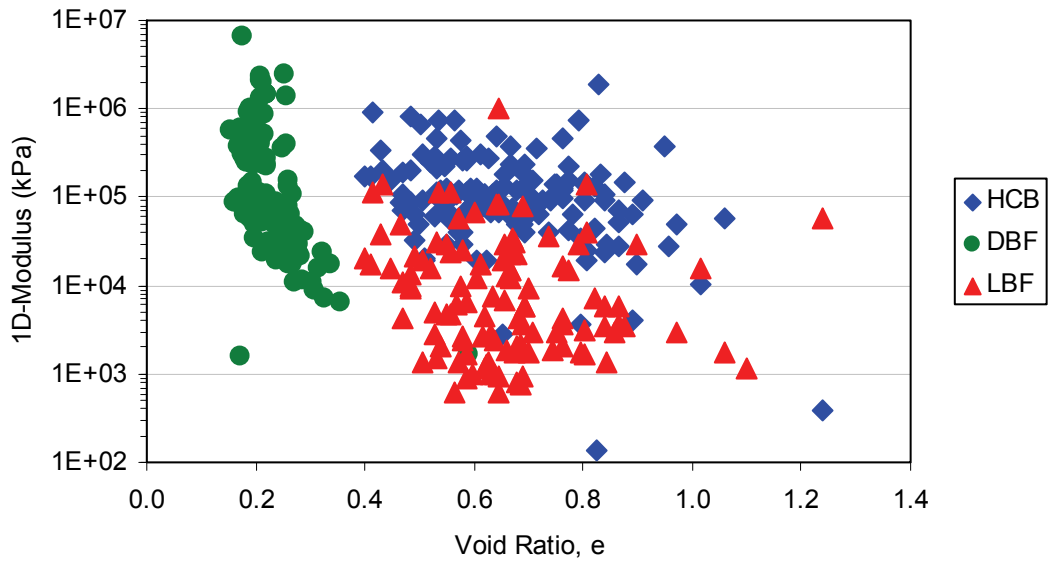


Figure 11: 1D-Modulus versus Void Ratio

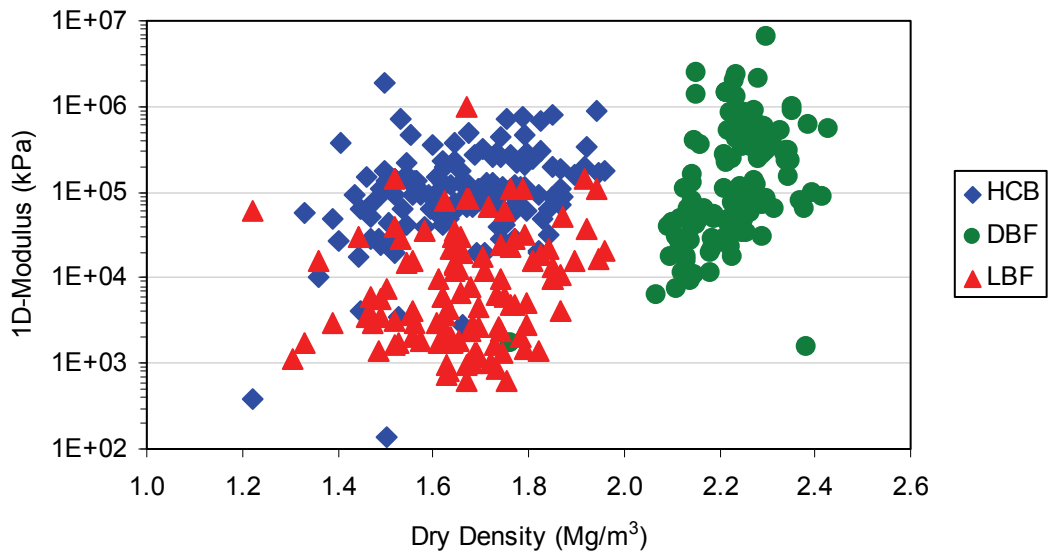


Figure 12: 1D-Modulus versus Dry Density

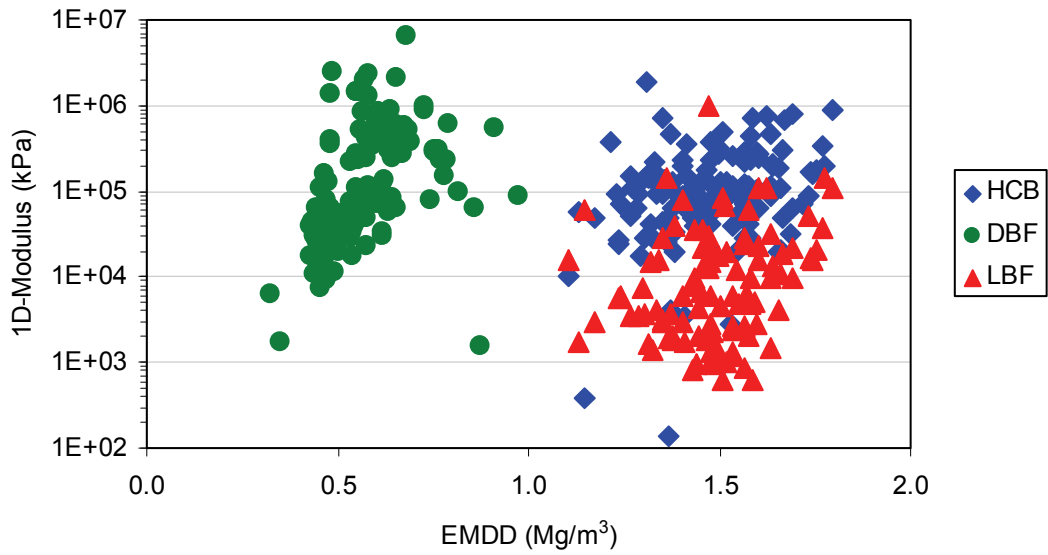
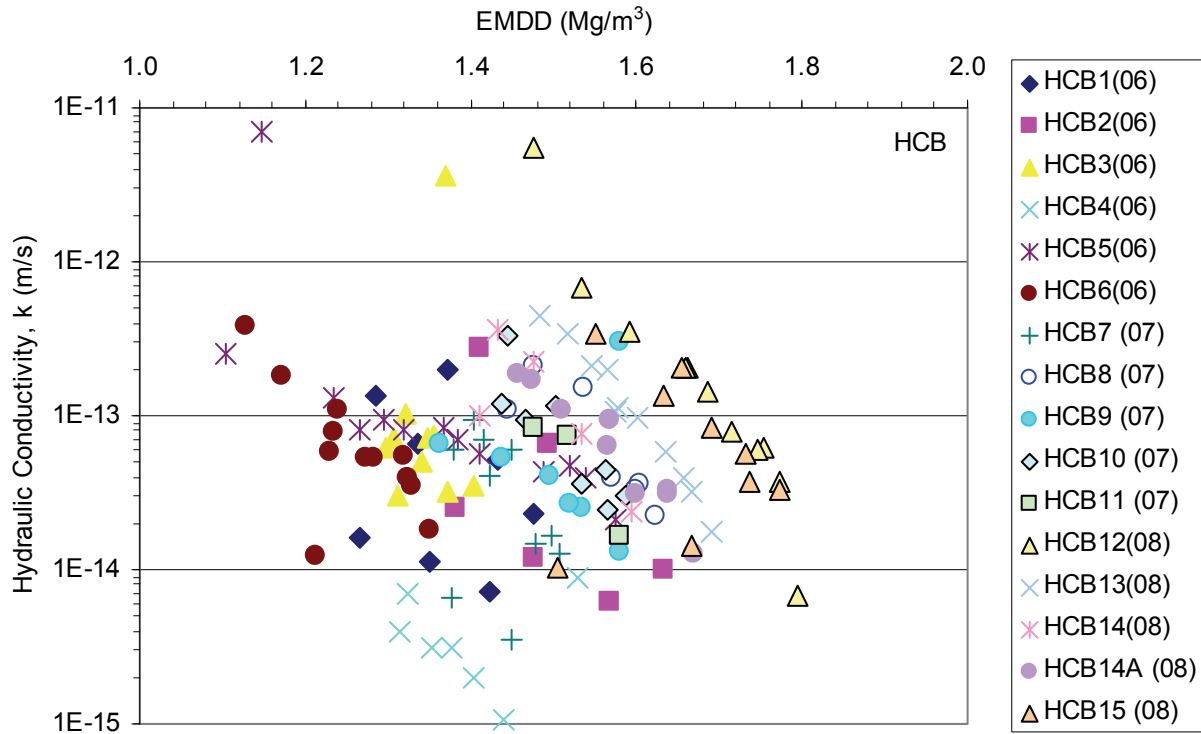
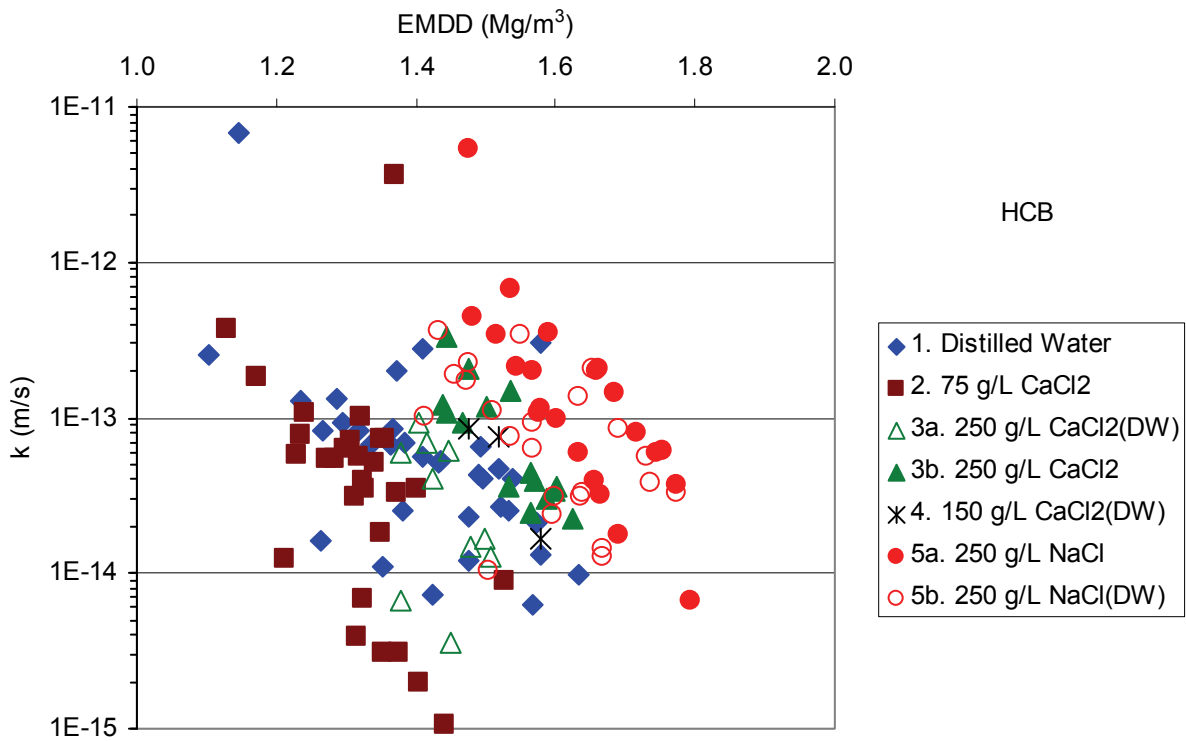


Figure 13: 1D-Modulus versus EMDD

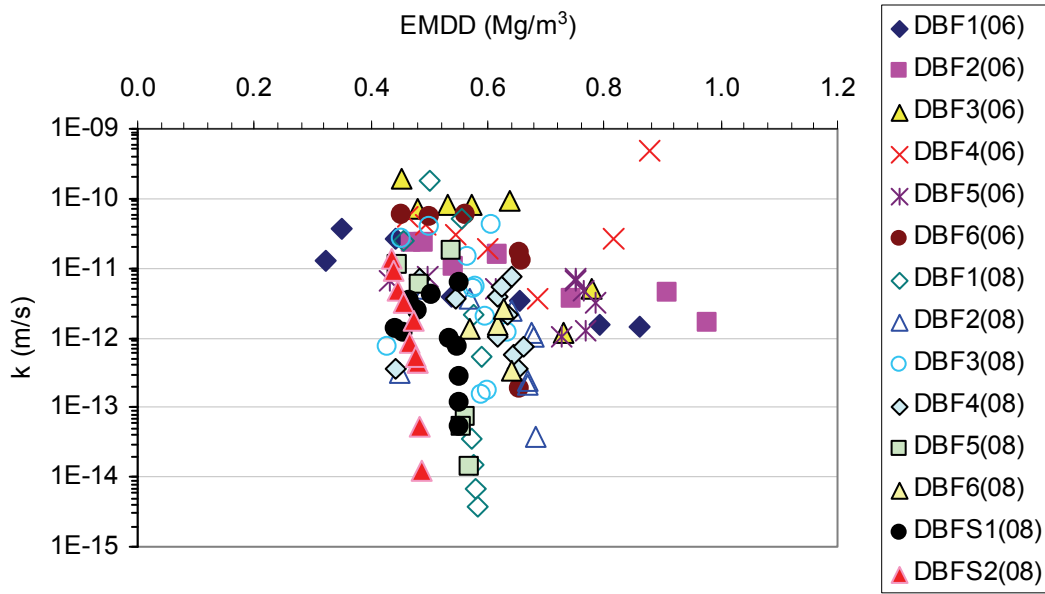


(a) Classified Based on the Specimen (See Table 2 for Tests Configurations)

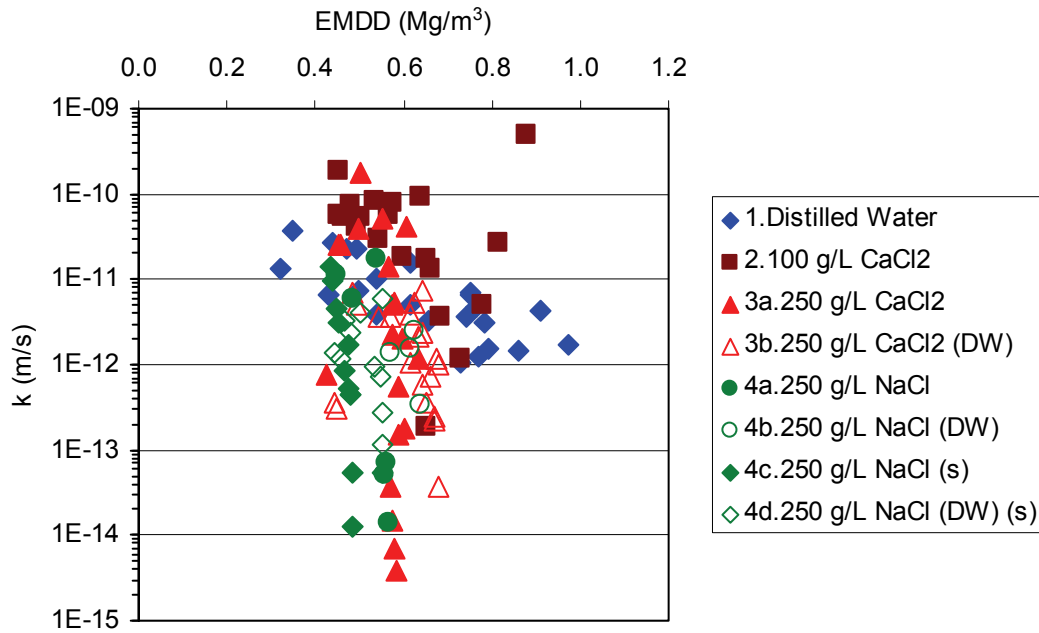


(b) Classified Based on the Fluid Type

Figure 14: EMDD versus Hydraulic Conductivity of HCB

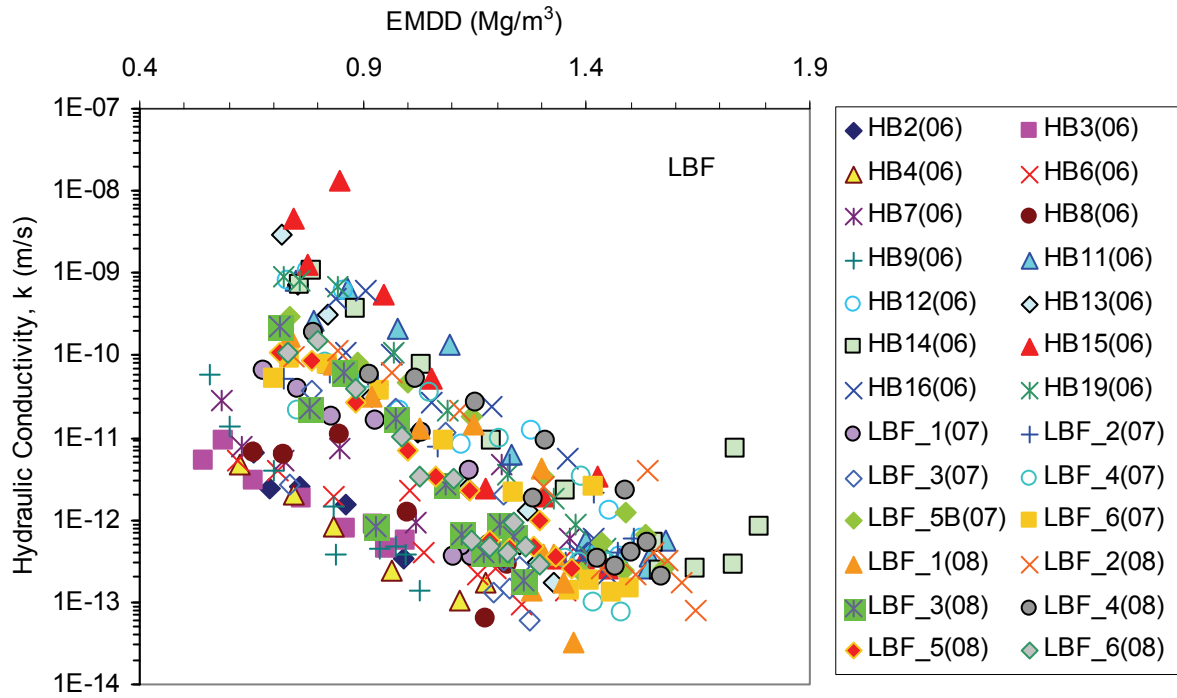


(a) Classified Based on the Specimen
(See Table 3 for Tests Configurations)

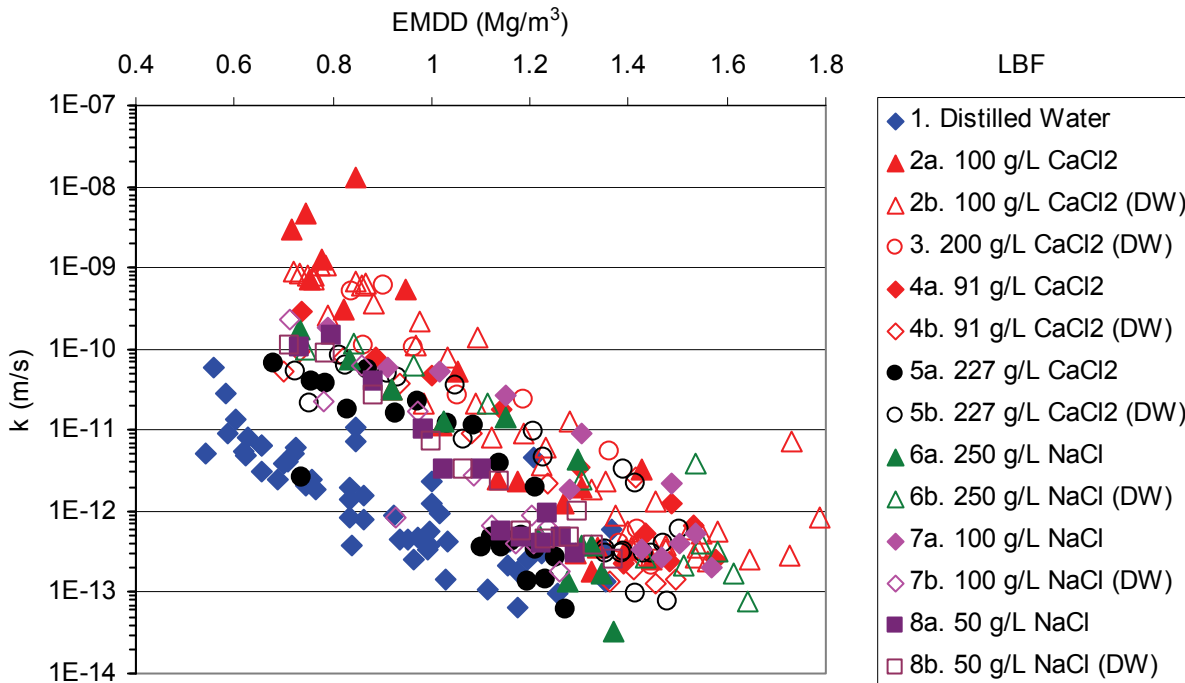


(b) Classified Based on the Fluid Type

Figure 15: EMDD versus Hydraulic Conductivity of DBF



(a) Classified Based on the Specimen
(See Table 4 for Tests Configurations)



(b) Classified Based on the Fluid Type

Figure 16: EMDD versus Hydraulic Conductivity of LBF

6.2 COMPRESSION AND SWELLING INDICES

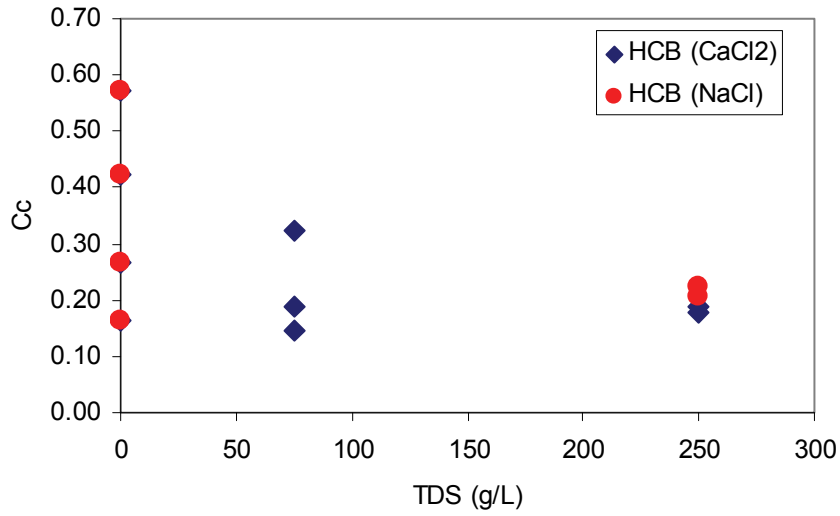
Priyanto et al. (2008) showed that the compression and swelling indices (C_c and C_s) of HCB, DBF and LBF specimens decrease with the presence of CaCl_2 in the pore fluid at concentrations > 75 g/L. The results of current testing programs compared to the previous tests (Baumgartner et al. 2008; Priyanto et al. 2008) allow comparison of the effects of CaCl_2 and NaCl solutions on the compression indices of the specimens.

Figure 17, Figure 18 and Figure 19 plot C_c and C_s versus the concentrations of CaCl_2 and NaCl solutions in the HCB, DBF and LBF specimens, respectively. The compression indices (C_c and C_s) are not obviously affected by whether the saline pore fluid solution contains NaCl or CaCl_2 .

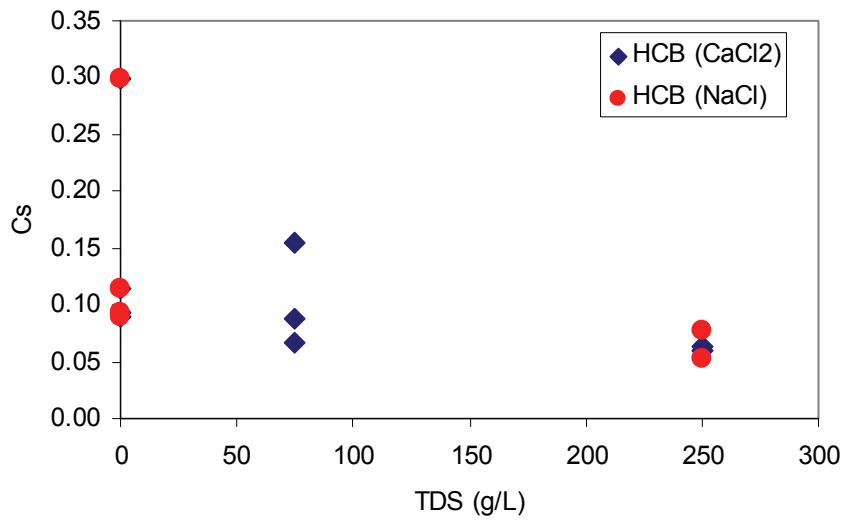
Figure 19 shows the relationships between C_c and C_s and salt concentration for LBF. There is more C_s and C_c data available from tests on LBF than for either HCB or DBF, particularly at NaCl concentrations less than 130 g/L. There are no obvious differences between the magnitudes of the indices for the two types of salt solutions (NaCl and CaCl_2) examined. Figure 19 also shows that the C_c of LBF decreases with increasing pore fluid salinity, up to TDS of 50 g/L, and beyond that concentration is relatively constant. The C_s of the LBF decreases with increasing TDS when the TDS is less than 100 g/L and is relatively constant for TDS greater than 100 g/L. Based on this observation, the C_c and C_s for the LBF are dependent on the pore fluid concentration up to about 100 g/L, but they are independent on the type of salt solution. Although the compression indices of DBF and HCB are less for saline pore fluid than for fresh water, they do not change with changes in solution concentration (Figures 17 and 18). However, this interpretation would benefit from additional tests in the range of 0 to 100 g/L concentration.

The relationship of C_c and C_s to the salt solution concentration (in TDS) was plotted in Figure 20 by assuming that the compression and swelling indices of HCB and DBF similarly decreased with increasing salt concentration up to 100 g/L. The C_c of the LBF is the greatest followed by the HCB and DBF. Considering that the HCB has the highest montmorillonite content and therefore the greatest content of highly swelling material, it is logical that the C_s of the HCB is the greatest, followed by the LBF and DBF (Figure 20).

This relationship of the C_c and C_s to the TDS for the HCB, DBF and LBF specimens can be used to include the effect of pore fluid salinity on the mechanical behaviour of the clay-based sealing materials using THM numerical models of the DGR system.

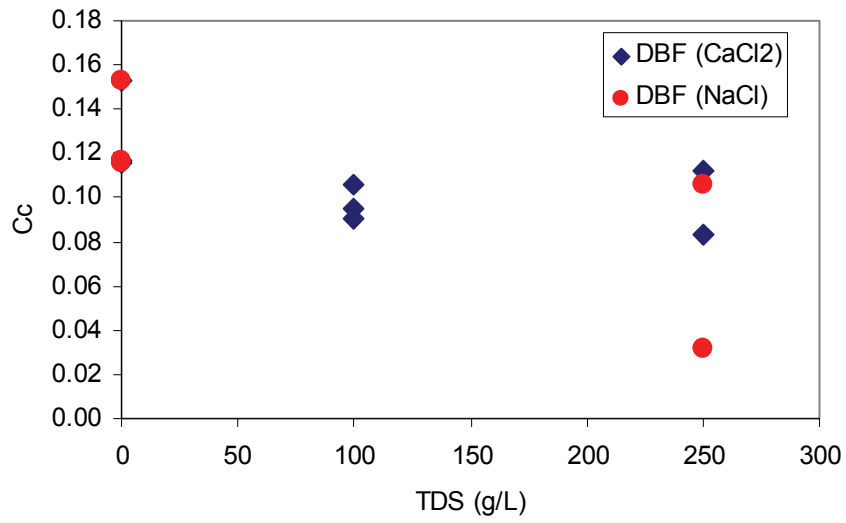


(a) Compression Index (C_c)

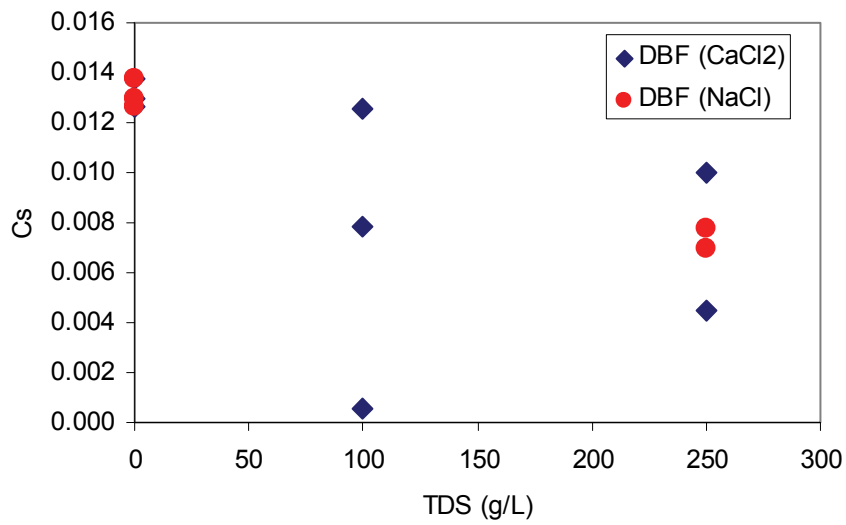


(b) Swelling Index (C_s)

Figure 17: The Effect of CaCl₂ and NaCl Solution to the Compression Index (C_c) and Swelling Index (C_s) of HCB

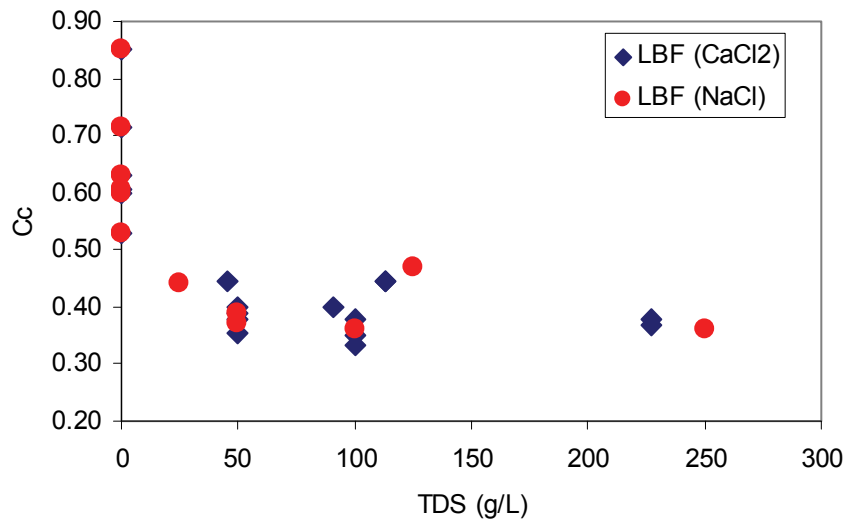


(a) Compression Index (C_c)

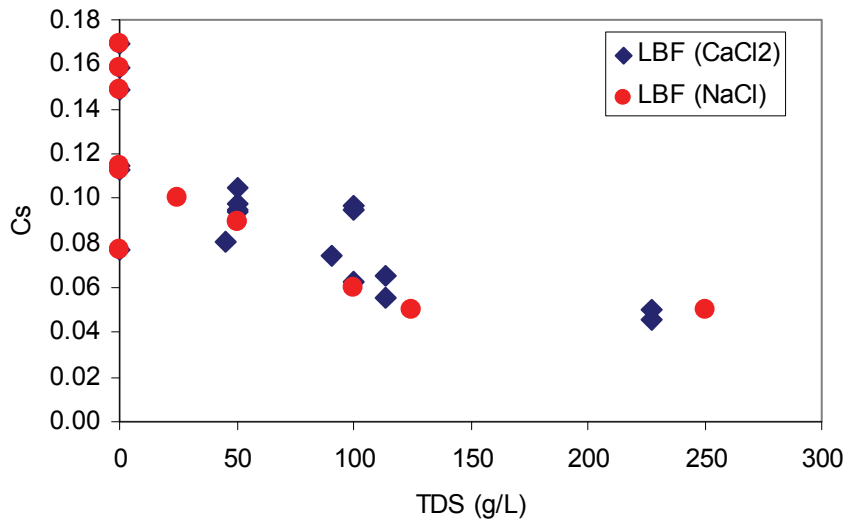


(b) Swelling Index (C_s)

Figure 18: The Effect of CaCl₂ and NaCl Solution to the Compression Index (C_c) and Swelling Index (C_s) of DBF

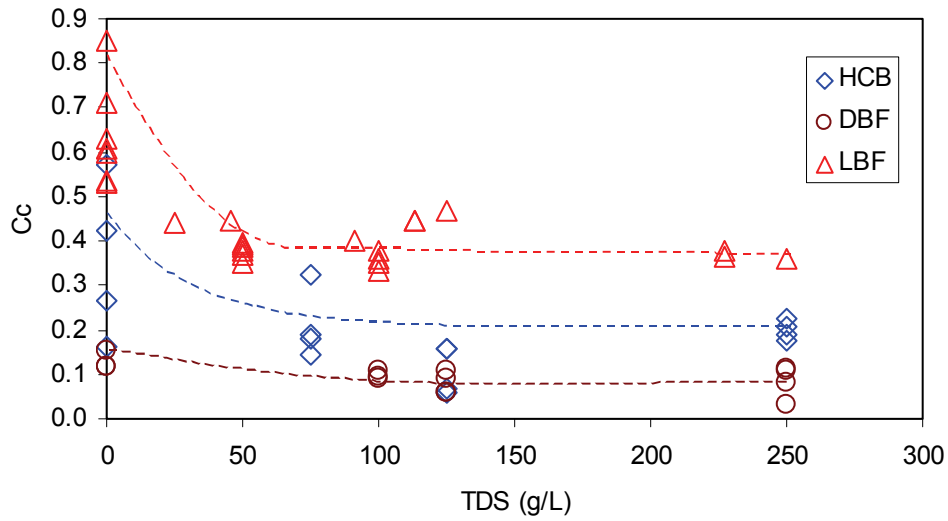


(a) Compression Index (C_c)

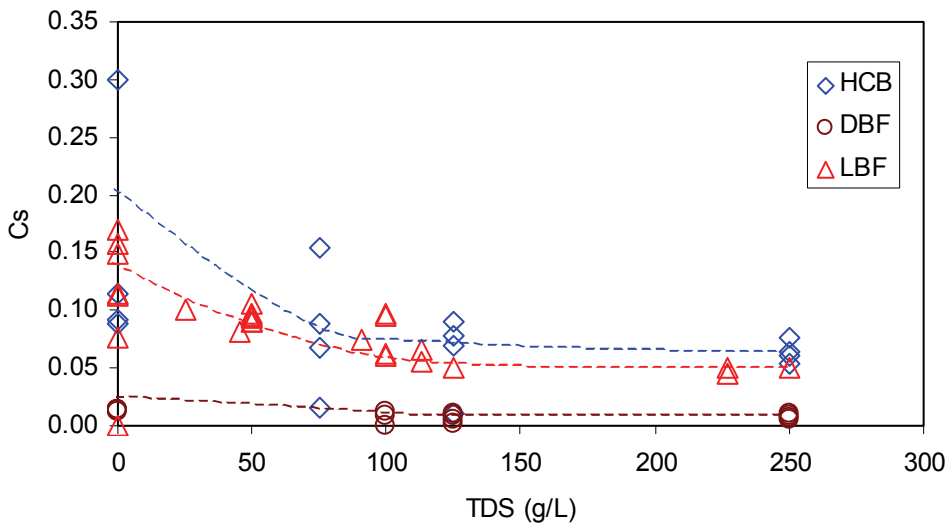


(b) Swelling Index (C_s)

Figure 19: The Effect of CaCl₂ and NaCl Solution to the Compression Index (C_c) and Swelling Index (C_s) of LBF



(a) Compression Index (Cc)



(b) Swelling Index (Cs)

Figure 20: Relationship of Compression Index (Cc) and Swelling Index (Cs) and TDS of Solution

6.3 SWELLING PRESSURE UNDER CONSTANT VOLUME (CV) OF HCB

Under constant volume boundary conditions during initial saturation, the vertical stress increases until the pressure required maintaining constant volume has been reached. Figure 21 and Figure 22 show the swelling pressures for specimens HCB9, HCB10, HCB12 and HCB14A. Table 7 summarizes the swelling pressure and fluid used in the tests. The breaks

appeared in swelling pressure of specimens HCB9 (Figure 21) and HCB14A (Figure 22b) were due to power disruption that occurred during the tests.

Specimen HCB9 having distilled water as mixing and reservoir fluid had the largest swelling pressure at 5 MPa compared to three similarly prepared specimens having 250 g/L NaCl or CaCl₂ reservoir fluids. For similar salt concentrations (250 g/L), specimen HCB10 prepared using CaCl₂ solution has significantly greater swelling pressure (approximately 2.5 MPa) than specimen HCB12 prepared with NaCl solution (swelling pressure was approximately 0.1 MPa). For systems having similar reservoir fluids (250 g/L NaCl solution), specimen HCB14A that was prepared with distilled water has a higher swelling pressure (approximately 0.3 to 1 MPa) than specimen HCB12 (approximately 0.1 MPa). Using distilled water in specimen preparation initially reduces the concentration of salt solution in the pore fluid, and consequently a higher swelling pressure develops.

Table 7: Swelling Stress of HCB Specimens During Initial Saturation

Specimen	Mixing Fluid	Reservoir Fluid	Swelling Stress (MPa)
HCB9	Distilled Water (DW)	Distilled Water (DW)	5.0
HCB10	250 g/L CaCl ₂	250 g/L CaCl ₂	2.5
HCB12	250 g/L NaCl	250 g/L NaCl	0.1
HCB14A	Distilled Water (DW)	250 g/L NaCl	0.3 to 1.0

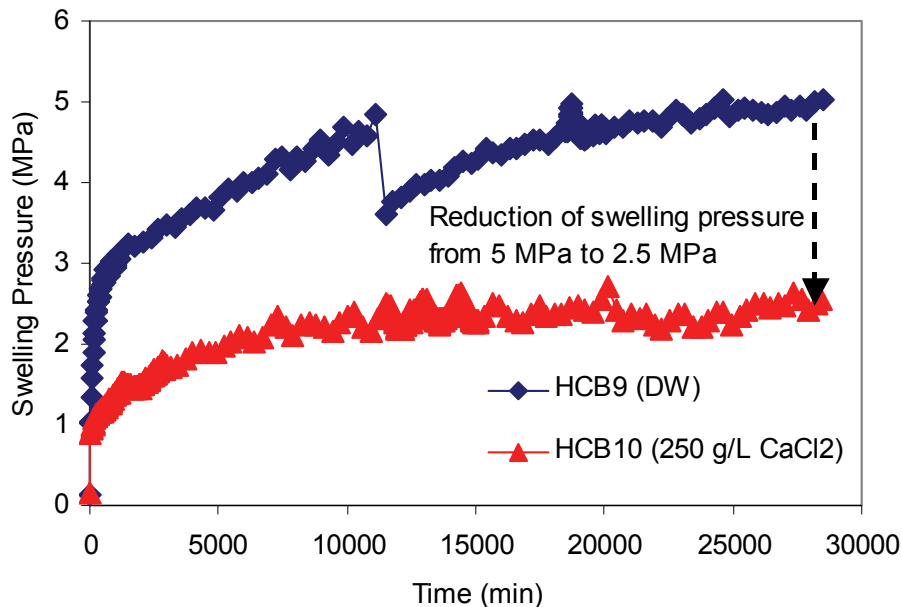
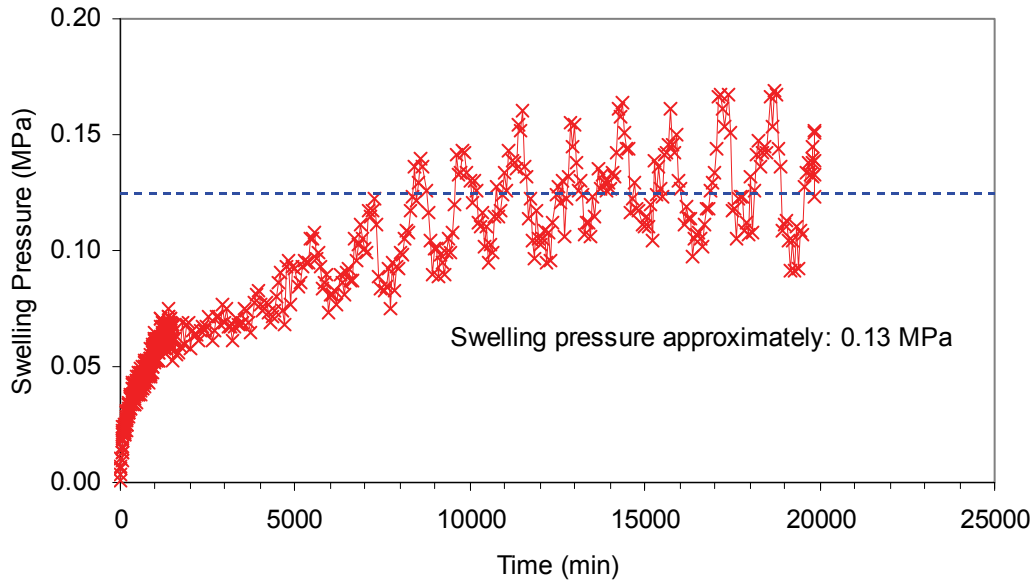
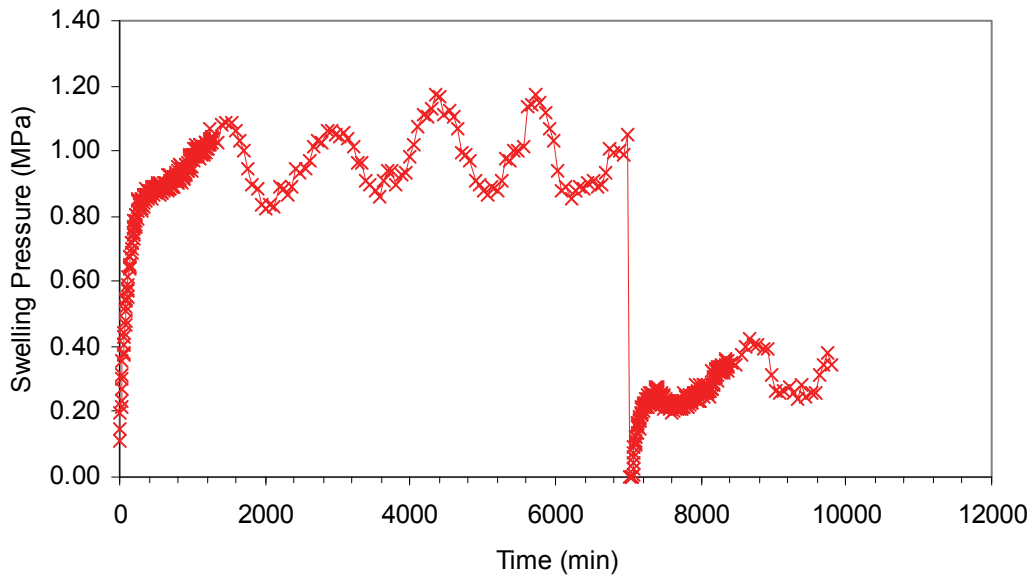


Figure 21: Swelling Stress for Specimens HCB9 and HCB10



(a) Specimen HCB12
(Mixing Fluid = Reservoir Fluid = 250 g/L NaCl Solution)



(b) Specimen HCB14A
(Mixing Fluid = Distilled Water; Reservoir Fluid = 250 g/L NaCl Solution)

Figure 22: Swelling Stress for Specimens HCB12 and HCB14A

7. CONCLUDING REMARKS AND RECOMMENDATIONS

7.1 CONCLUDING REMARKS

Based on the results of the 1D-consolidation tests of the three clay-based sealing materials, the following conclusions can be made.

- The compression indices (C_c) and swelling indices (C_s) decrease with the presence of either NaCl or CaCl_2 in the pore fluid for HCB, DBF and LBF. A decrease in the C_c indicates that the materials become stiffer and less compressible, while a decrease of the C_s indicates a reduction of the ability of the material to swell.
- The C_c and C_s for the LBF material are dependent on the pore fluid concentration up to about 100 g/L, but they are independent on the type of salt solution (i.e., NaCl or CaCl_2). This relationship may also be applicable for the HCB and DBF materials. Above salt solution concentrations of 100 g/L the magnitude of C_s and C_c is independent of the concentration.
- Higher salt solution concentrations in the pore fluid of HCB, DBF and LBF specimens reduce the swelling stress.
- For a similar salt concentration of 250 g/L, the NaCl solution reduces swelling pressure of the HCB specimen more than the CaCl_2 solution.

The determination hydraulic conductivity (k) has been completed for this test. The data show that within each individual test that k decreases with increasing density, although globally (all tests combined) that trend is not apparent. These data indicate the difficulty in making accurate determination of k from consolidation data. The permeability tests (e.g., Dixon et al. 1999; Dixon 2000) should give more reliable results to determine k .

7.2 RECOMMENDATIONS

The tests described in this report are limited in number and so cannot be considered to be conclusive. They do however provide valuable insight into the effects of the environment (i.e., groundwater salinity) and the mode of material preparation (mixing water used) on the hydraulic and mechanical properties of three materials being considered for use as repository sealing system components.

Other tests are needed to clarify the relationships of consolidation indices (i.e., C_c and C_s) and pore fluid salinity provided in this document. The results of the tests in this document suggest that there is a greater need to test the materials with pore fluid concentration in the range of 0 to 100 g/L, where the C_c and C_s vary the most and only limited number of tests in this range have been completed. The C_c and C_s do not vary in the tests with pore fluid concentration above 100 g/L, so that fewer new tests at high concentrations are warranted.

Considering application of test results to design or numerically model the DGR, it is recommended 1D-Consolidation tests be done with an artificial groundwater similar to the groundwater composition observed by Gascoyne et al. (1987) and Mazurek (2004) (e.g., mixture of NaCl and CaCl_2 solution).

ACKNOWLEDGEMENTS

This work is supported under a contract issued to AECL by the Nuclear Waste Management Organization. The authors acknowledge the valuable contributions and support provided by all personnel from AECL, University of Manitoba and Royal Military College of Canada.

REFERENCES

- ASTM (ASTM International). 2004. Standard test methods for one-dimensional consolidation properties of soils using incremental loading. Standard D2435-04, ASTM International, West Conshohocken, Pennsylvania, USA.
- ASTM (ASTM International). 2005. Standard test method for laboratory determination of water (moisture) content of soil and rock by mass. Standard D 2216-05, ASTM International, West Conshohocken, Pennsylvania, USA.
- ASTM (ASTM International). 2007. Standard test method for pore water extraction and determination of the soluble salt content of soils by refractometer. Standard D 4542-07, ASTM International, West Conshohocken, Pennsylvania, USA.
- Baumgartner, P., and G.R. Snider. 2002. Seal evaluation and assessment study (SEAS): Light backfill placement trials. Atomic Energy of Canada Limited Technical Record, TR-793.*.
- Baumgartner, P., D.G. Priyanto, J.R. Baldwin, J.A. Blatz, B.H. Kjartanson, and H. Batenipour. 2008. Preliminary results of one-dimensional consolidation testing on bentonite clay-based sealing components subjected to two-pore liquid chemistry conditions. Nuclear Waste Management Organization (NWMO) Technical Report No. TR-2008-04. Toronto, Canada.
- Dixon, D.A. and M.N. Gray. 1985. The engineering properties of buffer material – research at Whiteshell Nuclear Research Establishment. Atomic Energy of Canada Limited Technical Record, TR-350*, 1985.
- Dixon, D.A., J. Graham, and M.N. Gray. 1999. Hydraulic conductivity of clays in confined tests under low hydraulic gradients. *Can. Geotech.* 36, 815-825.
- Dixon, D.A. 2000. Porewater salinity and the development of swelling pressure in bentonite-based buffer and backfill materials. Helsinki, Posiva Report, POSIVA 2000-04 (ISBN 951-652-090-1).
- Gascoyne, M., C.C. Davison, J.D. Ross, and R. Pearson. 1987. Saline groundwaters and brines in plutons in the Canadian Shield. *In* Saline Water and Gases in Crystalline Rocks. (Fritz, P. and Frape, S.K., Eds.), Geological Association of Canada Special Paper 33, Ottawa.
- JNC (Japan Nuclear Cycle Development Institute). 2000. H12: Project to establish the scientific and technical basis for HLW disposal in Japan. Supporting report 2: Repository design and engineering technology. Japan Nuclear Cycle Development Institute Report, JNC TN 1400 2000-003.
- Mazurek, M. 2004. Long-term used nuclear fuel waste management – Geoscientific review of the sedimentary sequence in southern Ontario. Institute of Geological Sciences, Univ. of Bern, Technical Report TR 04-01, Bern, Switzerland, available from Nuclear Waste Management Organization, Toronto, Canada (www.nwmo.ca).

NUKEM. 2003. Deep geological in-floor borehole emplacement. Design changes from in-room emplacement concept. RWE NUKEM Limited Report 89125/REP/02. November, 2003.

Priyanto, D.G., J.A. Blatz, G.A. Siemens, R. Offman, J.S. Boyle, and D.A. Dixon. 2008. The effects of initial conditions and liquid composition on the one-dimensional consolidation behaviour of clay-based sealing materials. Nuclear Waste Management Organization (NWMO) Technical Report No. TR-2008-06. Toronto, Canada.

Roscoe, K.H., and J.B. Burland. 1968. On the generalized stress-strain behaviour of 'wet' clay. In (J. Heyman & F. Leckie, Eds.), Engineering Plasticity (pp. 535-609). Cambridge: Cambridge University Press.

Russell, S.B., and G.R. Simmons. 2003. Engineered barrier system for a deep geologic repository. Presented at the 2003 International High-Level Radioactive Waste Management Conference. 2003 March 30-April 2, Las Vegas, NV.

Terzaghi, K. 1943. Theoretical Soil Mechanics. Wiley, New York.

* Available from SDDO, Atomic Energy of Canada Limited, Chalk River Laboratories, Chalk River, Ontario K0J 1J0.

**APPENDIX A: DETAILED DESCRIPTION: TESTING OF
HIGHLY COMPACTED BENTONITE (HCB)**

D.G. Priyanto and D.A. Dixon
Atomic Energy of Canada Limited

CONTENTS

	<u>Page</u>
A1. HIGHLY COMPACTED BENTONITE (HCB)	39
A2. EQUIPMENT	39
A2.1 OEDOMETER CELL AND LOADING SYSTEM	39
A2.2 STRAIN AND PRESSURE MEASUREMENT	39
A3. TEST PROCEDURE	40
A3.1 TEST MATRIX FOR HCB SPECIMENS	40
A3.2 SPECIMEN PREPARATION.....	41
A4. RESULTS	42
A5. DISCUSSION	48
A6. CONCLUDING REMARKS.....	51
ACKNOWLEDGEMENTS	51
REFERENCES	52

LIST OF TABLES

	<u>Page</u>
Table A1: 1-D Consolidation Test Matrix for HCB Specimens in 2008	41
Table A2: Initial Properties of the Highly Compacted Bentonite (HCB) Specimens	42
Table A3: 1-D Consolidation Test Matrix for HCB Specimens in 2008	48

LIST OF FIGURES

	<u>Page</u>
Figure A1: Specimen HCB12	43
Figure A2: Specimen HCB13	44
Figure A3: Specimen HCB14	45
Figure A4: Specimen HCB14A.....	46
Figure A5: Specimen HCB15	47
Figure A6: Void Ratio versus Vertical Stress of Specimens HCB8 and HCB13.....	49
Figure A7: Hydraulic Conductivity (k) versus EMDD	49
Figure A8: Comparison of Swelling Stress	50

A1. HIGHLY COMPACTED BENTONITE (HCB)

Highly Compacted Bentonite (HCB) is a clay-based sealing-system component proposed for use in either full contact or very close proximity to the used-fuel container (Maak and Simmons 2005). HCB is composed of 100% bentonite (Russell and Simmons 2003), compacted to high dry densities. The test specimens are fabricated from 80-mesh granules of Wyoming bentonite (MX80) with an assumed minimum Na-montmorillonite content of 75%. The 1D consolidation tests of HCB specimens are conducted at the Atomic Energy of Canada Limited (AECL) geotechnical engineering laboratory.

A2. EQUIPMENT

A2.1 OEDOMETER CELL AND LOADING SYSTEM

A standard dead weight oedometer with a 50-mm diameter cell is unable to apply the high stresses required to counteract the high swelling pressure of HCB. Small-diameter oedometer cells (28.1-mm diameter) with two types of custom-built loading systems were constructed to achieve a maximum stress of 16 MPa. The two loading systems were as follows.

1. Frame 1 was a compression frame with a double-action hydraulic ram (e.g., a 222 kN spring-return ram and a 445 kN double-acting ram). Each hydraulic ram was actuated by a high-pressure nitrogen-gas cylinder acting on a gas-over-oil accumulator rather than the conventional mechanical hydraulic pumps to achieve the most stable possible loading condition.
2. Frame 2 was a frame using a servo-hydraulic testing system manufactured by MTS[®] (Materials Testing Services). This equipment enabled an application of different boundary conditions during initial saturation (i.e., constant volume or constant pressure).

Two filter stones were installed at the top and bottom of the specimen. All components of the oedometer cells were fabricated from stainless steel to avoid corrosion.

A2.2 STRAIN AND PRESSURE MEASUREMENT

Displacements are measured with calibrated Linear Variable Differential Transformers (LVDT). Stresses are measured with calibrated strain-gauge load cells (i.e., 17.8-kN capacity). All instruments are connected to a data logger. The scan rates of the data logger was set at 5 minutes for the first 24 hours of a load/unload increment and every hour thereafter until the load/unload increment was deemed complete. The laboratory temperature ranged between 19°C and 24°C, producing maximum dimensional variance of 0.011 mm or about a 0.1% variation for 10-mm-thick specimen (Baumgartner et al. 2008). This small variation was considered insignificant and no thermal compensation was included in any calculation.

A3. TEST PROCEDURE

A3.1 TEST MATRIX FOR HCB SPECIMENS

The testing program in 2008 included HCB specimens prepared with two different mixing liquids (i.e., distilled water or 250 g/L NaCl solution) and two types of boundary conditions during initial saturation (i.e., constant volume (CV) or constant stress (CS)). Solution of 250-g/L NaCl was used as reservoir fluid in all four tests. Table A1 shows the test matrix of HCB specimens in 2008.

Four 1D-consolidation tests on the HCB specimen were planned in 2008. However, Specimen HCB14 was terminated during unloading because of the mechanical failure the cell restraint system due to rod cell failure caused by steel fatigue and damage to the LVDT due to exposure to salt vapour. It was also discovered that the HCB materials of the specimen HCB14 was squeezed out of the cell during dismantling of the specimen. The LVDT set-up was subsequently modified to avoid contact of the LVDT with the salt solution and new cell restraint rods were fabricated. Specimen HCB14A having similar configuration was installed in the new test set-up to replace the specimen HCB14.

Combined with the previous tests (Baumgartner et al. 2008; Priyanto et al. 2008), this testing program examines the effect of three different types of fluids (i.e. NaCl, CaCl₂ and distilled water). The results of the testing program can also be used to examine the effects of the initial boundary conditions (i.e., Constant Volume (CV) and Constant Vertical Stress (CS)) applied during initial saturation.

The results of the previous tests (Baumgartner et al. 2008; Priyanto et al. 2008) indicated that the primary consolidation of the HCB specimens has already been completed after 7 days. To maintain consistency between all the tests, the similar duration of 7 days for each load increment was used in these tests.

Table A1: 1-D Consolidation Test Matrix for HCB Specimens in 2008

Specimen No.	Mixing Fluid	Reservoir Fluid	Target Initial Dry Density (kg/m ³)	Target Initial Degree of Saturation (%)	Initial Boundary Condition During Saturation	Load Sequence
HCB12	250 g/L NaCl	250 g/L NaCl	1650	95	Constant pressure at 1 MPa	Load to 16 MPa, Unload to 0.1 MPa
HCB13	250 g/L NaCl	250 g/L NaCl	1650	95	Constant volume	Load to 16 MPa, Unload to 0.1 MPa
HCB14	Distilled water	250 g/L NaCl	1650	95	Constant volume	Load to 16 MPa.
HCB14A	Distilled water	250 g/L NaCl	1650	95	Constant volume	Load to 16 MPa, Unload to 0.1 MPa
HCB15	Distilled water	250 g/L NaCl	1650	95	Constant pressure at 1 MPa	Load to 16 MPa, Unload to 0.1 MPa

* This specimen was added to the test plan at the end of 2007.

A3.2 SPECIMEN PREPARATION

All the specimens were compacted to a target dry density of ~1650 kg/m³ with a target degree of saturation of approximately 95%. The HCB specimens were fabricated from 80-mesh granules of Wyoming bentonite (MX80). Dry Wyoming bentonite (MX80) was placed in a small beaker and solution was added slowly using a syringe to achieve uniform gravimetric water content and to avoid lumps during the mixing process. Compared to mixing of the HCB with distilled water, mixing with 250 g/L NaCl was easier with less formation of lumps.

The target mass compacted in the cell was calculated based on the target dry density and degree of saturation. This target mass was added to the cell and the gravimetric water content analysis was made from the remaining specimen mixture. The specimen was compacted in one lift in the oedometer ring with a hydraulic press (target thickness ~10-mm). The actual initial thickness was measured using callipers by measuring the piston stick-up of the cell. Filter papers and filter stones were installed on the top and bottom of the specimen. Finally, the specimen assembly was installed in the oedometer frame.

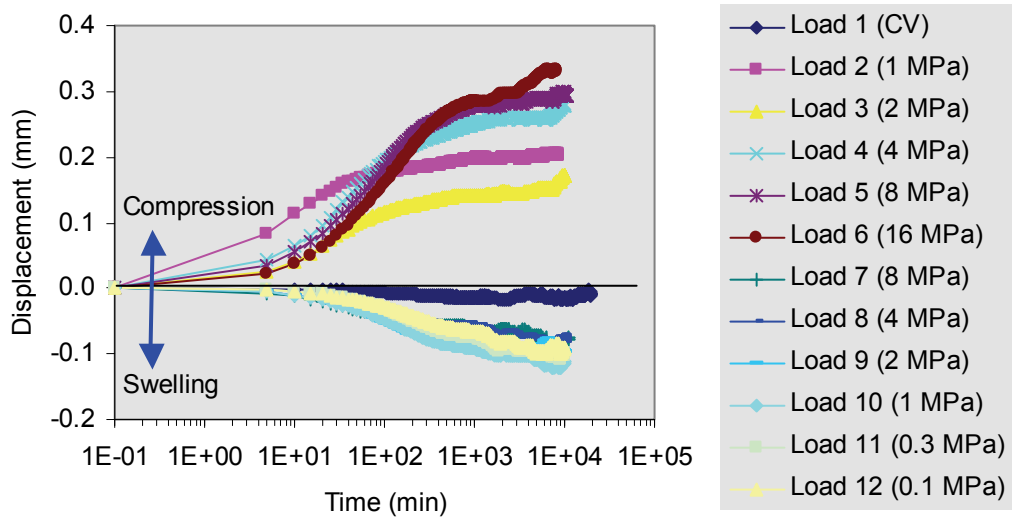
For specimens HCB12 and HCB15, a constant pressure load of 1 MPa was applied to settle the specimen assembly. The specified fluid was added to the reservoir after that. For specimens HCB13, HCB14 and HCB14A with the initial constant volume boundary condition during initial saturation, the servo-hydraulic testing system was set to zero strain and a small vertical stress of approximately 0.1 MPa was initially applied. After fluid was added to the reservoir, the load on the piston increased due to the constrained swelling of the specimen. Table A2 shows the initial gravimetric water content, height and dry density of the five specimens.

Table A2: Initial Properties of the Highly Compacted Bentonite (HCB) Specimens

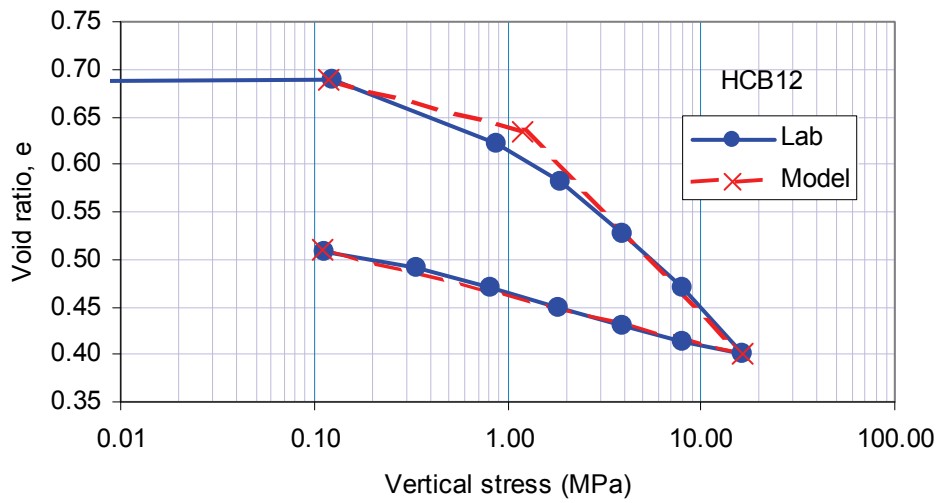
Test	Gravimetric Water Content (%)	Height (mm)	Dry Density (Mg/m³)
HCB12	20.8	10.07	1.63
HCB13	20.8	9.96	1.64
HCB14	22.2	9.92	1.68
HCB14A	24.1	10.00	1.65
HCB15	22.2	10.36	1.64

A4. RESULTS

Test results of the specimens HCB12, HCB13, HCB14, HCB14A and HCB15 are plotted in Figures A1 to A5 including displacement versus time and void ratio (e) versus vertical stress. Using these figures, the mechanical and hydraulic parameters can be calculated.

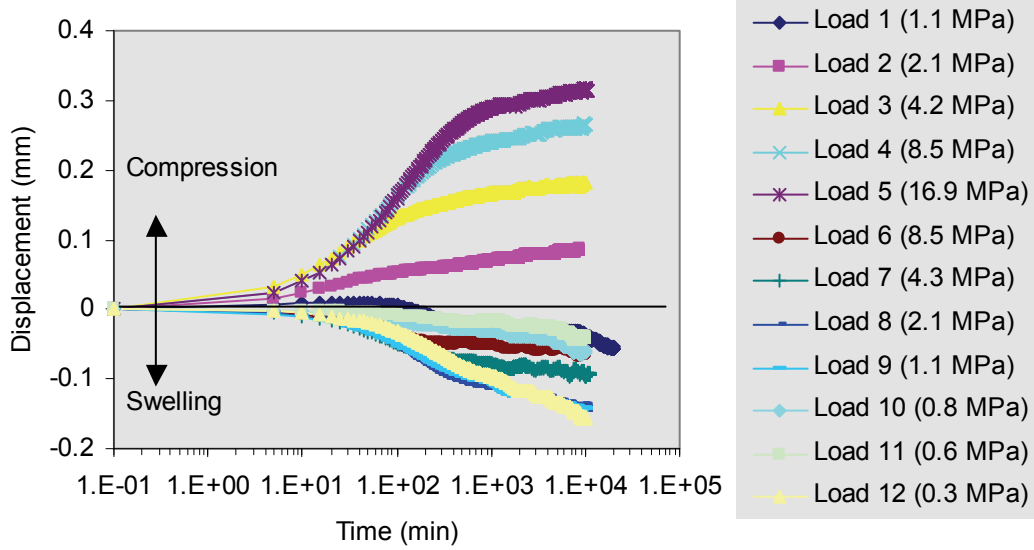


(a) Void Ratio versus Vertical Stress

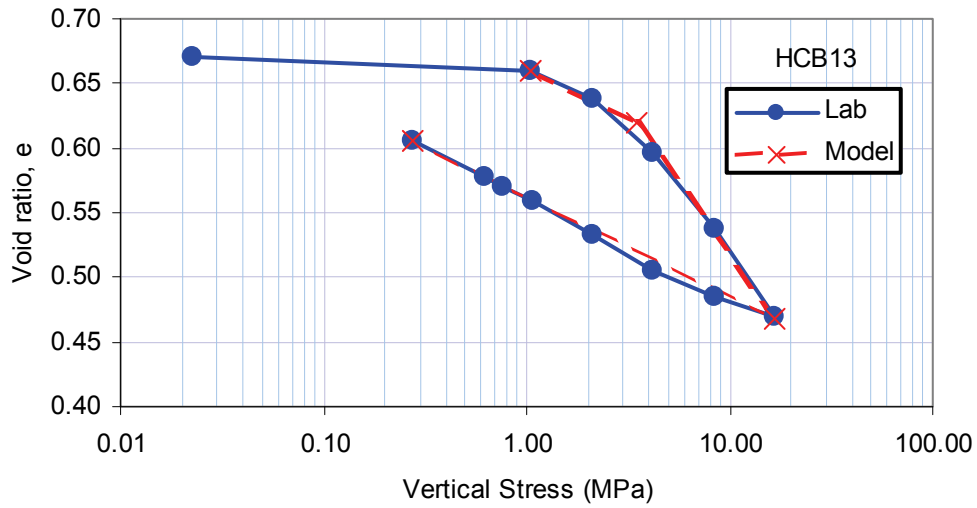


(b) Displacement versus Time in Log Scale

Figure A1: Specimen HCB12

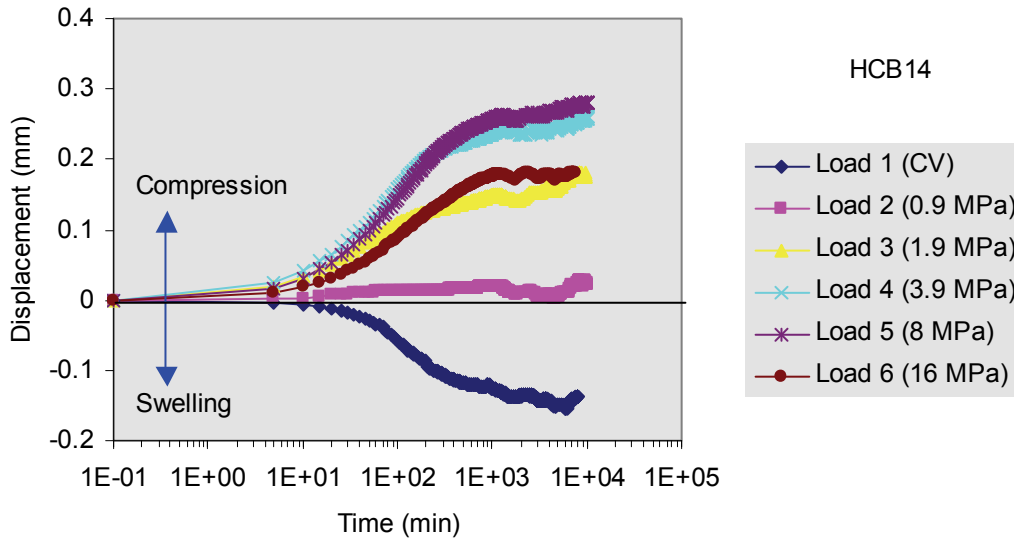


(a) Void Ratio versus Vertical Stress

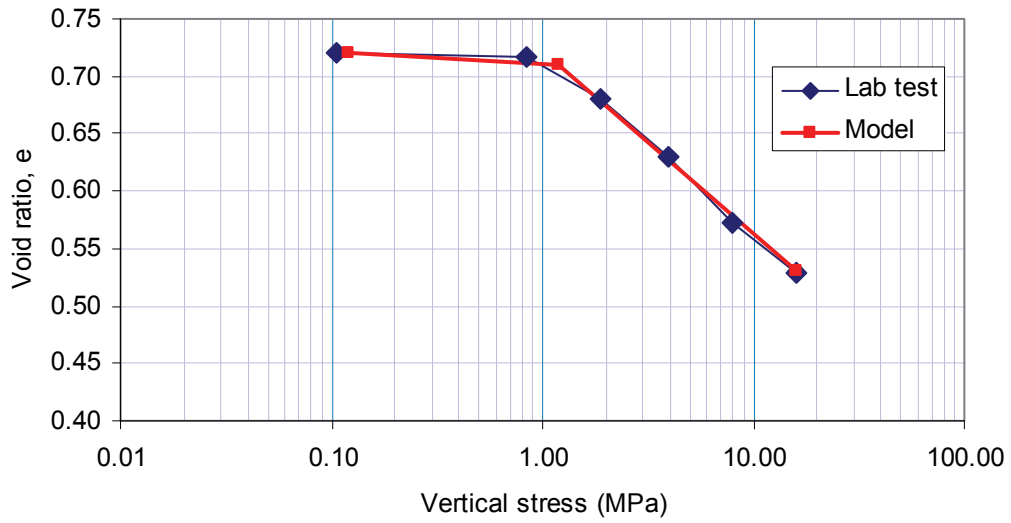


(b) Displacement versus Time in Log Scale

Figure A2: Specimen HCB13

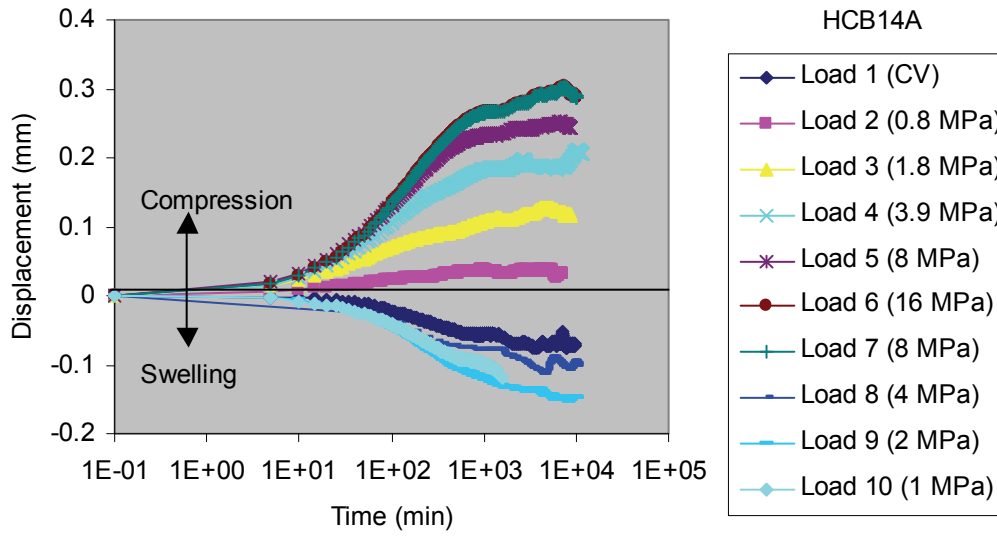


(a) Void Ratio versus Vertical Stress

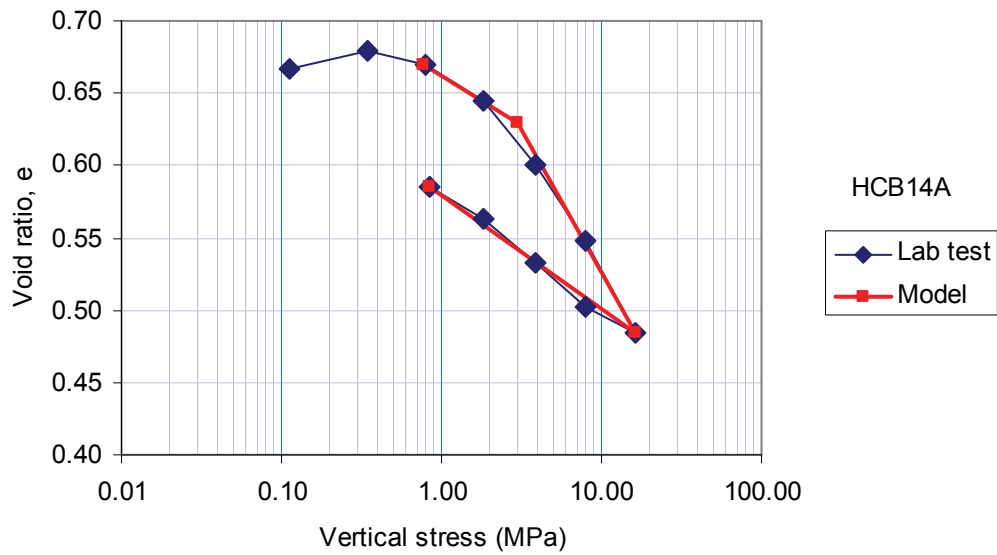


(b) Displacement versus Time in Log Scale

Figure A3: Specimen HCB14

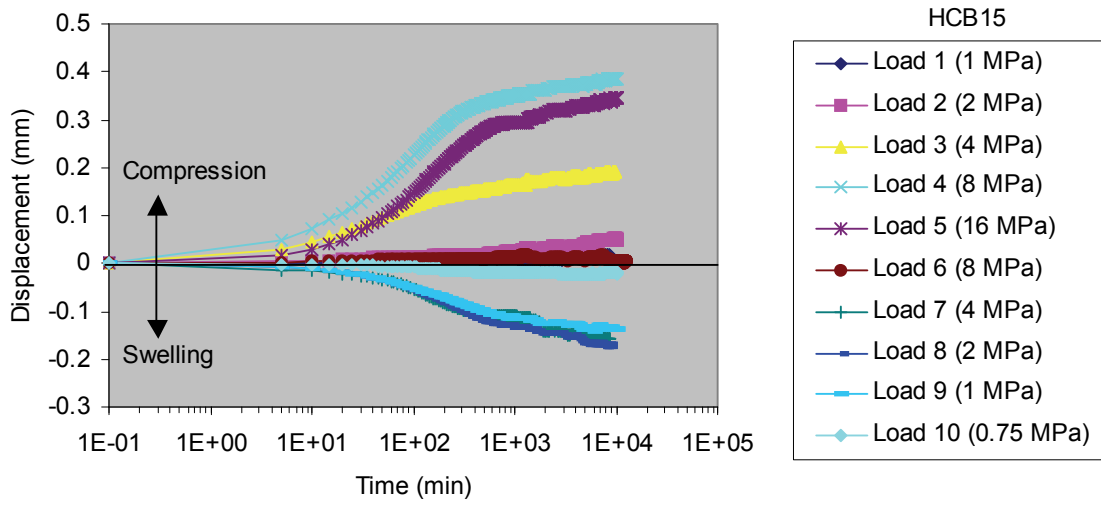


(a) Void Ratio versus Vertical Stress

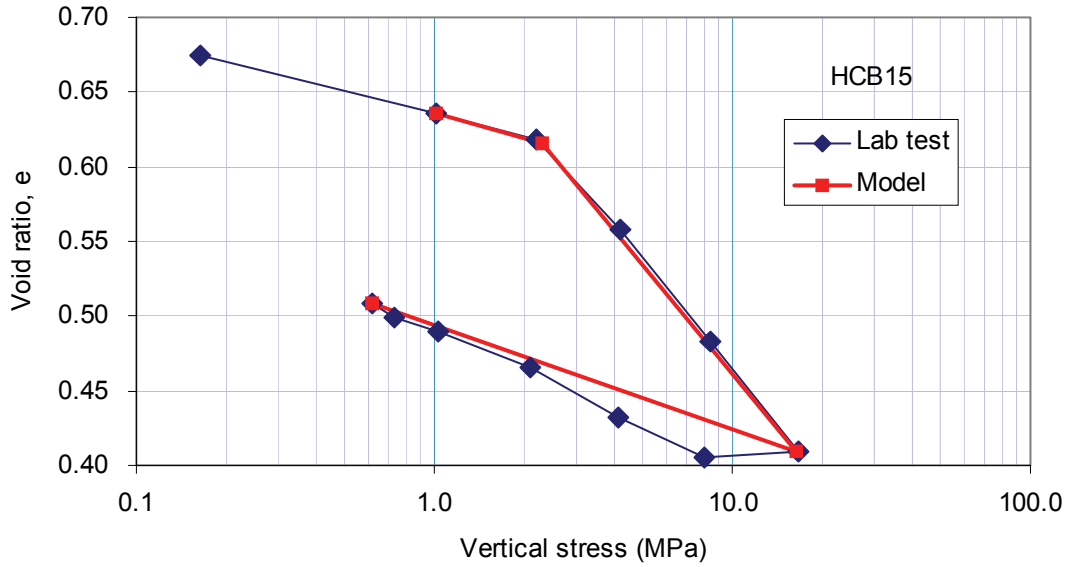


(b) Displacement versus Time in Log Scale

Figure A4: Specimen HCB14A



(a) Void Ratio versus Vertical Stress



(b) Displacement versus Time in Log Scale

Figure A5: Specimen HCB15

A5. DISCUSSION

The compression index (C_c), swelling index (C_s), consolidation stress (σ_c) and void ratio corresponding to the consolidation stress ($e(\sigma_c)$) are determined from the void ratio (e)-log vertical stress relationship. The definitions of C_c and C_s are illustrated in Figure 2 in the main text. Table A3 summarizes the compression and swelling indices (C_c and C_s) of HCB specimens having 250 g/L NaCl or CaCl_2 as mixing or reservoir fluids.

The HCB specimens having NaCl solutions have C_c values of approximately 0.16 to 0.24, while specimens having CaCl_2 have slightly lower C_c values of approximately 0.16 to 0.18. The HCB specimens in NaCl solutions have C_s value of approximately 0.05 to 0.08, while specimens having CaCl_2 have slightly higher values of C_s , approximately 0.06 to 0.09. There is no clear dependency of the C_c and C_s to the type of salt in the solutions. Figure A6 shows that the void ratio (e) versus vertical stress (σ_v) of specimen HCB8 is parallel to the HCB13 indicating relatively similar loading-unloading mechanical properties.

Figure A7 shows the relationship of the hydraulic conductivity (k) to Effective Montmorillonite Dry Density (EMDD) for five HCB specimens in the 2008 testing program. For specimens having 250 g/L NaCl as mixing and reservoir fluids (HCB12), specimens having constant volume (CV) boundary conditions during initial saturation have greater hydraulic conductivity (k) than those having constant pressure (CP) (HCB13). However, it is the opposite for specimens having 250 g/L NaCl as reservoir fluid, but prepared with distilled water (HCB14, HCB14A and HCB15). There is no consistency in the dependency of the hydraulic conductivity to the type of boundary conditions during initial saturation. The initial boundary conditions during initial saturation may establish the initial void ratio prior to the stress increments and cause this variation. In general, there is no clear evidence that the hydraulic conductivity is dependent on the boundary condition during initial saturation.

For similar boundary conditions during initial saturation (CV or CP) and similar reservoir fluid of 250 g/L NaCl, HCB specimen prepared with water (HCB14, HCB14A and HCB15) has lower hydraulic conductivity than HCB specimens prepared with 250 g/L NaCl solution (HCB12 and HCB13).

Table A3: 1-D Consolidation Test Matrix for HCB Specimens in 2008

Compression Index (C_c), Swelling Index (C_s), Consolidation Stress (σ_c) and Void Ratio ($e(\sigma_c)$)

Specimen	Compression index (C_c)	Swelling Index (C_s)	Consolidation Stress, σ_c (kPa)	Void Ratio $e(\sigma_c)$
HCB12 (250 g/L NaCl, CV)	0.21	0.05	1.2	0.64
HCB13 (250 g/L NaCl, CP)	0.22	0.08	3.5	0.62
HCB14 (250 g/L NaCl, DW, CV)	0.16	NA	1.2	0.71
HCB14A (250 g/L NaCl, DW, CV)	0.20	0.08	3.0	0.63
HCB15 (250 g/L NaCl, DW, CP)	0.24	0.07	2.3	0.62
HCB7 (250 g/L CaCl_2 , DW, CP)	0.16	0.09	4.0	0.74
HCB8 (250 g/L CaCl_2 , CP)	0.18	0.06	2.4	0.68

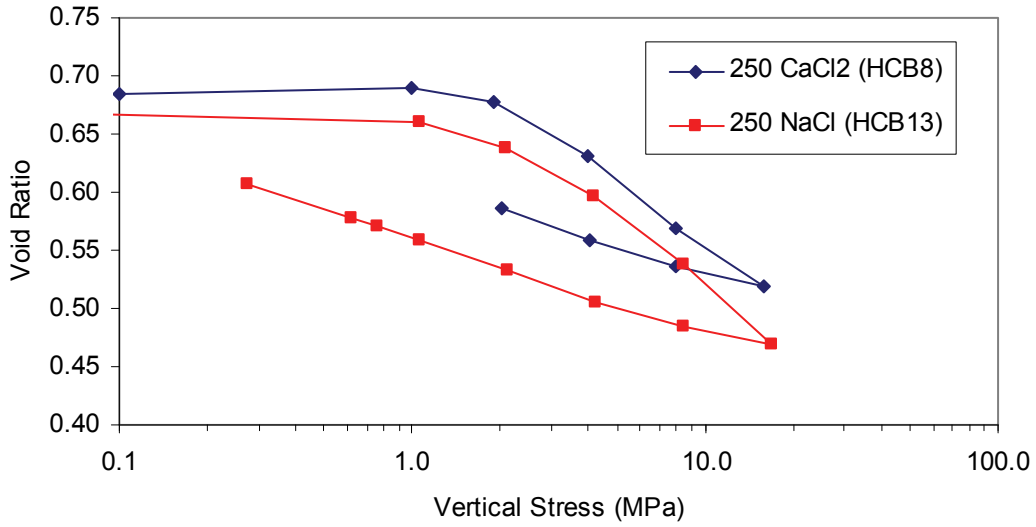


Figure A6: Void Ratio versus Vertical Stress of Specimens HCB8 and HCB13

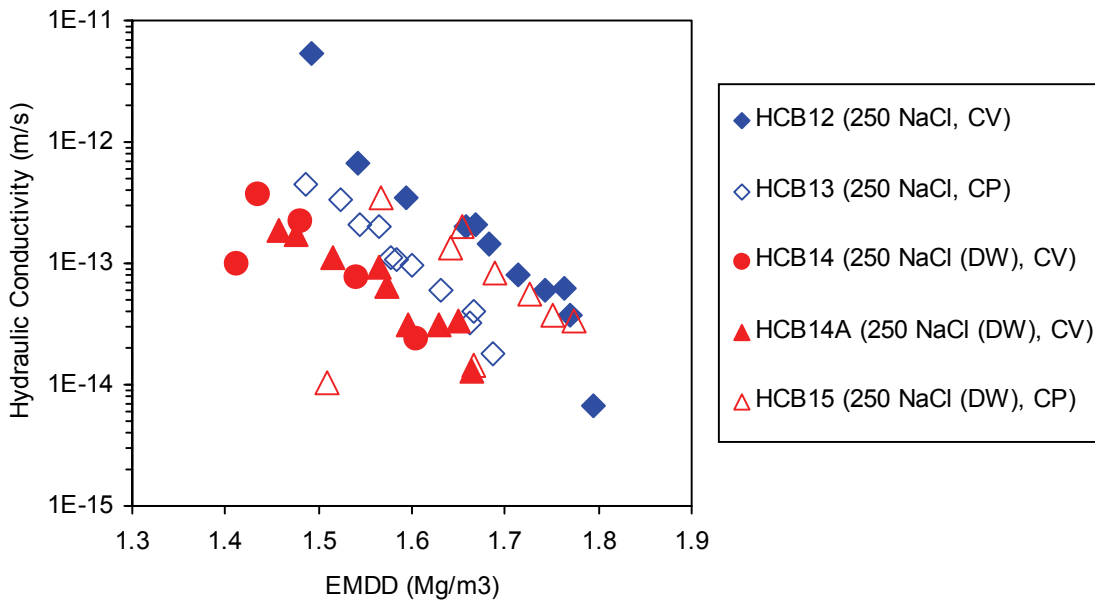
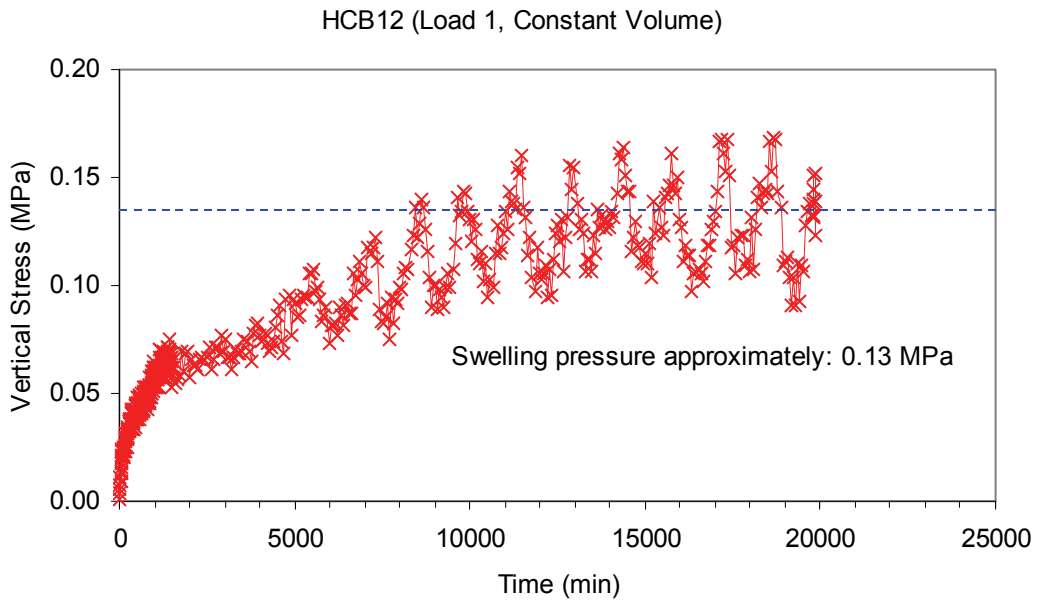


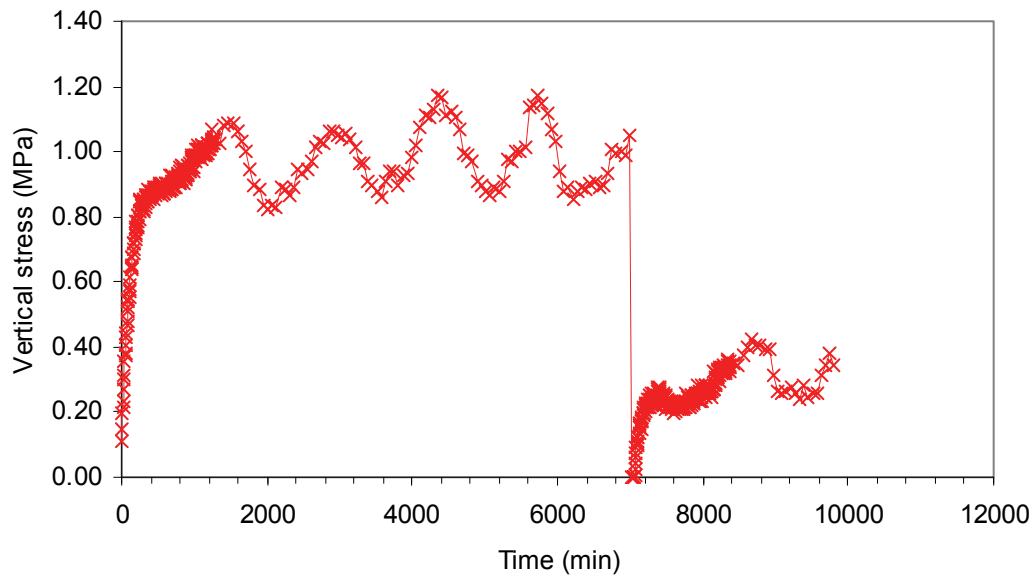
Figure A7: Hydraulic Conductivity (k) versus EMDD

Figure A8 shows the vertical stress measurements during initial saturation of specimens HCB12 and HCB14A under constant volume (CV). The stress measurements reflect the swelling pressure of the HCB. The decrease of compression and swelling indices (C_c and C_s) with an increase of concentration of salt solution indicates a decrease of swelling pressure with an increase of salt concentration. The swelling stresses for specimens HCB12 and HCB14A are approximately 0.1 MPa and 0.4 to 1 MPa. Specimen HCB14A used distilled water as mixing

fluid resulting in pore fluid salinity that is lower than 250 g/L. This resulted a higher swelling stress than specimen HCB12 having 250 g/L NaCl solution as mixing fluid.



(a) Specimen HCB12
(Mixing Fluid = Reservoir Fluid = 250 g/L NaCl Solution)



(b) Specimen HCB14A
(Mixing Fluid = Distilled Water; Reservoir Fluid = 250 g/L NaCl Solution)

Figure A8: Comparison of Swelling Stress

A6. CONCLUDING REMARKS

The following conclusions can be made based on the results of 2008 1D-consolidation tests on the HCB material:

- There is no clear dependency of the compression and swelling indices (C_c and C_s) on the type of salt in the solutions (NaCl or CaCl_2) for observed concentration of 250 g/L.
- The hydraulic conductivity is independent of the boundary condition during initial saturation.
- The HCB specimen prepared with distilled water has lower hydraulic conductivity than a similar specimen having an initial porefluid condition of 250 g/L NaCl when subsequently tested using 250 g/L NaCl as the reservoir fluid.
- For similar EMDD and initial conditions, the HCB specimen prepared using NaCl solution has higher hydraulic conductivity than the HCB specimen using CaCl_2 solution.
- In all cases, an increase of EMDD results in a decrease of hydraulic conductivity

ACKNOWLEDGEMENTS

The authors would like to acknowledge the assistance from the AECL's Underground Research Laboratory personnel supporting laboratory works, especially C-S. Kim, S. Jones, F. Johnston, K. Clarke, B. Evenden, M. Ruta, C. Kohle, T. Reimer, D. Drew and K. Avanthay.

REFERENCES

- Baumgartner, P., D.G. Priyanto, J.R. Baldwin, J.A. Blatz, B.H. Kjartanson, and H. Batenipour. 2008. Preliminary results of one-dimensional consolidation testing on bentonite clay-based sealing components subjected to two pore-liquid chemistry conditions. Nuclear Waste Management Organization (NWMO) Technical Report No. TR-2008-04. Toronto, Canada.
- Maak P. and G.R. Simmons. 2005. Deep geologic repository concepts for isolation of used fuel in Canada, Canadian Nuclear Society, Waste Management, Decommissioning and Environmental Restoration for Canada's Nuclear Activities: Current Practices and Future Needs, Ottawa May 8-11 2005.
- Priyanto, D.G., J.A. Blatz., G.A.Siemens, R. Offman, S.J. Boyle, D.A. Dixon. 2008. The effects of initial conditions and liquid composition on the one-dimensional consolidation behaviour of clay-based sealing materials. Nuclear Waste Management Organization (NWMO) Technical Report No. TR-2008-06. Toronto, Canada.
- Russell, S.B. and G.R. Simmons. 2003. Engineered barrier system for a deep geologic repository. Presented at the 2003 International High-Level Radioactive Waste Management Conference. 2003 March 30 – April 2, Las Vegas, NV.

**APPENDIX B: DETAILED DESCRIPTION:
TESTING OF DENSE BACKFILL (DBF)**

R.B. Offman¹, J.A. Blatz¹ and D.G. Priyanto²
¹University of Manitoba, ²Atomic Energy of Canada Limited

CONTENTS

	<u>Page</u>
B1. SUMMARY	55
B2. DENSE BACKFILL.....	55
B3. EQUIPMENT	55
B4. TESTING AT THE UNIVERSITY OF MANITOBA.....	55
B4.1 SPECIMEN PREPARATION.....	55
B4.2 TESTING PROCEDURES	56
B4.2.1 Free Swell Testing	56
B4.2.2 Rigidly Confined Testing	56
B4.3 SUMMARY	58
B5. TESTING AT AECL	66
B6. DISCUSSION	69
B7. CONCLUSIONS AND RECOMMENDATIONS	71
REFERENCES	72

LIST OF TABLES

	<u>Page</u>
Table B1: Dense Backfill (DBF) Specimen Names and Configurations	58

LIST OF FIGURES

	<u>Page</u>
Figure B1: Results of Specimen DBF1(08)	60
Figure B2: Results of Specimen DBF2(08)	61
Figure B3: Results of Specimen DBF3(08)	62
Figure B4: Results of Specimen DBF4(08)	63
Figure B5: Results of Specimen DBF5(08)	64
Figure B6: Results of Specimen DBF6(08)	65
Figure B7: Results of Specimen DBFS1(08)	67
Figure B8: Results of Specimen DBF1(08)	68
Figure B9: Void Ratio (e) versus Vertical Stress (σ_v) of Eight (8) Specimens	69
Figure B10: Void Ratio versus Vertical Stress for Specimen With Different Scales.....	70
Figure B11: Void Ratio versus Vertical Stress for Specimens having Different Granularities	70

B1. SUMMARY

This Appendix summarizes the results of 1D-Consolidation Tests of Dense Backfill (DBF) completed at two locations: the Geotechnical Laboratory of the University of Manitoba and AECL's geotechnical laboratory at the Underground Research Laboratory.

B2. DENSE BACKFILL

Dense Backfill (DBF) is defined as a mixture of natural glacial lake clay, crushed host rock and bentonite clay, either installed at high dry density by in-situ compaction or prefabricated as blocks. The DBF in this study composed of 75% (by weight) crushed granite, 18.75% crushed illite clay (Sealbond) and 6.25% (by weight) Avonlea bentonite (montmorillonite content ~80%). This material is similar to the "backfill" material used in AECL's large scale Buffer Container Experiment (BCX) (Dixon et al. 2002).

B3. EQUIPMENT

Two different sizes of specimens were used to test the DBF.

1. Large cells, 101-mm-in-diameter, allowing a 101-mm-thick specimen, are used to test the DBF. This size is needed to accommodate the large size of the aggregate (i.e., up to 35-mm granite chips). These cells were used to test the DBF at the University of Manitoba.
2. Small cells, 50-mm-diameter consolidation cells that allow 40-mm-thick specimens, were added to test the DBF in 2008. Replacement of the largest size component of the aggregate with a smaller-sized aggregate allowed conventional dead-weight-type oedometers to be used as a loading system. A LVDT was connected to a data logger to measure the displacement of the specimen. These cells were used to test the DBF at AECL's geotechnical laboratory.

B4. TESTING AT THE UNIVERSITY OF MANITOBA

B4.1 SPECIMEN PREPARATION

The specimens were prepared in the laboratory from the dense backfill (DBF) material provided by AECL. Specimens were prepared by first separating out the fines from the rocks and rock chips by putting the soil mixture through a 2.38 mm sieve. The fines were pulverized and remixed with the rocks and rock chips. Following drying, the soil specimen was mixed with predetermined fluids (either distilled water, 250 g/L CaCl₂ or 250 g/L NaCl) to produce an initial gravimetric water content of 11.3%. The procedure from previous experiments (Baumgartner et al. 2008, Appendix B) was followed. The target moisture content was approximately 10.6% when the specimens were placed in the oedometers.

The mixing procedure was completed as follows: Mix in mixing fluid (~2 min); Compact and scarify (~2 min); Mix (~6 min); Compact (~1 min); Scarify (~2 min); Light mixing (~2 min). The mixed soil was sealed in plastic bags and placed in a fridge for two days to equilibrate.

The soil was then compacted into the ring in four equal lifts of 237 g, with a target height of 2 inches and diameter of 4 inches. (The mass per lift was calculated assuming a dry density of the soil equal to 2100 kg/m³.)

B4.2 TESTING PROCEDURES

The procedure for determining the gravimetric water content was done as per ASTM D 2216-05 (2005). The calculations for determining the final dry density excluding the CaCl₂ and NaCl solution were used as shown in Baumgartner et al. (2008).

B4.2.1 Free Swell Testing

Free swell tests were conducted on two specimens prepared in the lab. The tests were labelled according to the test matrix received from AECL with the specified “mixing fluid”. The specimen number and preparation description for each test are shown below.

- Test 1: Specimen No. 003
 - Mixing Fluid – 250 g/L CaCl₂
 - Reservoir Fluid - 250 g/L CaCl₂
- Test 2: Specimen No. 004
 - Mixing Fluid - Distilled Water
 - Reservoir Fluid - 250 g/L CaCl₂

Swell testing was conducted in general accordance with Method A from ASTM D 4546 (2003). In both tests, the inundation fluid was 250g/L CaCl₂. Following the swell phase, each test underwent the load-unload-load cycle provided by AECL. The only deviation from this procedure occurred at loading step two of Test 1 when the data became abruptly constant. To ensure that the top cap had not become bound, the load was quickly removed and the top cap was inspected. The inspection showed that the top cap rotated freely and was therefore not bound. Following this inspection, the load was replaced and no additional movement was observed.

The large oedometer constructed specifically for testing DBF specimens (Baumgartner et al. 2008) was used in these tests.

B4.2.2 Rigidly Confined Testing

Confined tests were conducted on four specimens prepared in the lab. The tests were labelled according to the test matrix received from AECL with the specified “mixing fluid”. The specimen number and preparation description for each test are shown below.

- Test 3: Specimen No. 005
 - Mixing Fluid - 250g/L CaCl₂
 - Reservoir Fluid - 250 g/L CaCl₂
- Test 4: Specimen No. 006
 - Mixing Fluid - Distilled Water
 - Reservoir Fluid - 250 g/L CaCl₂

- Test 5: Specimen No. 007
 - Mixing Fluid - 250g/L NaCl
 - Reservoir Fluid - 250 g/L NaCl

- Test 6: Specimen No. 008
 - Mixing Fluid - Distilled Water
 - Reservoir Fluid - 250 g/L NaCl

Rigidly confined testing was carried out in general accordance with ASTM D 2435-04 (2004). These tests were inundated with the reservoir solution listed above.

Tests 3 and 4 were loaded according to the modified loading schedule provided by AECL on 2008 February 14. The tests were loaded as shown below:

- Load to: 1 MPa, 2 MPa, 4 MPa
- Unload to: 2 MPa, 1 MPa, 0.5 MPa, 200 kPa, 75 kPa
- Load to: 1 MPa, 2 MPa, 4 MPa

Tests 5 and 6 were loaded according to the loading schedule supplied by AECL specifically for the tests involving NaCl. The loading schedule for these tests is shown below.

- Load to: 1 MPa, 2 MPa, 4 MPa
- Unload to: 2 MPa, 1 MPa, 0.5 MPa

This objective of this modification was to observe the behaviour of the DBF during loading on the smaller stress that was suspected to be different based on the results of 1D-consolidation tests on the bentonite-sand mixtures with different composition (N. A. Chandler, personal communication, 2007). It was discovered that there were no changes in the behaviour of the DBF for loading less than 75 kPa. Consequently, the numbers of the load increments were reduced again for Tests 5 and 6.

The specimens from Tests 1 to 6 were renamed to simplify the discussion of these specimens. Table B1 shows these names with the mixing and reservoir fluids, boundary condition during initial saturation and loading sequences.

The duration of each loading sequence for the DBF tests at the U of M is in the range of 2 days to 1 month. Due to the size of specimen, the time to reach initial saturation could be up to 1 month. After specimen was saturated, the duration of each load increment was reduced. The load was changed, when the time was greater than t_{90} from the square-root time method (i.e., ASTM Standard D 2435-04 (2004)).

Table B1: Dense Backfill (DBF) Specimen Names and Configurations

Specimen Name	U of Manitoba Label	Mixing Fluid	Reservoir Fluid	Boundary Condition during Initial Saturation	Loading sequence
DBF1(08)*	Test 1: Specimen No. 003	250 g/L CaCl ₂	250 g/L CaCl ₂	Free swell	Load to 1, 2, 4 MPa, Unload to 2, 1, 0.5 MPa; and Load to 1, 2, 4 MPa.
DBF2(08)*	Test 2: Specimen No. 004	Distilled Water	250 g/L CaCl ₂	Free swell	Load to 1, 2, 4 MPa, Unload to 2, 1, 0.5 MPa; and Load to 1, 2, 4 MPa.
DBF3(08)*	Test 3: Specimen No. 005	250 g/L CaCl ₂	250 g/L CaCl ₂	Rigidly Confined	Load to 1, 2, 4 MPa, Unload to 2, 1, 0.5, 0.2, 0.075 MPa; and Load to 1, 2, 4 MPa.
DBF4(08)*	Test 4: Specimen No. 006	Distilled Water	250 g/L CaCl ₂	Rigidly Confined	Load to 1, 2, 4 MPa, Unload to 2, 1, 0.5, 0.2, 0.075 MPa; and Load to 1, 2, 4 MPa.
DBF5(08)*	Test 5: Specimen No. 007	250 g/L NaCl	250 g/L NaCl	Rigidly Confined	Load to 1, 2, 4 MPa, Unload to 2, 1, 0.5 MPa
DBF6(08)*	Test 6: Specimen No. 008	Distilled Water	250 g/L NaCl	Rigidly Confined	Load to 1, 2, 4 MPa, Unload to 2, 1, 0.5 MPa
DBFS1(08)**	N/A	Distilled Water	250 g/L NaCl	Constant Stress	Load up to 1.6 MPa; Unload to 0.070 MPa.
DBFS2(08)**	N/A	250 g/L NaCl	250 g/L NaCl	Constant Stress	Load up to 1.6 MPa; Unload to 0.070 MPa.

* Tests at the University of Manitoba; ** Tests at AECL.

B4.3 SUMMARY

Results from tests of Specimens DBF1(08) to DBF6(08) are summarized below. Due to the nature of this project, in contrast to ASTM D 4546-03 (2003) percent heave, swell pressure (σ_{sp}), corrected swell pressure (σ'_{sp}), compression index (C_c), and the swell index (C_s) for the specimens tested are not reported. The U of M provided the electronic files of all tests completed, while the interpretation of these parameters was left to the discretion of AECL.

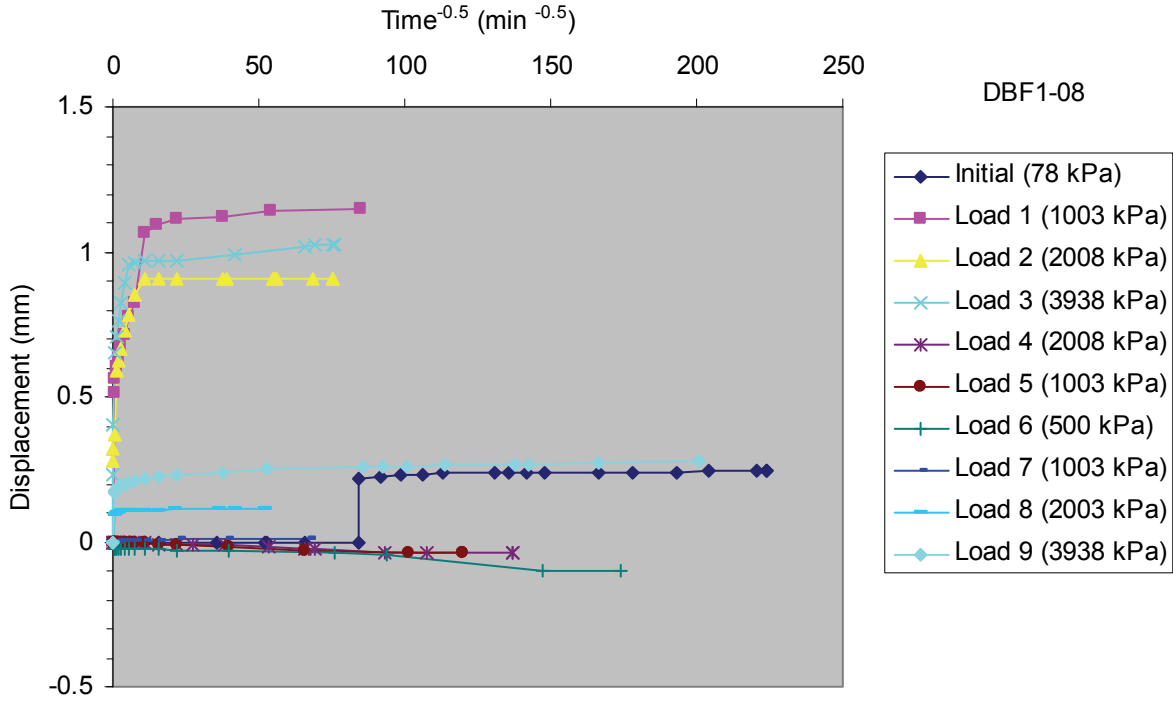
Figure B1 and Figure B2 show displacement versus square root of time and void ratio versus vertical stress in log scale for Specimens DBF1(08) and DBF2(08) (the two free swell tests), respectively. The initial vertical stress portion of the plots denotes the free swell phase of the test. Following the free swell, the specimens underwent the load-unload-load cycle.

Figure B3 and Figure B4 show displacement versus square root of time and void ratio (e) versus vertical stress (σ_v) in log scale for Specimens DBF3(08) and DBF4(08) (free swell tests),

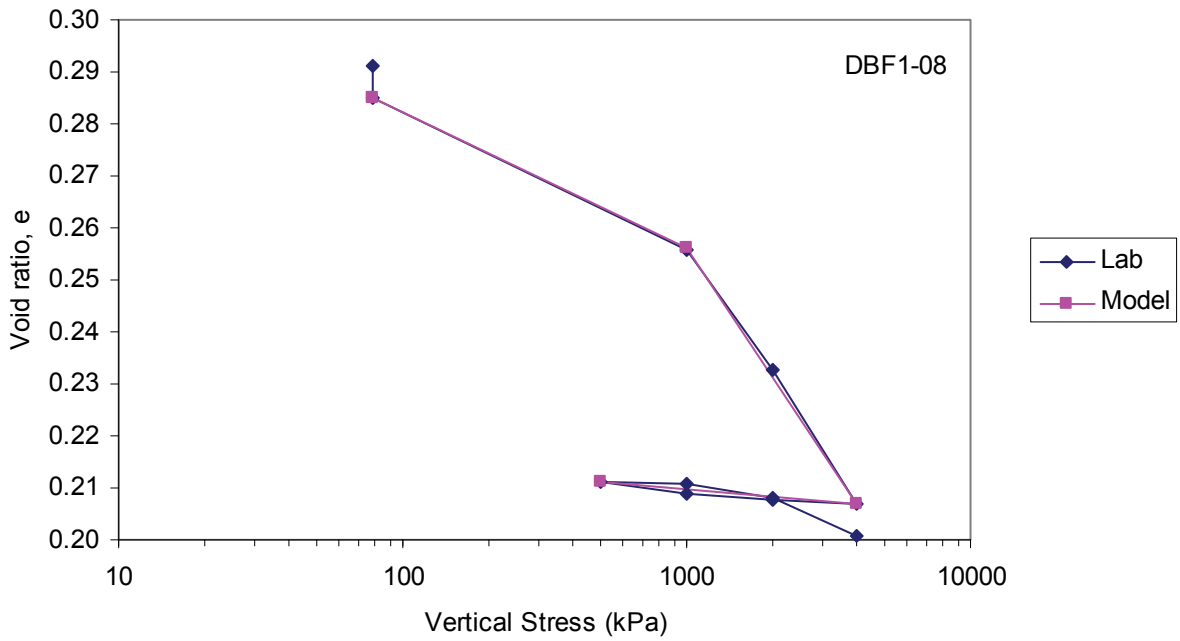
respectively. The initial vertical stress portion of the plots denotes the free swell phase of the test. Following the free swell, the specimens underwent the load-unload-load cycle.

Figure B5 and Figure B6 show displacement versus square root of time and void ratio (e) versus vertical stress (σ_v) in log scale for Specimens DBF5(08) and DBF6(08) (free swell tests), respectively. These specimens were loaded according to their individual loading schedules provided to us by AECL.

It should be noted that the specific gravity used for these tests was estimated at 2.7, which was used for all testing reported. Further, it should be emphasized that the results given in this report are only valid for the specimens tested. Any differences that might occur between values measured from these specimens and values of swell pressure, percent heave or water contents that occur in the field are not the responsibility of the University of Manitoba.

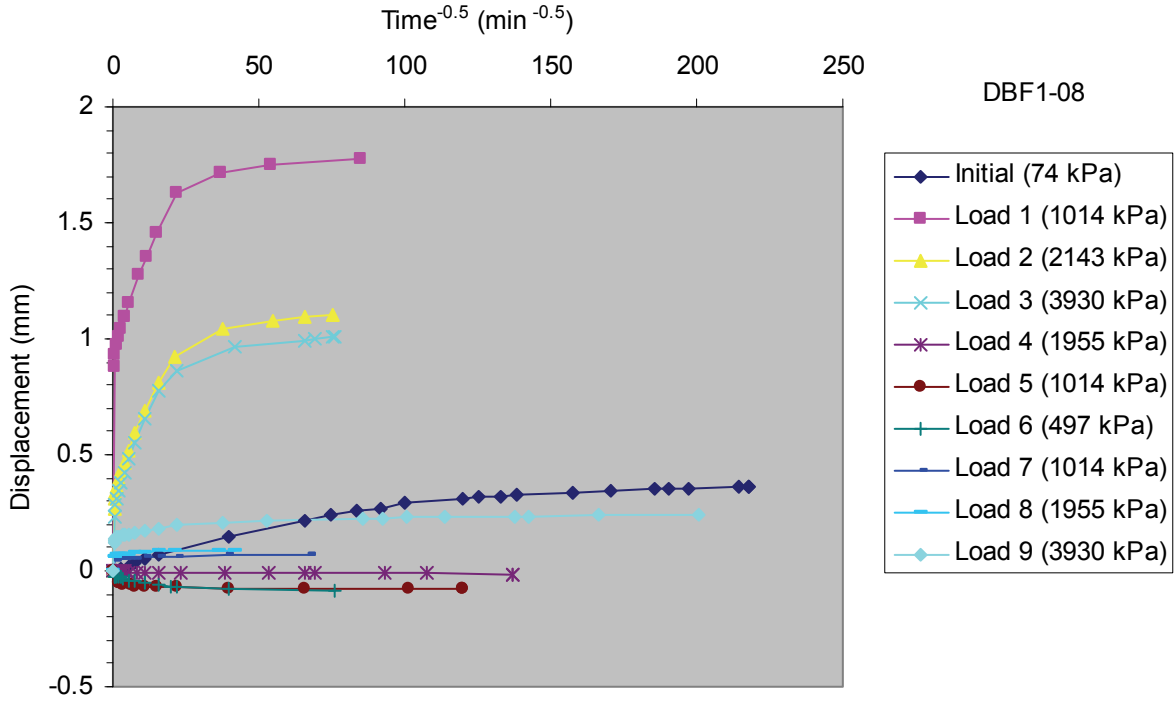


(a) Displacement versus Square Root of Time

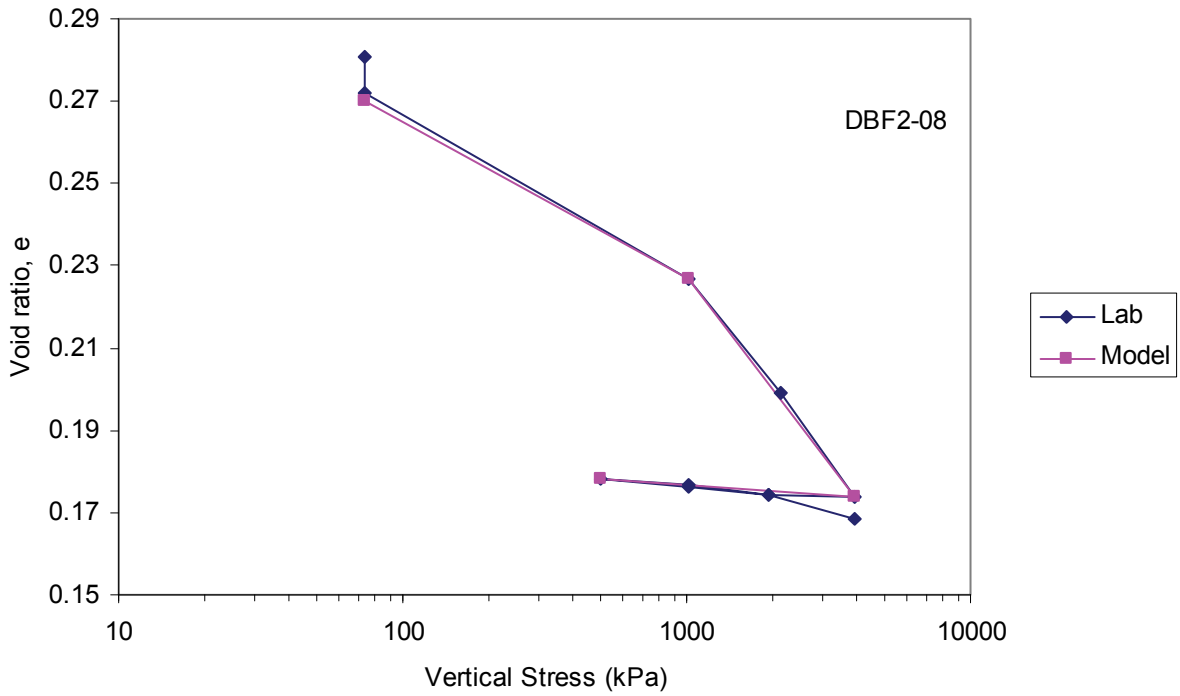


(b) Void Ratio versus Vertical Stress

Figure B1: Results of Specimen DBF1(08)

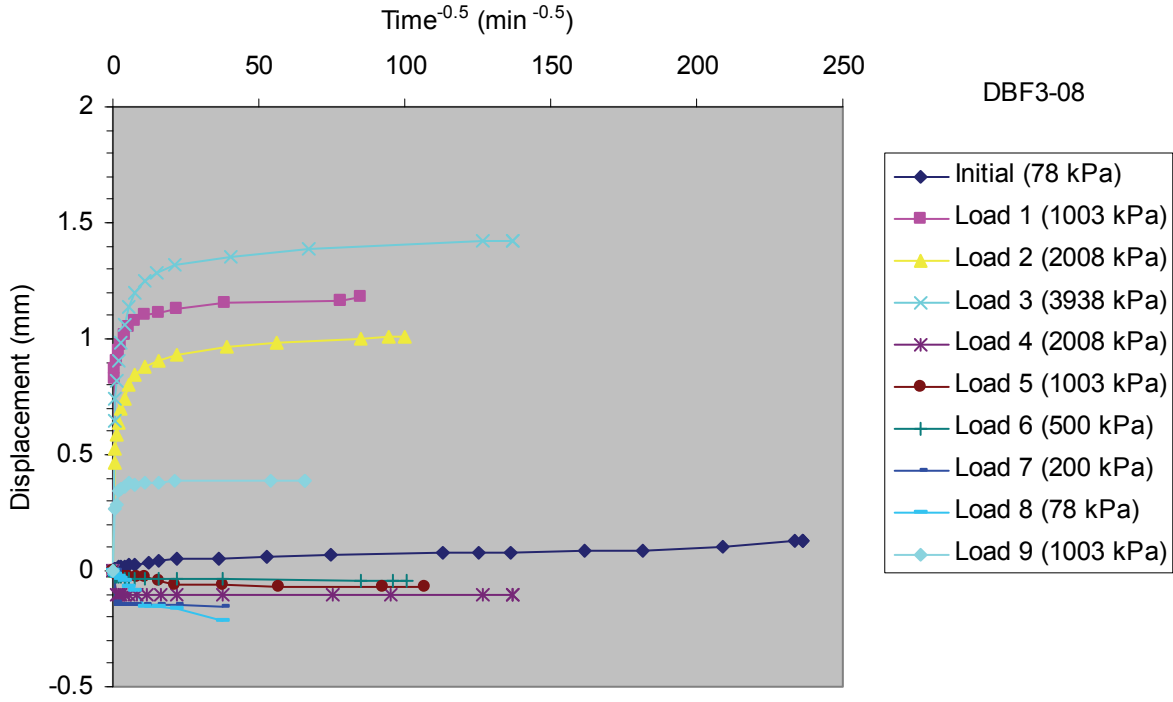


(a) Displacement versus Square Root of Time

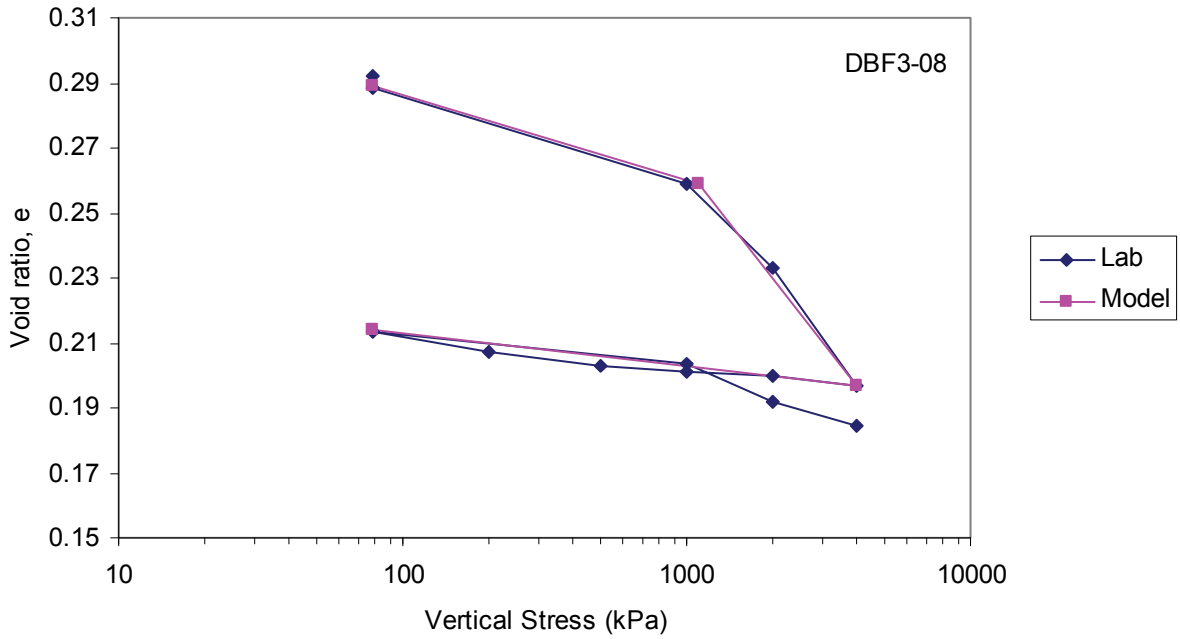


(b) Void Ratio versus Vertical Stress

Figure B2: Results of Specimen DBF2(08)

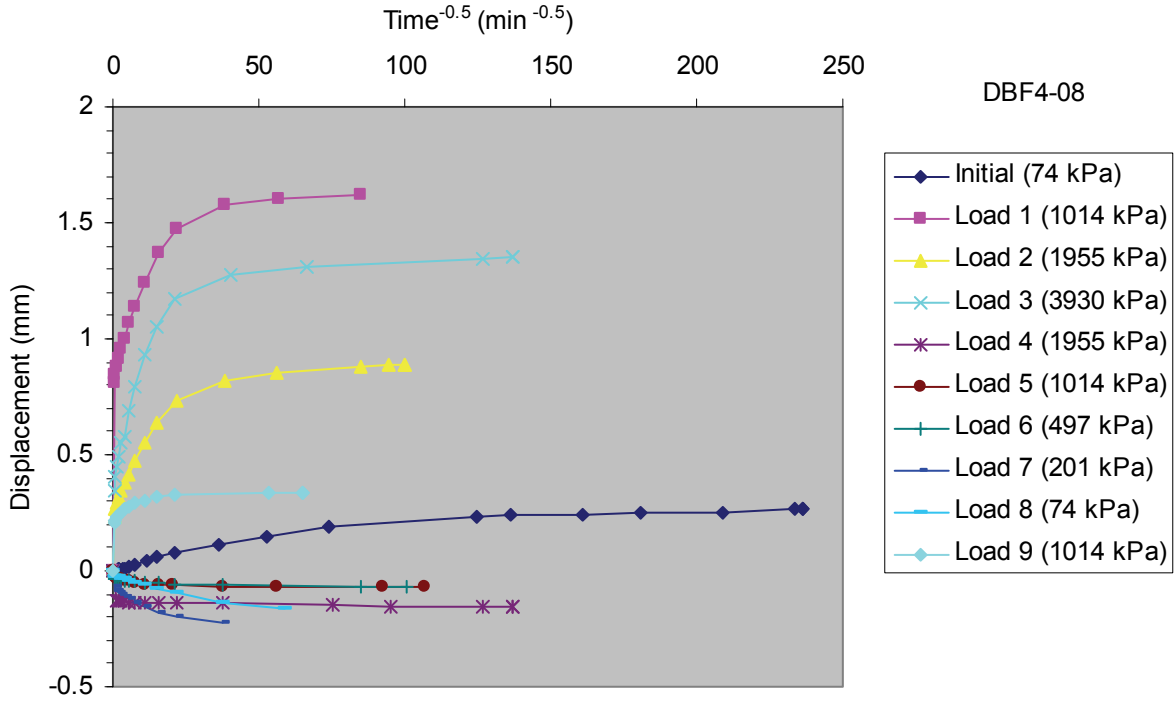


(a) Displacement versus Square Root of Time

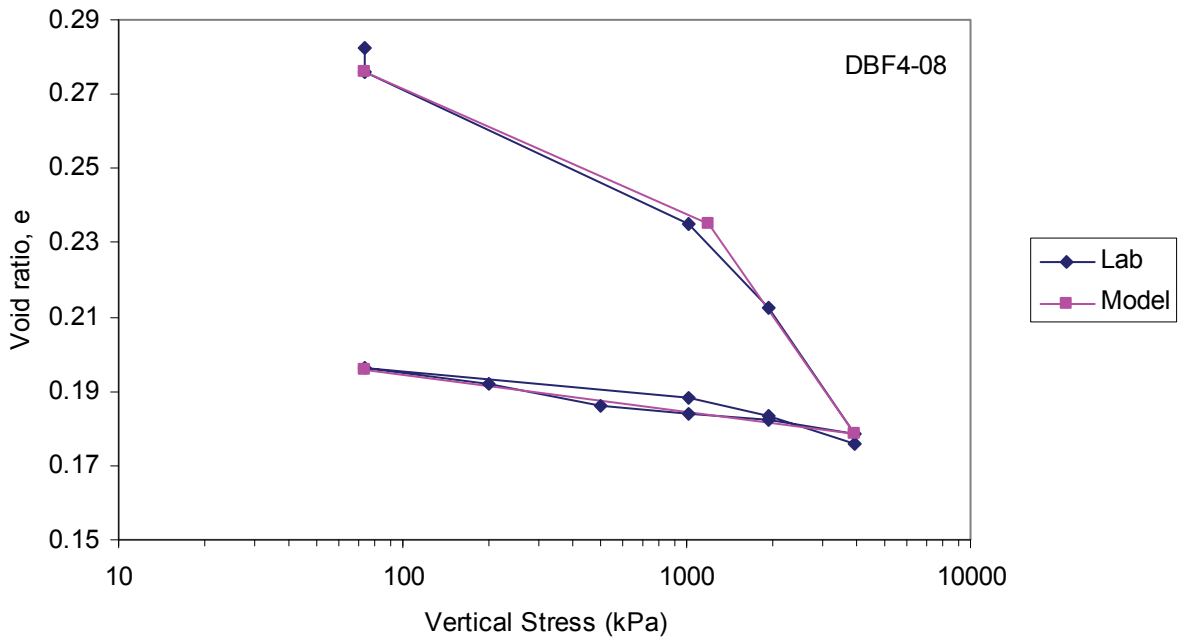


(b) Void Ratio versus Vertical Stress

Figure B3: Results of Specimen DBF3(08)

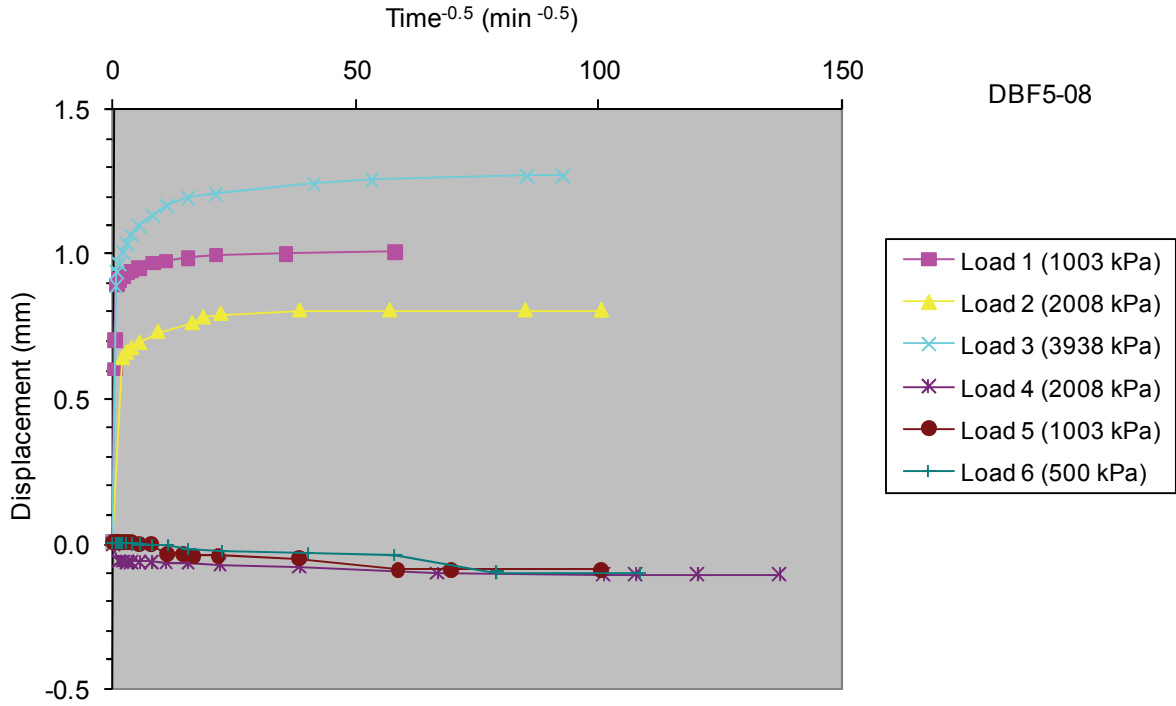


(a) Displacement versus Square Root of Time

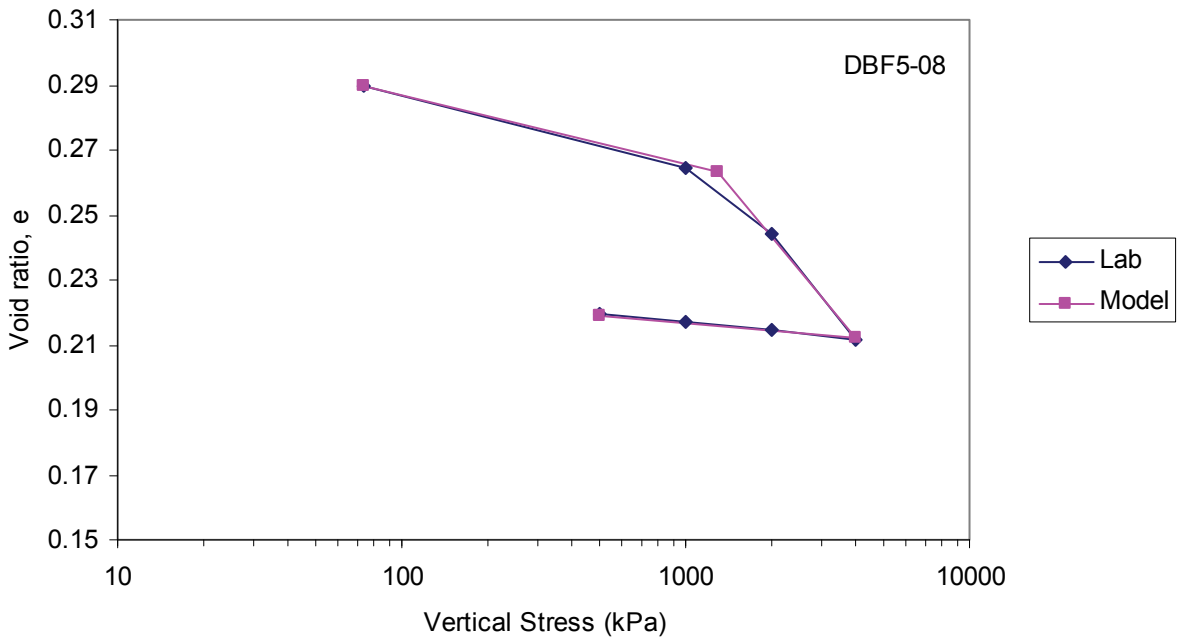


(b) Void Ratio versus Vertical Stress

Figure B4: Results of Specimen DBF4(08)

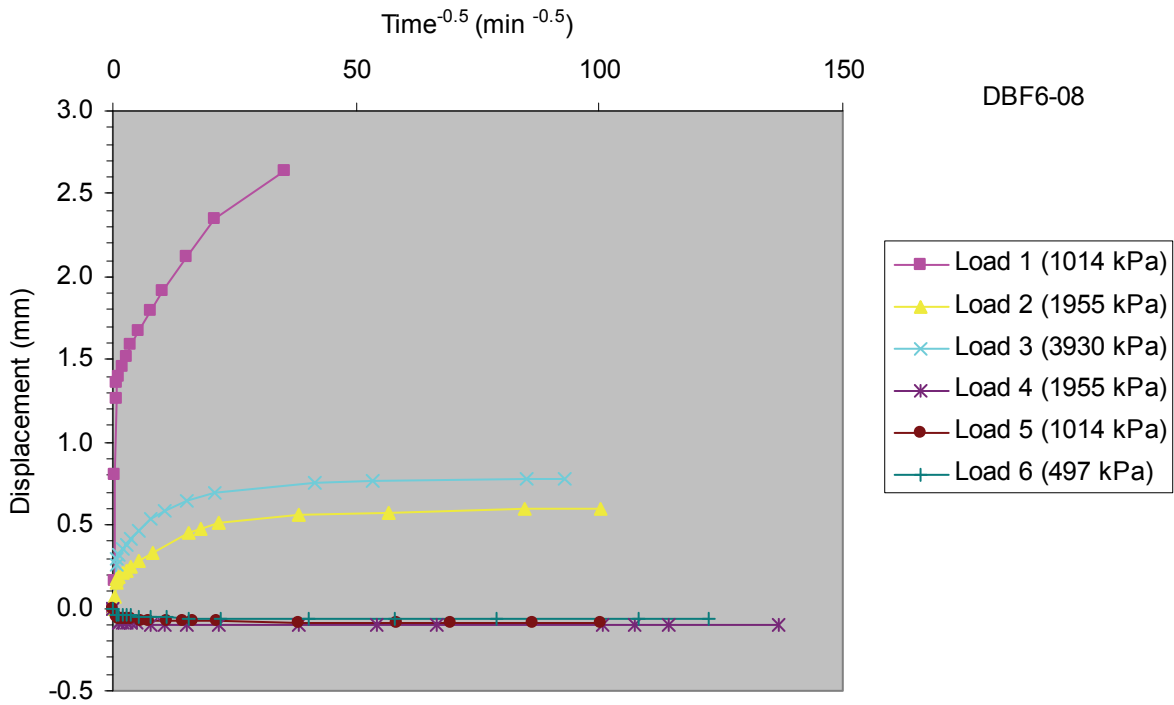


(a) Displacement versus Square Root of Time

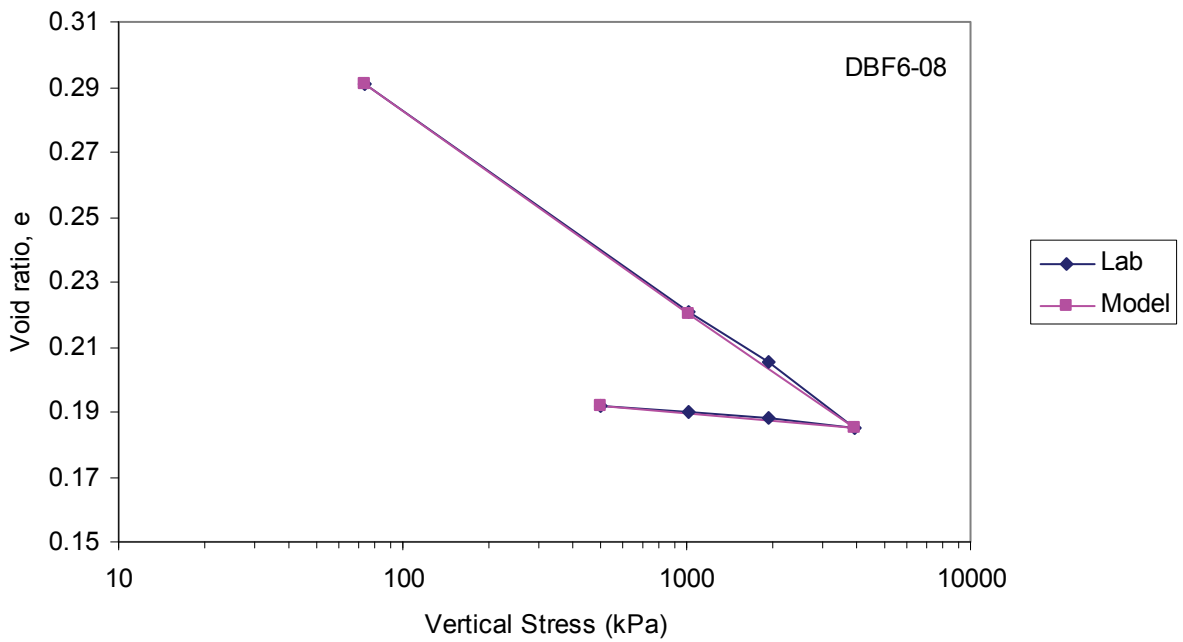


(b) Void Ratio versus Vertical Stress

Figure B5: Results of Specimen DBF5(08)



(a) Displacement versus Square Root of Time



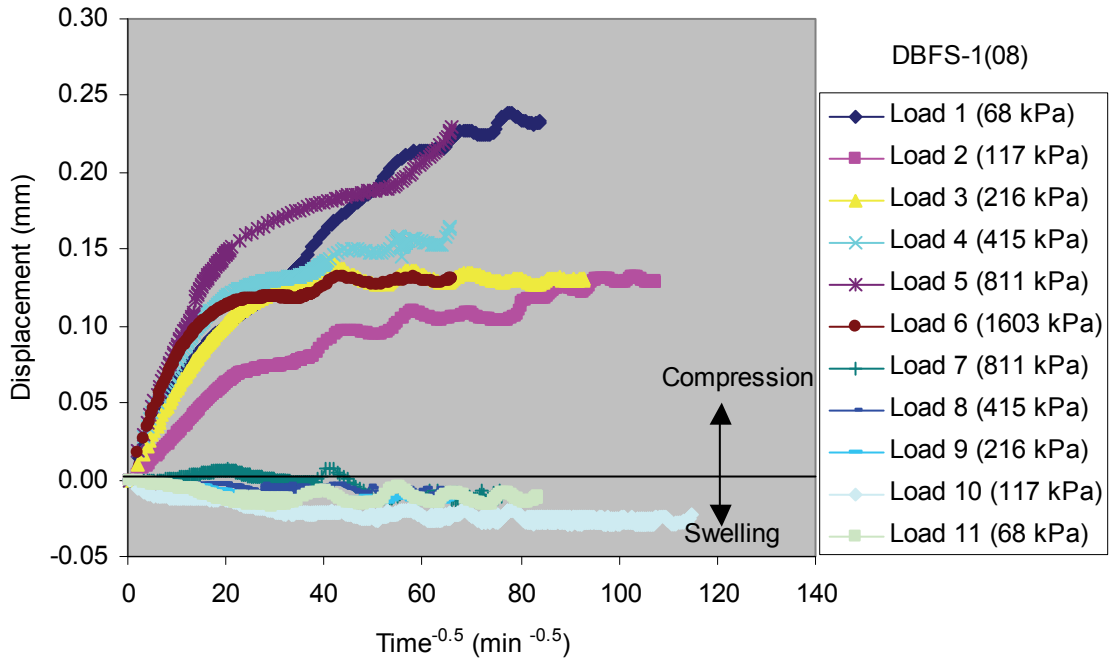
(b) Void Ratio versus Vertical Stress

Figure B6: Results of Specimen DBF6(08)

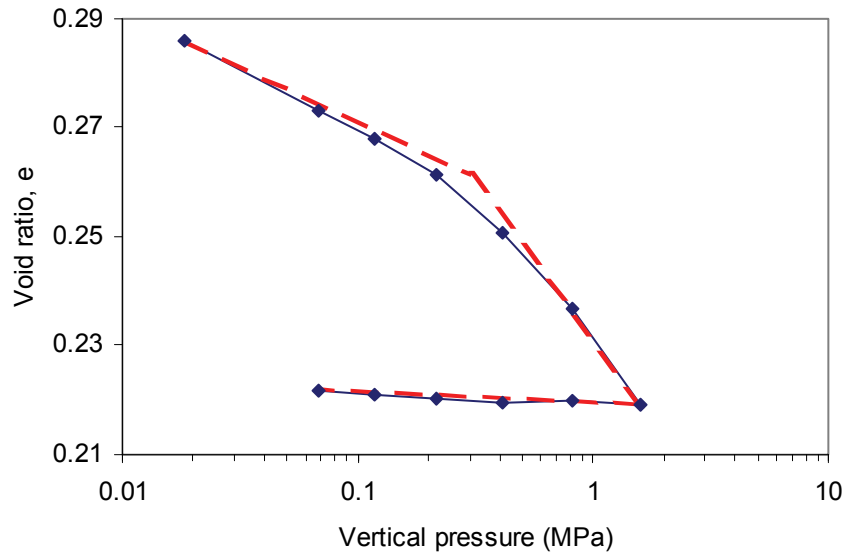
B5. TESTING AT AECL

Two additional oedometer cells were added at AECL in 2008 to test the Dense Backfill (DBF) materials. The specimens were smaller than those at the University of Manitoba having a 50-mm-diameter and 40-mm-height. Prior to the compaction of the specimens, DBF material of the type used at the U of M was oven dried and crushed using a small rock-crusher to accommodate testing using smaller oedometer cells. Grinding the DBF mixture resulted in different grain size distribution, but it did not change the material composition. As this process did not affect the proportion of very fine (clay-sized) material present, it was not likely to cause a substantial change in the 1D-consolidation behaviour of the mixture. The objectives of using smaller specimens were to investigate scale effects and reduce the consolidation time. The minimum stress that could be achieved using smaller cells was less than that using larger cells.

Two specimens were tested in 2008 with configurations shown in Table B1. These tests include specimens DBFS1(08) and DBFS2(08) using Distilled Water and 250 g/L NaCl solution. The displacement versus square root of time and void ratio versus vertical stress for Specimens DBFS1(08) and DBFS2(08) are shown in Figure B7 and Figure B8, respectively. The maximum stresses applied in the test were lower than those done at the University of Manitoba.

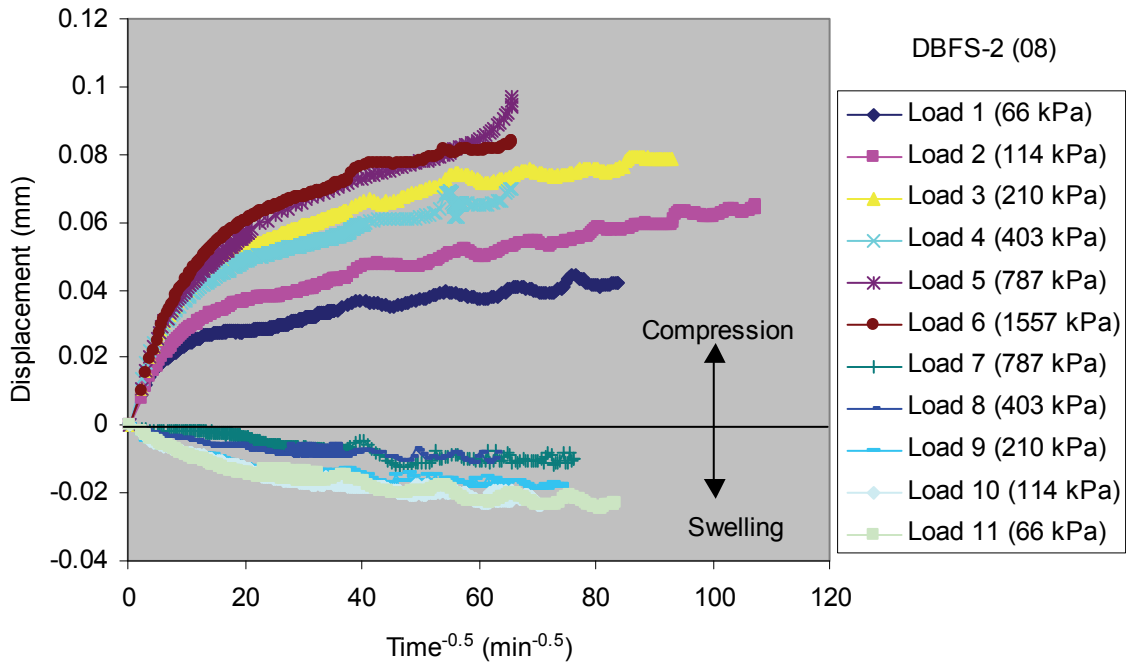


(a) Displacement versus Square Root of Time

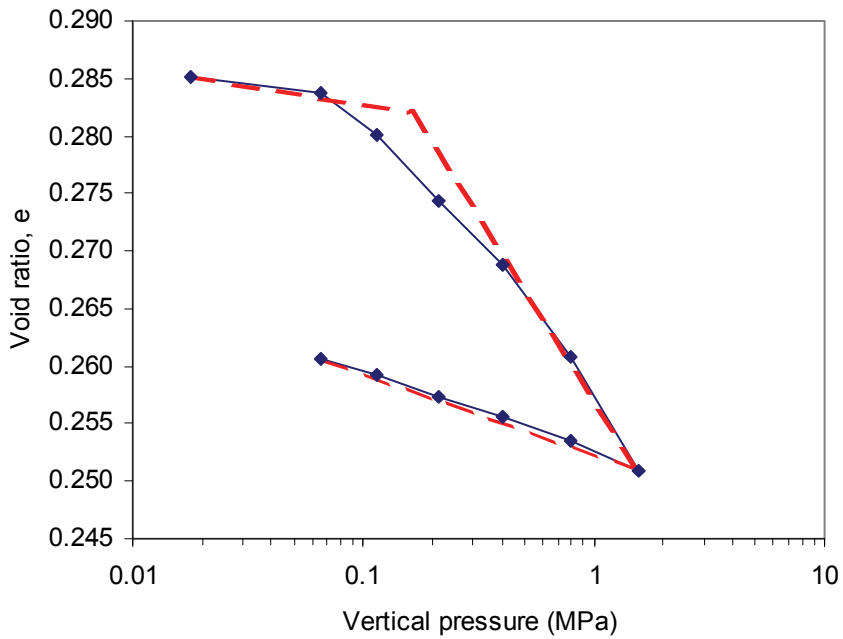


(b) Void Ratio versus Vertical Stress

Figure B7: Results of Specimen DBFS1(08)



(a) Displacement versus Square Root of Time



(b) Void Ratio versus Vertical Stress

Figure B8: Results of Specimen DBF1(08)

B6. DISCUSSION

Figure B9 shows the void ratio (e) versus vertical stress (σ_v) in log scale of the eight (8) specimens completed in 2008. The compression and swelling indices (C_c and C_s) of each specimen are interpreted and shown in Table 5 in the main document.

The effects of DBF specimen size are shown in Figure B10. Specimens DBF6(08) and DBFS1(08) having distilled water as a mixing fluid and 250 g/L NaCl as reservoir fluid, the $e - \sigma_v$ of both specimens are relatively matched to each other, similarly for Specimens DBF5(08) and DBFS2(08) having 250 g/L NaCl as mixing and reservoir fluid. This comparison indicates that the $e - \sigma_v$ relationship of the DBF specimen is relatively independent of the specimen size for specimens having similar fluid composition and initial dry density. Using smaller DBF specimen enables investigating up to lower vertical stress to determine the pre-consolidation stress.

For each load increment, the hydraulic conductivity of the DBF were determined from time-displacement relationship and summarized in Table 8. Figure B11 shows the hydraulic conductivity versus EMDD of the DBF5(08), DBF6(08), DBFS1(08) and DBFS2(08). The hydraulic conductivity is relatively similar for specimens with different scales (1×10^{-14} to 1×10^{-11} m/s). In both scales, the specimens mixed with distilled water (DBF6(08) and DBFS1(08)) have higher EMDD than specimens mixed with 250 g/L NaCl solution.

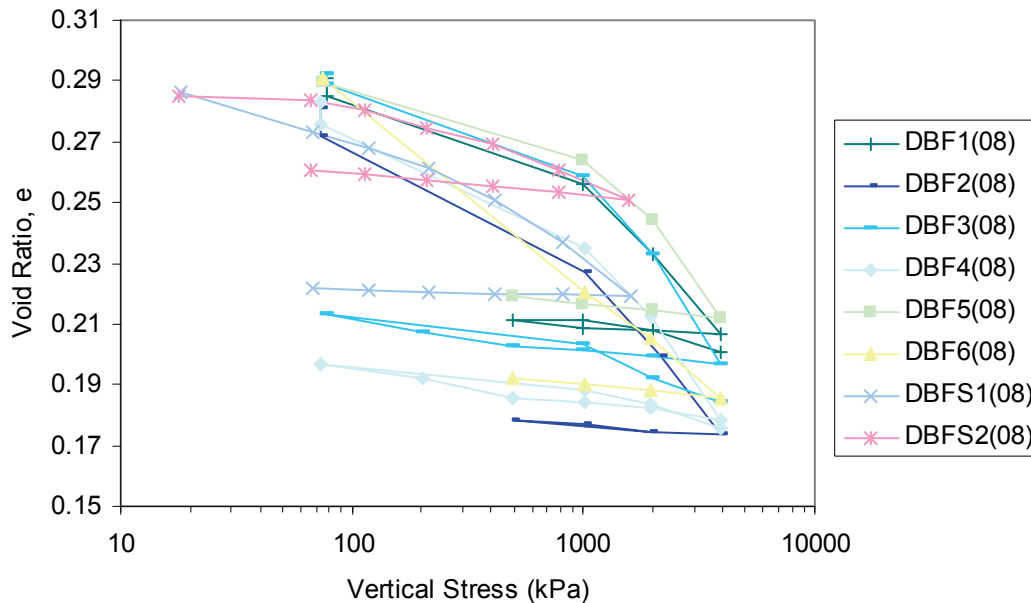
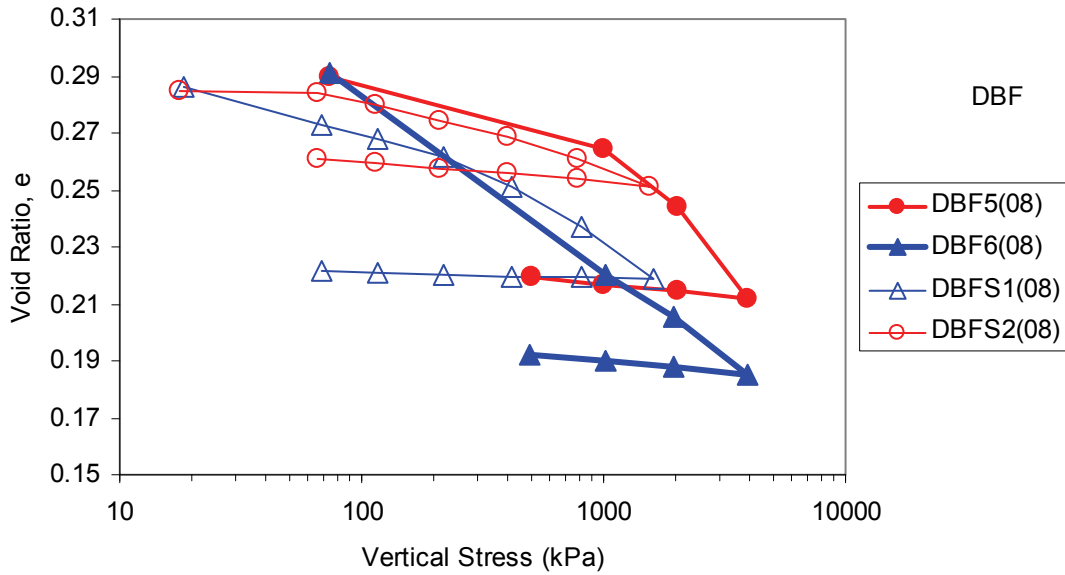
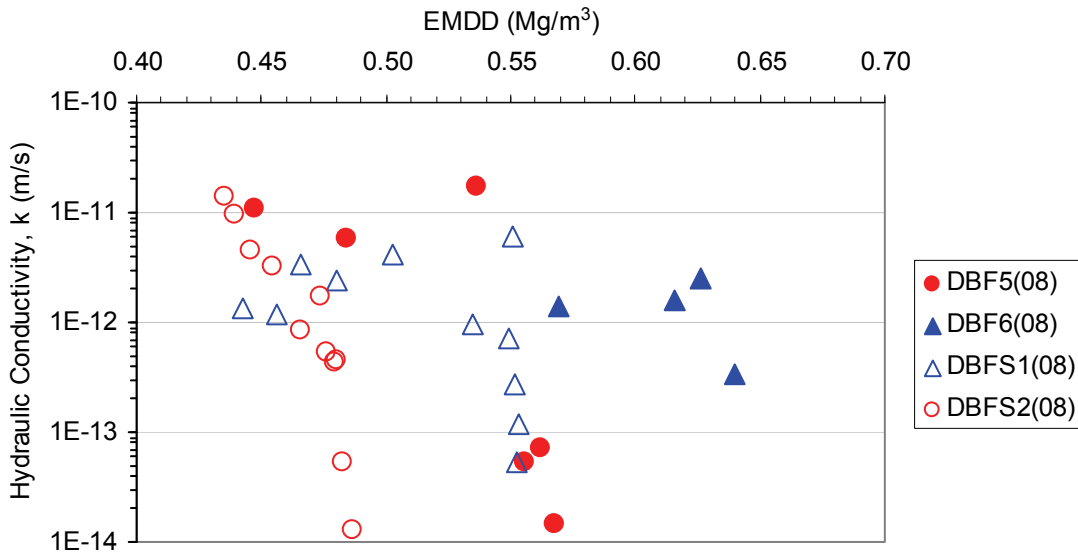


Figure B9: Void Ratio (e) versus Vertical Stress (σ_v) of Eight (8) Specimens



- DBF5(08)_Mixing: 250 g/L NaCl_Reservoir: 250 g/L NaCl; Large Scale
- DBF6(08)_Mixing: Distilled Water_Reservoir: 250 g/L NaCl; Large Scale
- DBFS1(08)_Mixing: Distilled Water_Reservoir: 250 g/L NaCl; Small Scale
- DBFS2(08)_Mixing: 250 g/L NaCl_Reservoir: 250 g/L NaCl; Small Scale

Figure B10: Void Ratio versus Vertical Stress for Specimen With Different Scales



- DBF5(08)_Mixing: 250 g/L NaCl_Reservoir: 250 g/L NaCl; Large Scale
- DBF6(08)_Mixing: Distilled Water_Reservoir: 250 g/L NaCl; Large Scale
- DBFS1(08)_Mixing: Distilled Water_Reservoir: 250 g/L NaCl; Small Scale
- DBFS2(08)_Mixing: 250 g/L NaCl_Reservoir: 250 g/L NaCl; Small Scale

Figure B11: Void Ratio versus Vertical Stress for Specimens having Different Granularities

B7. CONCLUSIONS AND RECOMMENDATIONS

The 1D-consolidation testing of the DBF have been completed using three types of fluids (i.e., distilled water, 250 g/L CaCl₂, and 250 g/L NaCl). Two different sizes of specimens were used in testing program. These different size specimens have similar material composition, but different pore-size distribution. The following conclusions and recommendations can be made based on results of the tests.

- The comparison of two different sizes of specimens indicates that the $e - \sigma_v$ relationship of the DBF specimen is relatively independent of the specimen size for specimens having similar fines content, mineralogic composition, fluid composition and initial dry density. However, the permeability of the DBF is dependent on the specimen size.
- Testing the DBF materials using smaller scale specimens is valuable in investigating the loading-unloading behaviour under lower stress, which cannot be investigated using larger scale tests.
- It is suggested for future work to increase the maximum stress used in the smaller-scale tests that would be comparable with the larger-scale tests. It would also provide valuable information on the behaviour of these materials under load conditions that might be encountered in a repository.

REFERENCES

- ASTM (ASTM International). 2003. Standard test methods for one-dimensional swell or settlement potential of cohesive soils. Standard D 4546-03, ASTM International, West Conshohocken, Pennsylvania, USA.
- ASTM (ASTM International). 2004. Standard test methods for one-dimensional consolidation properties of soils using incremental loading. Standard D 2435-04, ASTM International, West Conshohocken, Pennsylvania, USA.
- ASTM (ASTM International). 2005. Standard test method for laboratory determination of water (moisture) content of soil and rock by mass. Standard D 2216-05, ASTM International, West Conshohocken, Pennsylvania, USA.
- Baumgartner, P., D.G. Priyanto, J.R. Baldwin, J.A. Blatz, B. H. Kjartanson, and H. Batenipour. 2008. Preliminary results of one-dimensional consolidation testing on bentonite clay-based sealing components subjected to two pore fluid chemistry conditions. Nuclear Waste Management Organization (NWMO) Technical Report No. TR-2008-04. Toronto, Canada.
- Dixon, D., N. Chandler, J. Graham, and M.N. Gray. 2002. Two large-scale sealing tests conducted at Atomic Energy of Canada's underground research laboratory: the buffer-container experiment and the isothermal test. *Canadian Geotechnical* 39, 503-518.

**APPENDIX C: DETAILED DESCRIPTION OF TESTS:
LIGHT BACKFILL (LBF)**

S. Powell (Boyle) and G. Siemens
Royal Military College of Canada

CONTENTS

	<u>Page</u>
C1. INTRODUCTION	75
C1.1 LBF.....	75
C2. LBF OEDOMETER TESTING.....	75
C2.1 LBF TEST DESCRIPTION.....	75
C2.2 LBF TEST PROCEDURE	75
C2.2.1 Sodium Chloride Solution.....	75
C2.2.2 LBF	76
C3. LBF TEST RESULTS	77
C3.1 INDIVIDUAL TEST RESULTS	77
C3.2 COMPARISON OF MIXING AND RESERVOIR CONDITIONS	85
C4. SUMMARY	86
C5. CONCLUSIONS AND RECOMMENDATIONS	86
ACKNOWLEDGEMENTS	87
REFERENCES	87

LIST OF TABLES

	<u>Page</u>
Table C1: Actual Testing Matrix for LBF 1-D Consolidation Testing.....	76
Table C2: Properties of NaCl Solutions Used	76
Table C3: Initial Properties of LBF Specimens.....	77
Table C4: Compression and Swelling Indices	84

LIST OF FIGURES

	<u>Page</u>
Figure C1: LBF_1 a) Change in void ratio vs. pressure b) Specimen displacement vs. square root of time (Mixing Fluid = Reservoir Fluid = 250 g/L NaCl).....	78
Figure C2: LBF_2 a) Change in void ratio vs. pressure b) Specimen displacement vs. square root of time (Mixing Fluid = Distilled Water, Reservoir Fluid = 250 g/L NaCl)	79
Figure C3: LBF_3 a) Change in void ratio vs. pressure b) Specimen displacement vs. square root of time (Mixing Fluid = Distilled Water, Reservoir Fluid = 100 g/L NaCl)	80
Figure C4: LBF_4 a) Change in void ratio vs. pressure b) Specimen displacement vs. square root of time (Mixing Fluid = Reservoir Fluid = 100 g/L NaCl).....	81
Figure C5: LBF_5 a) Change in void ratio vs. pressure b) Specimen displacement vs. square root of time (Mixing Fluid = Distilled Water, Reservoir Fluid = 50 g/L NaCl)	82
Figure C6: LBF_6 a) Change in void ratio vs. pressure b) Specimen displacement vs. square root of time (Mixing Fluid = Reservoir Fluid = 50 g/L NaCl).....	83
Figure C7: Calculation of Compression and Swelling Indices.....	84
Figure C8: Void Ratio Comparison for Tests in Distilled Water	85
Figure C9: Void Ratio Comparison for Tests in Sodium Chloride (NaCl) Solution	86

C1. INTRODUCTION

This report summarizes the laboratory procedures used and results obtained from the one-dimensional (1D) consolidation testing of Light Backfill (LBF). Light Backfill (LBF) is one of the proposed engineered barrier components for the Deep Geologic Repository (DGR) concept (Russell and Simmons 2003; Gierszewski et al. 2004; Maak and Simmons 2005). The testing program consisted of six specimens with changes to the pore fluid chemistry. This testing is part of the ongoing work being undertaken to determine parameters for Hydraulic-Mechanical modelling of LBF by the Atomic Energy of Canada (AECL). The LBF was tested at Royal Military College of Canada (RMC).

C1.1 LBF

Light Backfill (LBF) is a clay based sealing-system component, proposed for the use in the proposed DGR. LBF is composed of 50% (by dry weight) of sand-sized aggregate and 50% of sodium bentonite (Russell and Simmons 2003). The Bentonite Sand Buffer (BSB) removed upon completion of the Buffer/Container Experiment (Dixon et al. 2002) was used to prepare the LBF mixture. As received from AECL, this LBF mixture was reconditioned and compacted to specified gravimetric water content and dry density.

C2. LBF OEDOMETER TESTING

C2.1 LBF TEST DESCRIPTION

The LBF material used in the following tests was dry and crushed when it arrived at the Royal Military College of Canada (RMC). Fluid was added to the material, using a spray bottle to achieve even distribution, to obtain target gravimetric water content of 19.1%. The mixing fluid used is specified in Table C1. The material was then mixed thoroughly. Once the target gravimetric water content was achieved, a predetermined quantity of material was placed into the oedometer ring and compacted to a target dry density of 1.3 Mg/m³. Two Wykeham Farrance Model 24001, rear-loading consolidation frames were used to conduct the 1D oedometer tests. Standard 50-mm-diameter and 19-mm-high, consolidation rings were used. Six specimens were tested according to the testing matrix, shown in Table C1.

C2.2 LBF TEST PROCEDURE

C2.2.1 Sodium Chloride Solution

Four different fluids (distilled water, 250 g/L NaCl, 100 g/L NaCl and 50 g/L NaCl solutions) were used during the course of this testing. Properties of each of the solutions can be found in Table C2. For the 250 g/L NaCl solution, 250 g of NaCl was mixed with distilled water until 1L of solution was obtained. The 100g/L solution was obtained by diluting the existing 250g/L NaCl from previous tests. In this case, 400 mL of 250 g/L NaCl was mixed with distilled water until 1L of solution was achieved. Prior to dilution the concentration of the 250g/L solution was verified. Following dilution, the concentration of the 100g/L solution was also verified. For the 50g/L NaCl solution, 50g of NaCl with distilled water until 1L of solution was obtained. To

minimize evaporation and maintain a constant concentration, the solutions were stored in sealed containers.

Table C1: Actual Testing Matrix for LBF 1-D Consolidation Testing

Test No.	Mixing Fluid	Reservoir Fluid	Initial Conditions During Water Uptake	Loading Path
LBF_1	250 g/L NaCl	250 g/L NaCl	Rigidly Confined	Load to 1762 kPa, Unload to 1.1 kPa
LBF_2	Distilled Water	250 g/L NaCl	Rigidly Confined	Load to 1760 kPa, Unload to 1.1 kPa
LBF_3	Distilled Water	100 g/L NaCl	Rigidly Confined	Load to 1762 kPa, Unload to 1.1 kPa
LBF_4	100 g/L NaCl	100 g/L NaCl	Rigidly Confined	Load to 1753 kPa, Unload to 1.1 kPa
LBF_5	Distilled Water	50 g/L NaCl	Rigidly Confined	Load to 1764 kPa, Unload to 1.1 kPa
LBF_6	50 g/L NaCl	50 g/L NaCl	Rigidly Confined	Load to 1756 kPa, Unload to 1.1 kPa

Table C2: Properties of NaCl Solutions Used

Solute	Molar Mass (g/mol)	TDS (g/L)	Mass Percent C_m (%)	Concentration c (mol/L)	Solution Density ρ_l (Mg/m ³)
NaCl	58.44	250	22	4.28	1.133
NaCl	58.44	100	9.4	1.71	1.067
NaCl	58.44	50	4.8	0.86	1.032

C2.2.2 LBF

Standard ASTM D2435-04 (2004) procedures were used for the consolidation testing, unless otherwise specified. Specimens were prepared from the oven dried, crushed LBF material supplied to RMC. Prior to testing, the LBF was placed overnight in the oven. The oven dried specimens were then wetted with the specified fluid, as outlined in the testing matrix (Table C1), to obtain a target water content of 19.1%. Using a target density of 1.3 Mg/m³, the wetted LBF was added to the oedometer ring and compacted, by hand, to a target height of 10 mm. Each specimen was then loaded according to the testing schedule. The initial properties for each test are outlined in Table C3. Using experience from previous testing, the oedometer cell lifting and tie down screws were replaced with stainless steel wing nuts coating in “Marine Goop”¹ to

¹ Marine Goop is a product of Eclectic Products, Inc. 101 Dixie Mae Drive Pineville, LA 71360-3993

alleviate rusting due to the NaCl solution. Primary consolidation was not always complete in the standard 24 increment, therefore each load and unload increment was changed when the vertical deformation rate was less than 0.02 mm/ day (change in specimen height divided by the change in time) rather than a traditional 24 hr increment. This end of loading increment criterion was specified by AECL. It was seen that as the salt concentration was decreased in later tests, primary consolidation was observed in the traditional 24 hr increment for some of the loading sequences. To maintain consistency between all the tests, the equilibrium reading was taken when the vertical deformation rate was less than 0.02 mm/day even if equilibrium was reached in 24 hr.

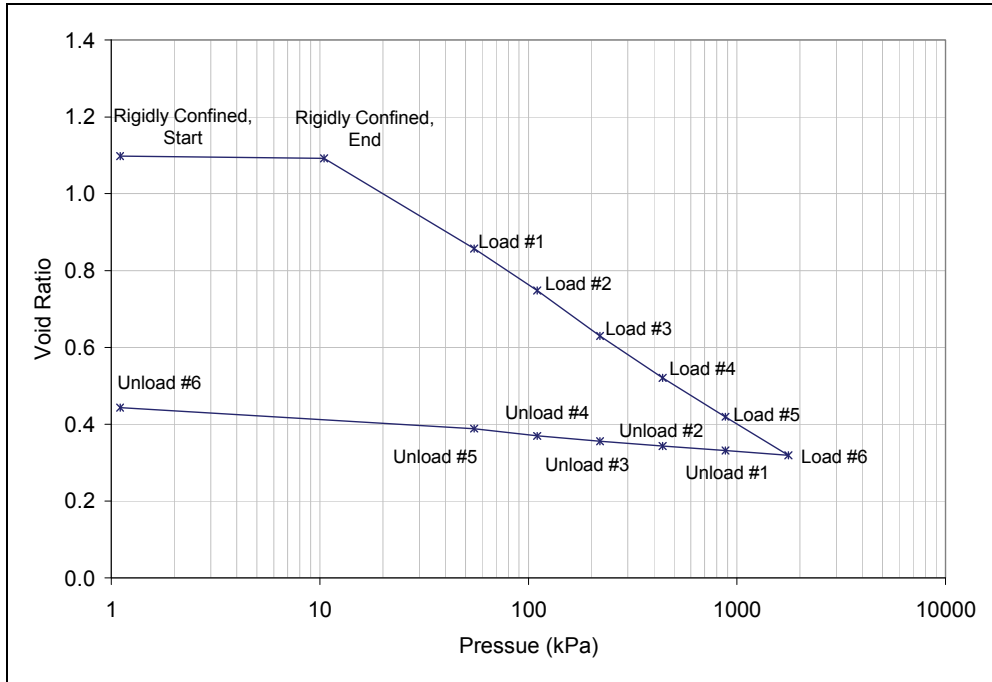
Table C3: Initial Properties of LBF Specimens

Test	Water Content (%)	Height (mm)	Bulk Density (Mg/m³)	Dry Density (Mg/m³)
LBF_1	19.1	10.32	1.52	1.28
LBF_2	16.6	10.65	1.47	1.26
LBF_3	18.9	10.69	1.45	1.22
LBF_4	18.2	10.30	1.52	1.28
LBF_5	19.1	10.55	1.49	1.25
LBF_6	18.4	10.32	1.52	1.28
Average	18.4	10.47	1.50	1.26

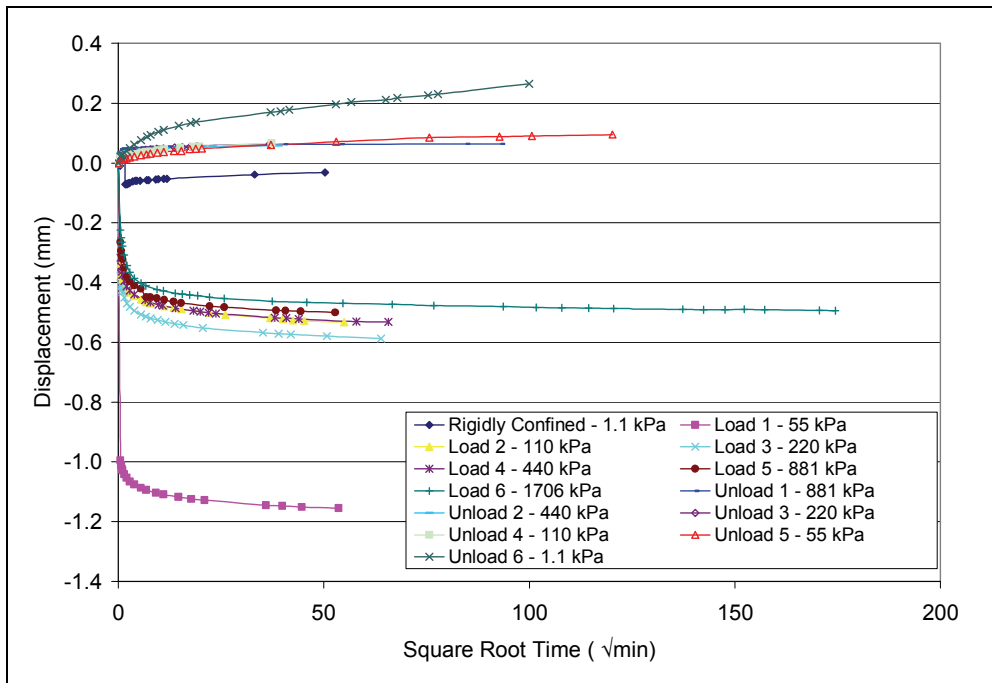
C3.LBF TEST RESULTS

C3.1 INDIVIDUAL TEST RESULTS

Test results of the six specimens are plotted in Figures C1 through C6 showing both void ratio versus applied pressure and displacement versus square root of time. All six tests were rigidly confined during water uptake resulting in uncorrected swell pressures ranging from 6.0 kPa to 13.8 kPa. All the tests resulted in a clear normal compression line with the exception of LBF_3. In this test, the normal compression line was not as distinct. The reason for this behaviour is unknown, the individual loading and unloading increments for this test did behave in a similar fashion to the other five tests. During the final unloading increment of LBF_6, there is a sudden jump in the data after equilibrium appeared to have been reached. This was due to nearby soil sieving that commenced and continued for the last day of the test. It is not believed this jump had a significant influence on the test as equilibrium had essentially been reached prior to the sieving.

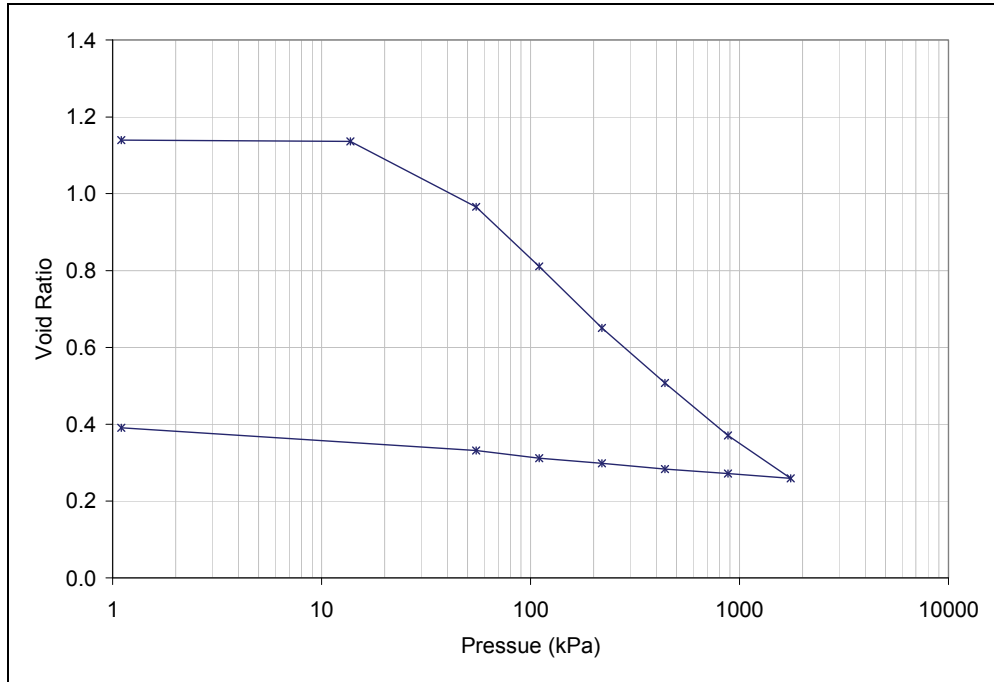


a)

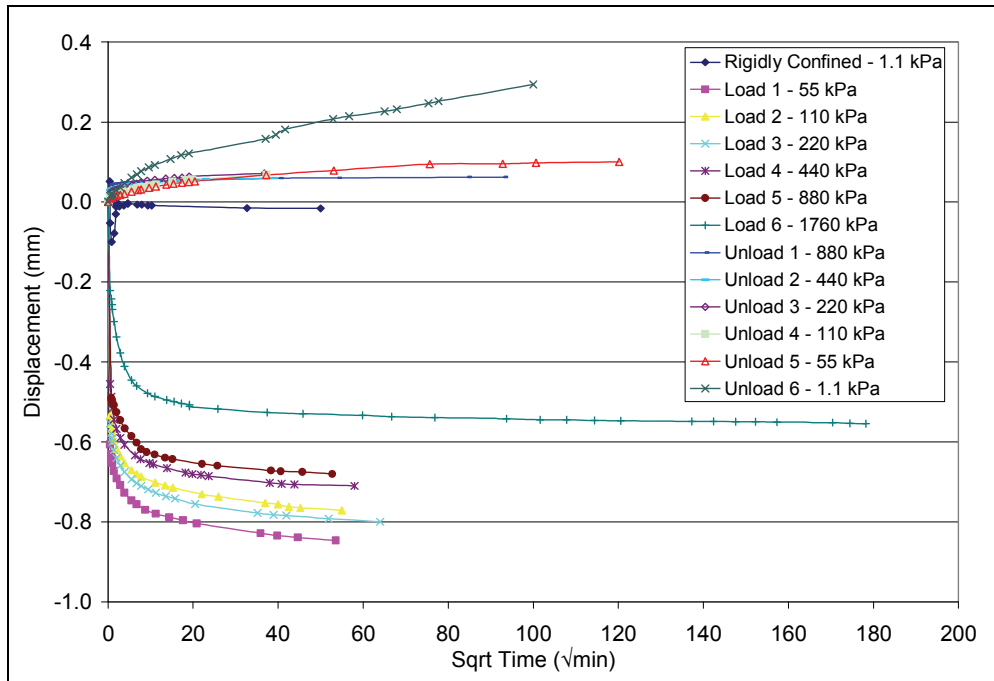


b)

Figure C1: LBF_1 a) Change in void ratio vs. pressure b) Specimen displacement vs. square root of time (Mixing Fluid = Reservoir Fluid = 250 g/L NaCl)

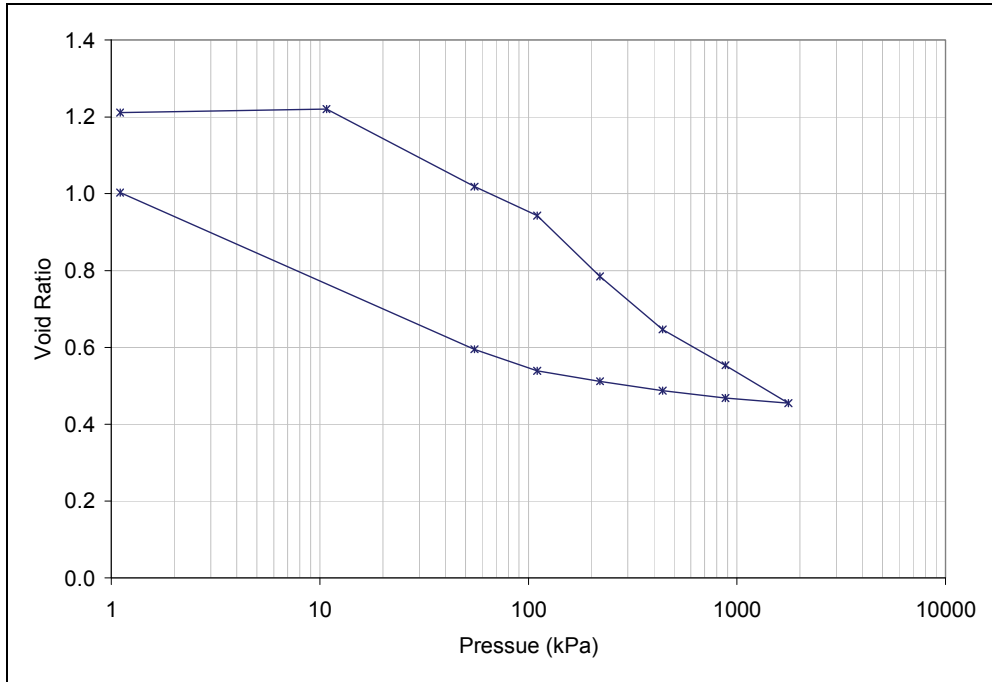


a)

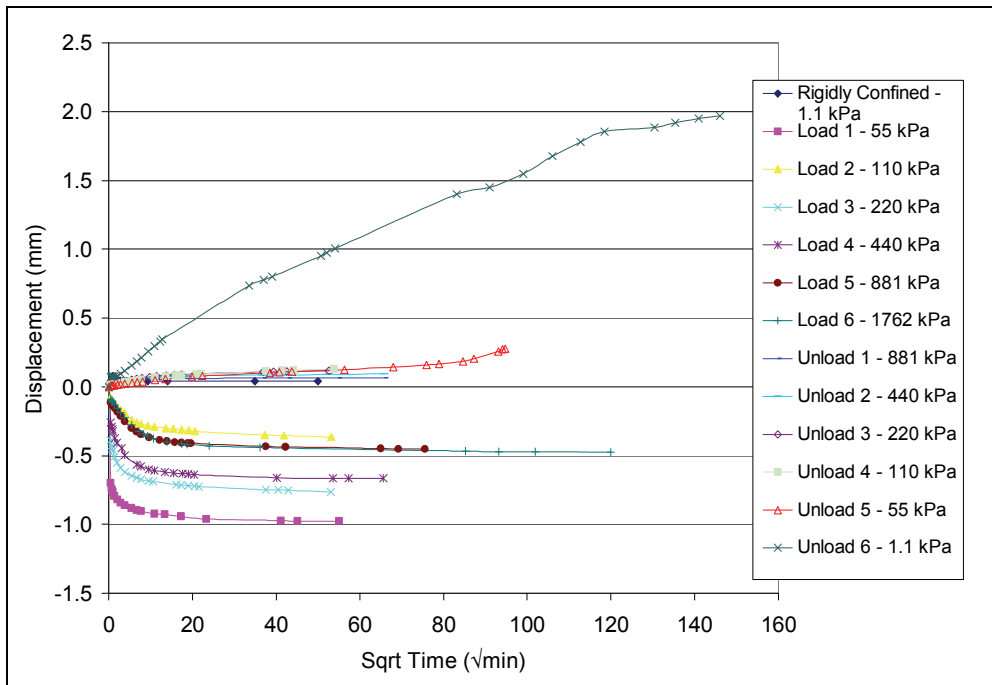


b)

Figure C2: LBF_2 a) Change in void ratio vs. pressure b) Specimen displacement vs. square root of time (Mixing Fluid = Distilled Water, Reservoir Fluid = 250 g/L NaCl)

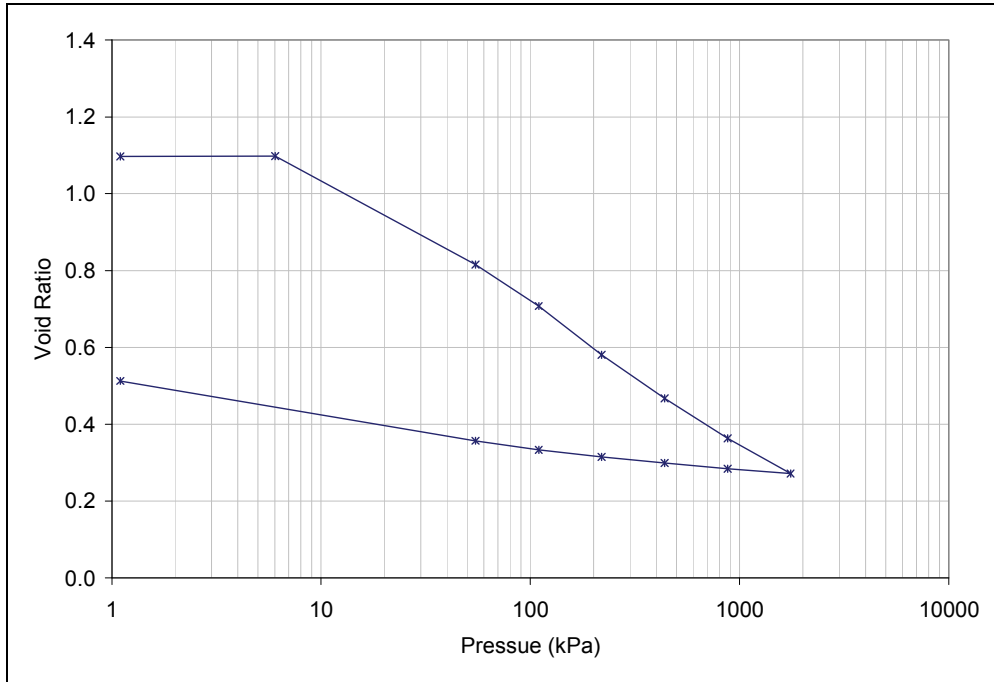


a)

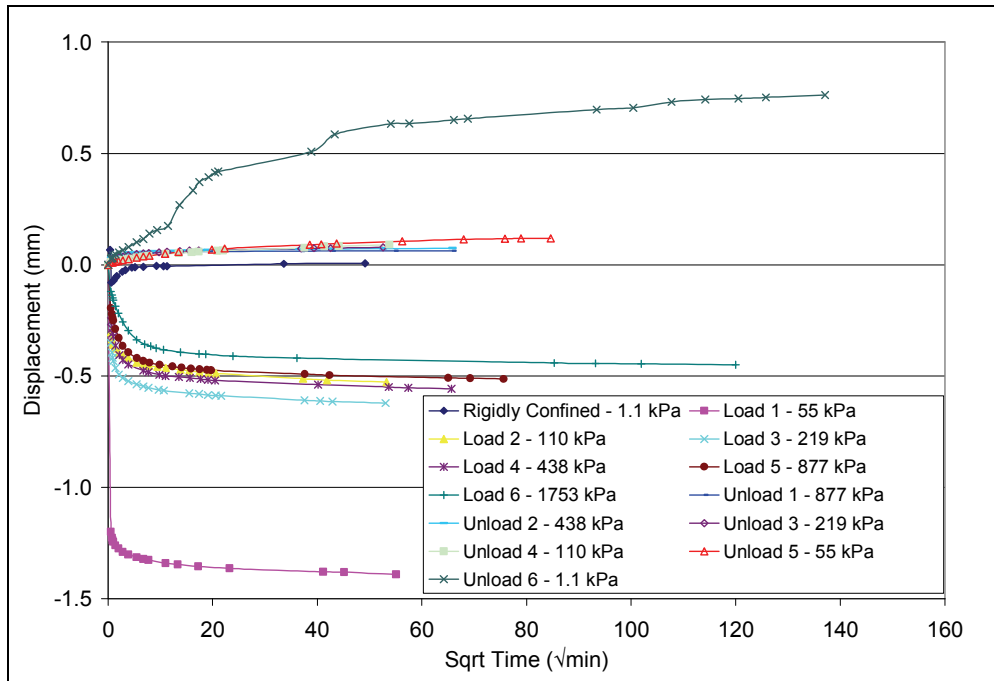


b)

Figure C3: LBF_3 a) Change in void ratio vs. pressure b) Specimen displacement vs. square root of time (Mixing Fluid = Distilled Water, Reservoir Fluid = 100 g/L NaCl)

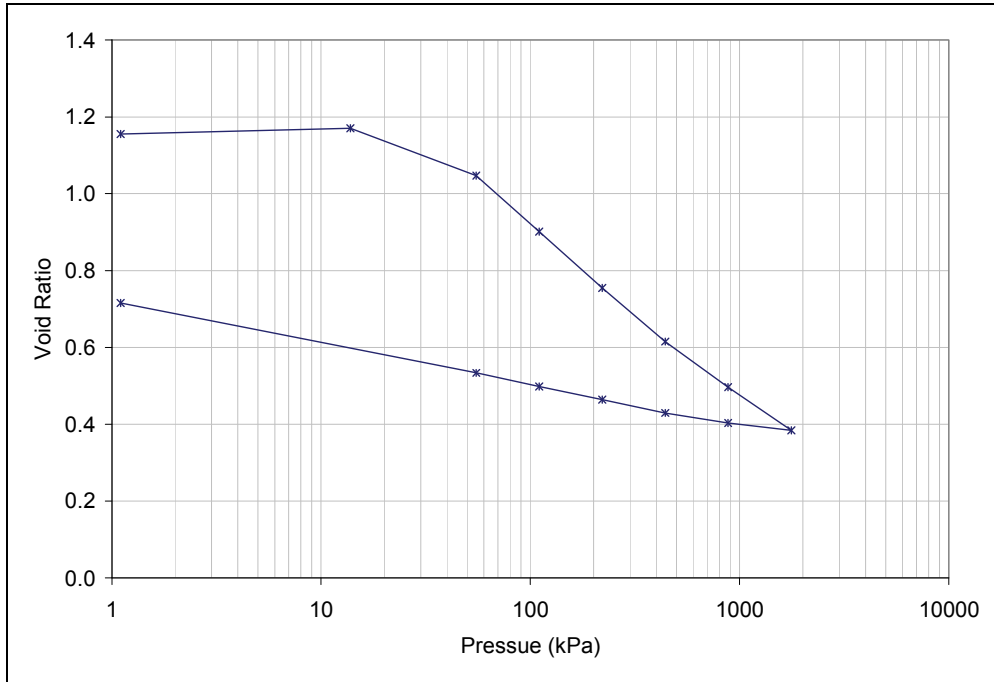


a)

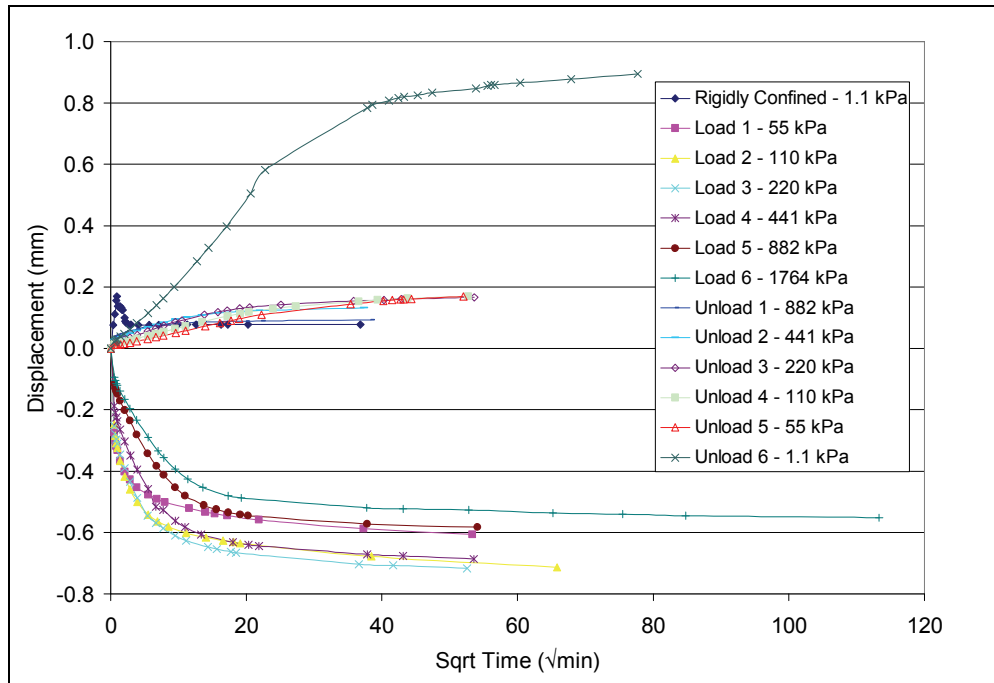


b)

Figure C4: LBF_4 a) Change in void ratio vs. pressure b) Specimen displacement vs. square root of time (Mixing Fluid = Reservoir Fluid = 100 g/L NaCl)

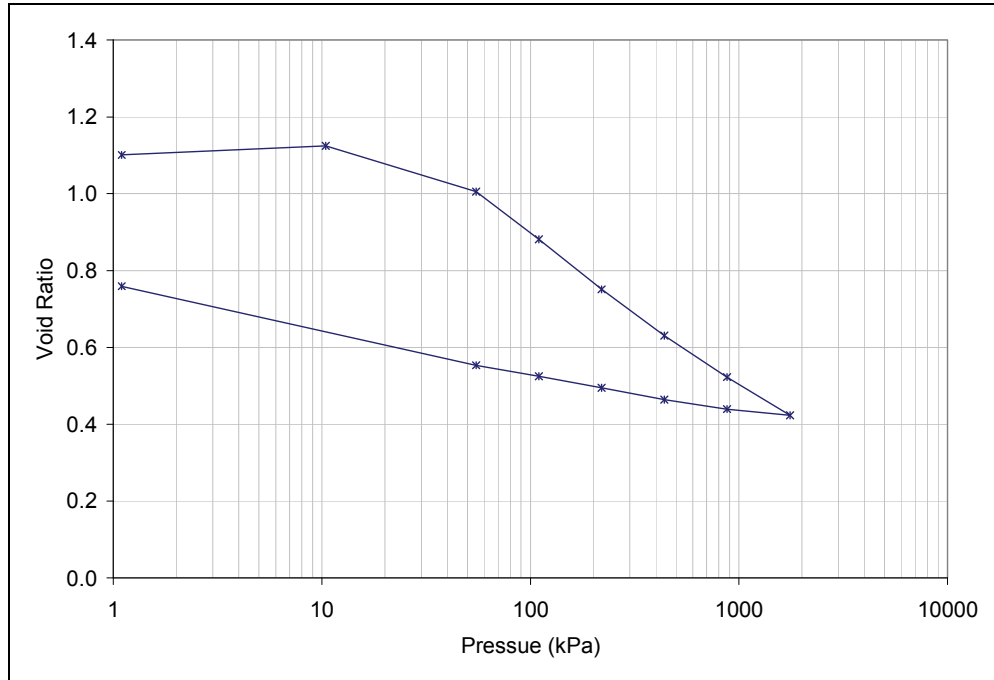


a)

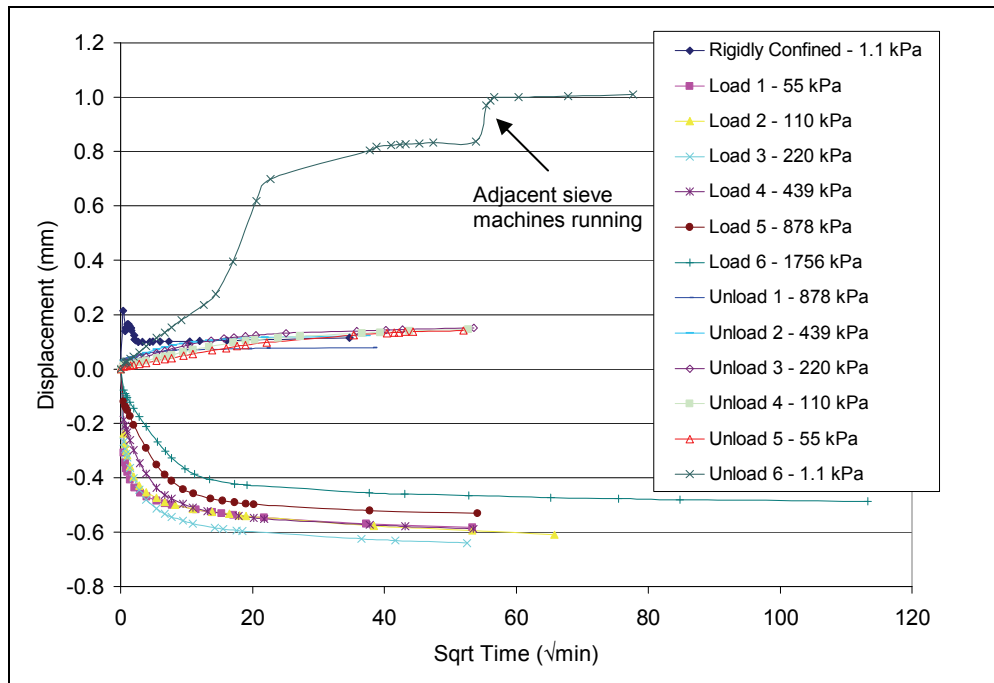


b)

Figure C5: LBF_5 a) Change in void ratio vs. pressure b) Specimen displacement vs. square root of time (Mixing Fluid = Distilled Water, Reservoir Fluid = 50 g/L NaCl)



a)



b)

Figure C6: LBF_6 a) Change in void ratio vs. pressure b) Specimen displacement vs. square root of time (Mixing Fluid = Reservoir Fluid = 50 g/L NaCl)

From the test data compression and swelling indices for each test were determined and summarized in Table C4. An example of the procedure used to calculate the indices is illustrated in Figure C7. The compression index (C_c) was calculated from the end of the first load increment to the end of the sixth load increment and the swelling index (C_s) was taken from the end of the sixth load increment to the end of the 5th unloading increment as shown in Figure C7. The 6th and final unloading increment was not included in the swelling index calculation due to the non-linearity of the curve, in most cases, between the 5th and 6th unloading increments.

Table C4: Compression and Swelling Indices

Test	Mixing Fluid	Reservoir Fluid	C_c	C_s
LBF_1	250 g/L NaCl	250 g/L NaCl	0.36	0.05
LBF_2	Distilled Water	250 g/L NaCl	0.47	0.05
LBF_3	Distilled Water	100 g/L NaCl	0.37	0.09
LBF_4	100 g/L NaCl	100 g/L NaCl	0.36	0.06
LBF_5	Distilled Water	50 g/L NaCl	0.44	0.10
LBF_6	50 g/L NaCl	50 g/L NaCl	0.39	0.09

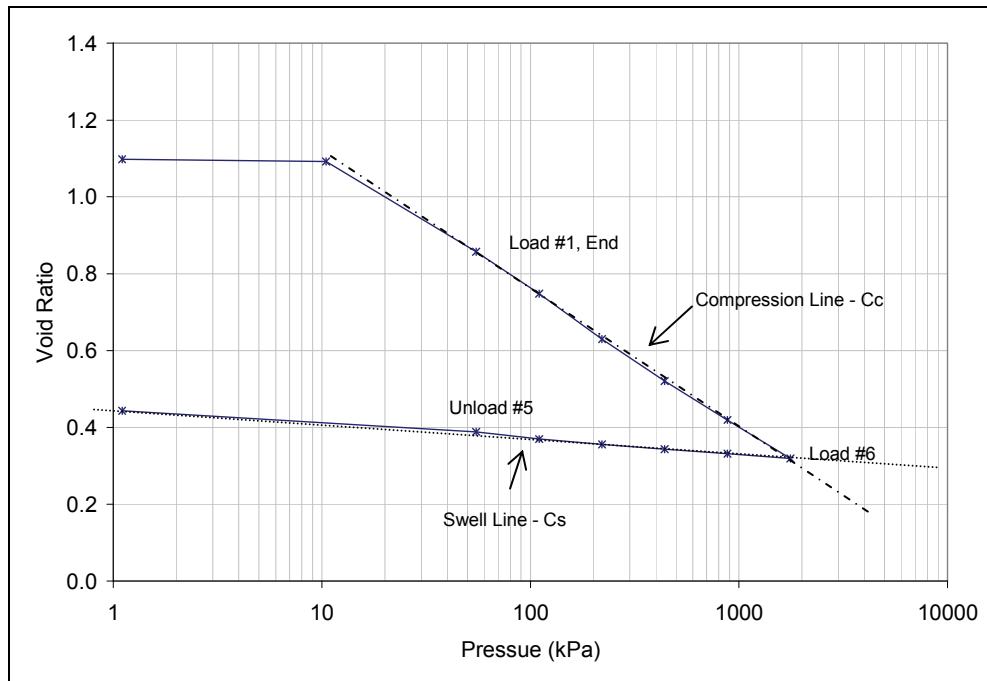


Figure C7: Calculation of Compression and Swelling Indices

C3.2 COMPARISON OF MIXING AND RESERVOIR CONDITIONS

For the specimens prepared with distilled water (LBF_2, LBF_3, and LBF_5), initial void ratios for the three distilled water tests were similar (Figure C8). The interpreted C_c values for LBF_2 and LBF_5 were similar at 0.47 and 0.44 where as LBF_3 yielded a value of 0.37 as seen in Table C3. This change in C_c value for LBF_3 is might be a result of the poorly defined normal compression line however changing the points used to calculate this value did not change C_c substantially. The C_s values from LBF_3 and LBF_5 were virtually the same at 0.09 and 0.10, however the C_s value from LBF_2 was 0.05. Behaviour observed during unloading (i.e., 1760 kPa to 1.1 kPa) is log-linear for the first five unloading increments (>50kPa), but when unloaded to 1.1 kPa the behaviour is not always longer log-linear.

The specimens prepared with the sodium chloride solutions at different concentrations (LBF_1, LBF_4 and LBF_6) resulted in essentially parallel curves with C_c values being 0.36 and 0.39 respectively (Figure C9). The prepared void ratios for these three tests are similar however the void ratios differed slightly following water uptake. This difference appears to be similar to the offset in the curves. The C_s values were similar ranging from 0.05 to 0.09 however it was noted that as the concentration of the sodium chloride solution decreased, the non-linearity of the unloading curve at pressures less than 50 kPa increased.

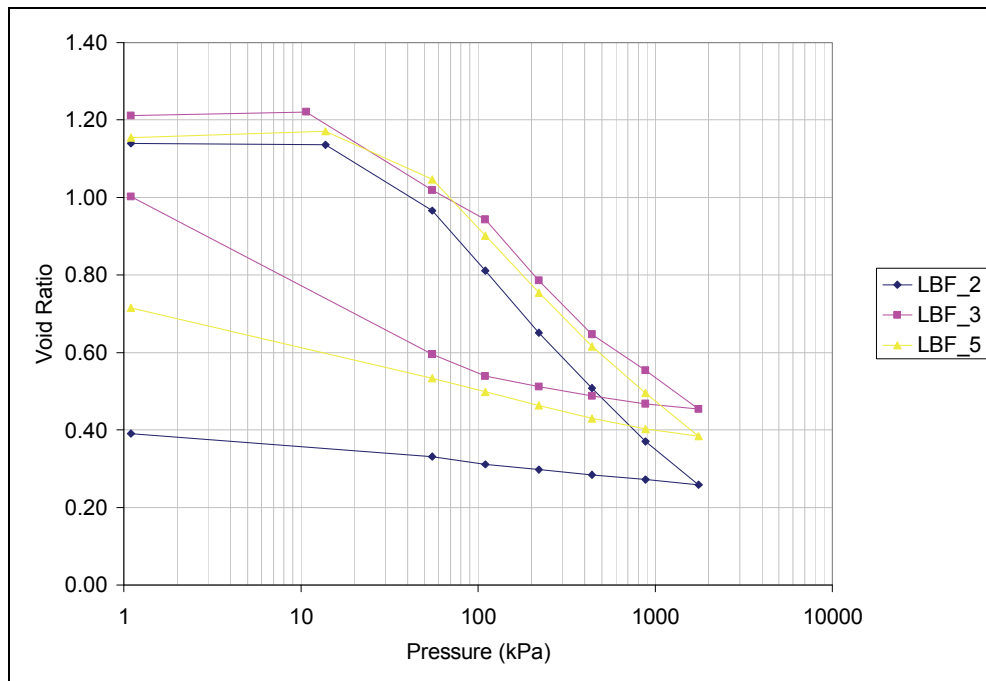


Figure C8: Void Ratio Comparison for Tests in Distilled Water

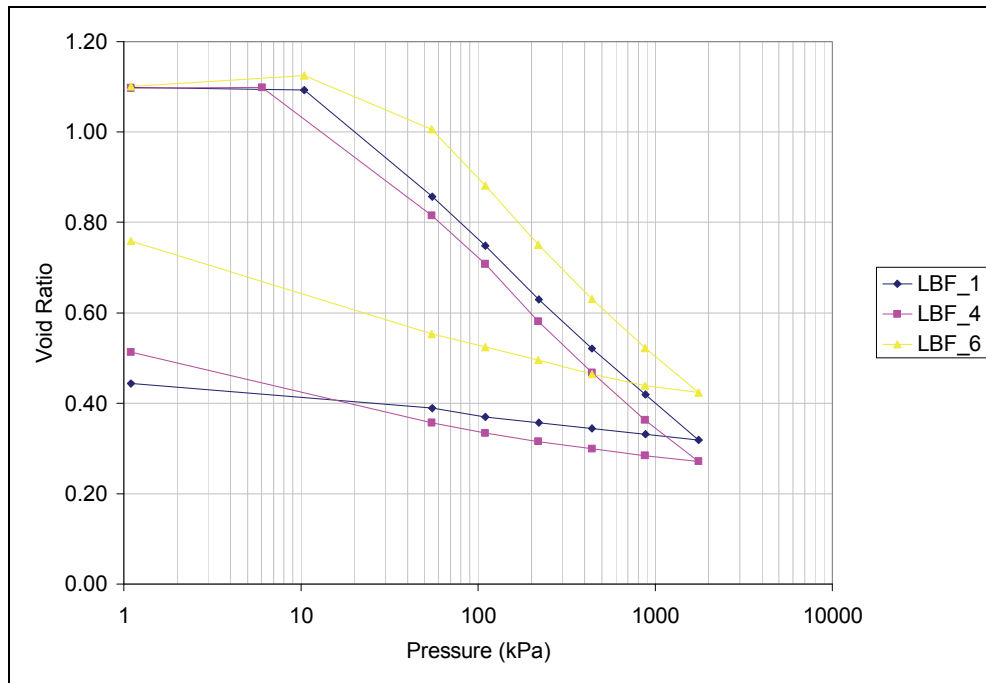


Figure C9: Void Ratio Comparison for Tests in Sodium Chloride (NaCl) Solution

C4. SUMMARY

One-dimensional consolidation tests were performed on LBF material. In total, six tests were conducted using a variety of pore water chemistries. All the tests were performed under rigidly confined conditions during water uptake. The resultant compression and swell indices, were determined for the Hydraulic-Mechanical modelling of LBF done by the Atomic Energy of Canada (AECL).

C5. CONCLUSIONS AND RECOMMENDATIONS

For the tests mixed with distilled water, the C_c values for LBF_2 and LBF_5 were similar at 0.47 and 0.44 where as LDF_3 yielded a value of 0.37. The C_s values for LBF_3 and LBF_5 were virtually the same at 0.09 and 0.10 where as LBF_2 was 0.05. The tests mixed with varying concentrations of NaCl show that as the solution concentration increases the swelling potential at pressures less than 50 kPa increases, and thus an increase in non-linearity of the curve. These tests yielded similar C_c values of 0.36 and 0.39. The C_s values were also similar ranging from 0.05 to 0.09. In general, all the tests yielded consistent results with the curves plotting on top or parallel to one another.

Prior to the first load increment at approximately 55 kPa, there are no data points and therefore this upper portion of the curve is poorly defined. It would be beneficial to have additional load increments between water uptake and 55 kPa. For instance, load increments in the range of 2, 4, 8, 16, 25 kPa would allow for better definition of the curve under small loads. Similarly there

are no unloading points between 55 kPa and 1.1 kPa. In some cases, the change in void ratio between these two points is substantial and therefore having more points in between would aid in better definition of the curve.

ACKNOWLEDGEMENTS

Funding provided by Nuclear Waste Management Organization (NWMO) through Atomic Energy of Canada Limited (AECL) is gratefully acknowledged. Technical assistance in the Geotechnical Laboratory at RMC was provided by Joe Dipietrantonio.

REFERENCES

ASTM (ASTM International). 2004. Standard test methods for one-dimensional consolidation properties of soils using incremental loading. Standard D2435-04, ASTM International, West Conshohocken, Pennsylvania, USA.

Dixon, D., N. Chandler, J. Graham, and M.N. Gray. 2002. Two large-scale sealing tests conducted at Atomic Energy of Canada's underground research laboratory: The buffer-container experiment and the isothermal test. *Canadian Geotechnical* 39, 503-518.

Gierszewski, P., J. Avis, N. Calder, A. D'Andrea, F. Garisto, C. Kitson, T. Melnyk, K. Wei and L. Wojciechowski. 2004. Third case study – Postclosure safety assessment. Ontario Power Generation, Nuclear Waste Management Division Report 06819-REP-01200-10109-R00. Toronto, Ontario.*

Maak P., and G.R. Simmons. 2005. Deep geologic repository concepts for isolation of used fuel in Canada, Canadian Nuclear Society, Waste Management, Decommissioning and Environmental Restoration for Canada's Nuclear Activities: Current Practices and Future Needs. Ottawa, Ontario, May 8-11 2005.

Russell, S.B., and G.R. Simmons. 2003. Engineered barrier system for a deep geologic repository. Presented at the 2003 International High-Level Radioactive Waste Management Conference. 2003 March 30 – April 2, Las Vegas, NV.

* Available from Nuclear Waste Management Organization, 22 St. Clair Avenue East, 6th Floor, Toronto, Ontario M4T 2S3 Canada.

APPENDIX D: DATA

CONTENTS

	<u>Page</u>
D1. SUMMARY	91

LIST OF TABLES

	<u>Page</u>
Table D1: Compression Index (Cc) and Swelling Index (Cs) of the Highly Compacted Bentonite (HCB)	92
Table D2: Compression Index (Cc) and Swelling Index (Cs) of the Dense Backfill (DBF)	93
Table D3: Compression Index (Cc) and Swelling Index (Cs) of the Light Backfill (LBF)	94
Table D4: Coefficient of Consolidation (cv), Hydraulic Conductivity (k), and 1-D Modulus of Highly Compacted Bentonite (HCB)	95
Table D5: Coefficient of Consolidation (cv), Hydraulic Conductivity (k), and 1-D Modulus of Dense Backfill (DBF)	104
Table D6: Coefficient of Consolidation (cv), Hydraulic Conductivity (k), and 1-D Modulus of Light Backfill (LBF)	111

D1. SUMMARY

This appendix summarizes the data from 1D-Consolidation Tests of the Highly Compacted Bentonite (HCB), Dense Backfill (DBF), and Light Backfill (LBF) specimens. The Compression (Cc) and Swelling (Cs) Indices of HCB, DBF, and LBF are shown in Tables D1, D2, and D3 respectively. The Coefficient of Consolidation (cv), Hydraulic Conductivity (k), and 1-D Modulus of HCB, DBF, and LBF are shown in Tables D4, D5, and D6 respectively.

Table D1: Compression Index (Cc) and Swelling Index (Cs) of the Highly Compacted Bentonite (HCB)

Test No.	Sample No.	Mixing Fluid	Reservoir Fluid	Mixing Fluid TDS (g/L)	Reservoir Fluid TDS (g/L)	Average TDS (g/L)	Boundary Condition During Saturation	Cc	Cs	σ_u (kPa)	Void ratio, $e(\sigma_u)$
1	HCB1(06)	DW	DW	0	0	0	CS	0.422	0.114	15930	0.634
2	HCB2(06)	DW	DW	0	0	0	CS	0.267	0.089	15980	0.506
3	HCB3(06)	CaCl ₂	CaCl ₂	75	75	75	CS	0.146	0.088	15880	0.689
4	HCB4(06)	CaCl ₂	CaCl ₂	75	75	75	CS	0.187	0.067	16000	0.693
5	HCB5(06)	DW	DW	0	0	0	CS	0.572	0.300	15780	0.534
6	HCB6(06)	CaCl ₂	CaCl ₂	75	75	75	CS	0.324	0.155	15940	0.774
7	HCB7 (07)	DW	CaCl ₂	0	250	125	CS	0.155	0.090	15901	0.613
8	HCB8 (07)	CaCl ₂	CaCl ₂	250	250	250	CS	0.177	0.064	15920	0.519
9	HCB9 (07)	DW	DW	0	0	0	CV	0.164	0.092	15974	0.549
10	HCB10 (07)	CaCl ₂	CaCl ₂	250	250	250	CV	0.187	0.061	15959	0.548
11	HCB11 (07)	DW	CaCl ₂	0	150	75	CS	0.180	0.016	15940	0.535
12	HCB12(08)	NaCl	NaCl	250	250	250	CV	0.207	0.053	16333	0.400
13	HCB13(08)	NaCl	NaCl	250	250	250	CS	0.223	0.077	16842	0.470
14	HCB14(08)	DW	NaCl	0	250	125	CV	0.159	0.010	16158	0.528
15	HCB14A (08)	DW	NaCl	0	250	125	CV	0.198	0.078	16162	0.485
16	HCB15 (08)	DW	NaCl	0	250	125	CS	0.242	0.070	16758	0.409

Note: CV: Constant Volume; CS: Constant Vertical Stress; DW: Distilled Water

Table D2: Compression Index (Cc) and Swelling Index (Cs) of the Dense Backfill (DBF)

Test No.	Sample No.	Mixing Fluid	Reservoir Fluid	Mixing Fluid TDS (g/L)	Reservoir Fluid TDS (g/L)	Average TDS (g/L)	Boundary Condition During Saturation	Cc	Cs	σ_u (kPa)	Void ratio, $e(\sigma_u)$
1	DBF1(06)	DW	DW	0	0	0	CS	0.153	0.013	3902	0.174
2	DBF2(06)	DW	DW	0	0	0	CV	0.116	0.013	3899	0.155
3	DBF3(06)	CaCl ₂	CaCl ₂	100	100	100	CS	0.091	0.008	3902	0.192
4	DBF4(06)	CaCl ₂	CaCl ₂	100	100	100	CV	0.106	0.013	3899	0.167
5	DBF5(06)	DW	DW	0	0	0	CS	0.116	0.014	3998	0.191
6	DBF6(06)	CaCl ₂	CaCl ₂	100	100	100	CS	0.095	0.001	4002	0.210
7	DBF1(08)	CaCl ₂	CaCl ₂	250	250	250	CS	0.083	0.005	3938	0.204
8	DBF2(08)	DW	CaCl ₂	0	250	125	CS	0.090	0.005	3930	0.174
9	DBF3(08)	CaCl ₂	CaCl ₂	250	250	250	CV	0.112	0.010	3938	0.197
10	DBF4(08)	DW	CaCl ₂	0	250	125	CV	0.110	0.010	3930	0.178
11	DBF5(08)	NaCl	NaCl	250	250	250	CV	0.106	0.008	3938	0.212
12	DBF6(08)	DW	NaCl	0	250	125	CV	0.060	0.008	3930	0.185
13	DBFS1(08)	DW	NaCl	0	250	125	CS	0.058	0.002	1603	0.219
14	DBFS2(08)	NaCl	NaCl	0	250	125	CS	0.032	0.007	1557	0.251

Note: CV: Constant Volume; CS: Constant Vertical Stress; DW: Distilled Water

Table D3: Compression Index (Cc) and Swelling Index (Cs) of the Light Backfill (LBF)

Test No.	Sample No.	Mixing Fluid	Reservoir Fluid	Mixing Fluid TDS (g/L)	Reservoir Fluid TDS (g/L)	Average TDS (g/L)	Boundary Condition During Saturation	Cc	Cs	σ_u (kPa)	Void ratio, $e(\sigma_u)$
1	HB2(06)	DW	DW	0	0	0	CV	0.537	NA	2651	0.619
2	HB3(06)	DW	DW	0	0	0	CS	0.851	0.169	1326	0.672
3	HB4(06)	DW	DW	0	0	0	CV	0.531	0.077	2654	0.510
4	HB6(06)	DW	DW	0	0	0	CS	0.629	0.158	3987	0.374
5	HB7(06)	DW	DW	0	0	0	CV	0.608	0.149	3986	0.366
6	HB8(06)	DW	DW	0	0	0	CS	0.600	0.113	2652	0.477
7	HB9(06)	DW	DW	0	0	0	CV	0.713	0.114	2659	0.663
8	HB11(06)	DW	CaCl ₂	0	100	50	CS	0.353	0.097	3990	0.297
9	HB12(06)	DW	CaCl ₂	0	100	50	CS	0.387	0.095	2675	0.305
10	HB13(06)	CaCl ₂	CaCl ₂	100	100	100	CS	0.351	0.097	2650	0.412
11	HB14(06)	DW	CaCl ₂	0	100	50	CV	0.398	0.105	4000	0.206
12	HB15(06)	CaCl ₂	CaCl ₂	100	100	100	CS	0.334	0.095	3985	0.338
13	HB16(06)	DW	CaCl ₂	0	200	100	CS	0.380	0.062	2650	0.347
14	HB19(06)	DW	CaCl ₂	0	100	50	CS	0.379	0.094	2660	0.348
15	LBF_1(07)	CaCl ₂	CaCl ₂	227	227	227	CS	0.366	0.050	1702	0.512
16	LBF_2(07)	DW	CaCl ₂	0	227	113.5	CS	0.446	0.065	1709	0.319
17	LBF_3(07)	CaCl ₂	CaCl ₂	227	227	227	CV	0.378	0.046	1703	0.448
18	LBF_4(07)	DW	CaCl ₂	0	227	113.5	CV	0.445	0.056	1709	0.332
19	LBF_5B(07)	CaCl ₂	CaCl ₂	91	91	91	CS	0.400	0.074	1701	0.286
20	LBF_6(07)	DW	CaCl ₂	0	91	45.5	CV	0.446	0.081	1711	0.322
21	LBF_1(08)	NaCl	NaCl	250	250	250	CV	0.360	0.050	1761	0.389
22	LBF_2(08)	DW	NaCl	0	250	125	CV	0.470	0.050	1760	0.260
23	LBF_3(08)	DW	NaCl	0	100	50	CV	0.370	0.090	1762	0.456
24	LBF_4(08)	NaCl	NaCl	100	100	100	CV	0.360	0.060	1753	0.291
25	LBF_5(08)	DW	NaCl	0	50	25	CV	0.440	0.100	1764	0.386
26	LBF_6(08)	NaCl	NaCl	50	50	50	CV	0.390	0.090	1756	0.433

Note: CV: Constant Volume; CS: Constant Vertical Stress; DW: Distilled Water

Table D4-1: Coefficient of Consolidation (cv), Hydraulic Conductivity (k), and 1-D Modulus of Highly Compacted Bentonite (HCB) (Continued)

Test No.	Sample No.	Vertical Stress (kPa)	Vertical Stress (MPa)	Void Ratio, e	Dry Density (Mg/m ³)	EMDD (Mg/m ³)	EMDD-mid (Mg/m ³)	cv (m ² /sec)	mv (Pa ⁻¹)	k (m/s)	Volume strain (%)	1D-Modulus (kPa)
1	HCB1(06)											
		380	0.4	0.644	1.67	1.484					0.0	
		990	1.0	0.891	1.45	1.259	1.372	8.3E-11	2.5E-07	2.0E-13	15.0	4060
		2100	2.1	0.877	1.46	1.270	1.265	2.5E-10	6.7E-09	1.6E-14	14.2	149929
		3980	4.0	0.838	1.49	1.302	1.286	1.2E-09	1.1E-08	1.3E-13	11.8	90481
		7970	8.0	0.761	1.56	1.368	1.335	6.4E-10	1.0E-08	6.6E-14	7.1	95242
		15930	15.9	0.634	1.68	1.495	1.431	5.8E-10	9.1E-09	5.1E-14	-0.6	110374
		8010	8.0	0.668	1.64	1.459	1.477	9.0E-10	2.6E-09	2.3E-14	1.5	380626
		4020	4.0	0.741	1.57	1.387	1.423	6.7E-11	1.1E-08	7.2E-15	5.9	91169
		2000	2.0	0.821	1.51	1.316	1.351	5.0E-11	2.3E-08	1.1E-14	10.8	43960
2	HCB2(06)											
		980	1.0	0.644	1.67	1.484	1.484				0.0	
		1310	1.3	0.796	1.53	1.337	1.411	1.0E-10	2.8E-07	2.7E-13	9.2	3569
		15980	16.0	0.506	1.82	1.648	1.492	6.1E-10	1.1E-08	6.6E-14	-8.4	90853
		8590	8.6	0.530	1.79	1.617	1.632	4.7E-10	2.2E-09	9.9E-15	-6.9	463723
		4270	4.3	0.614	1.70	1.516	1.566	5.0E-11	1.3E-08	6.2E-15	-1.8	78686
		2340	2.3	0.691	1.62	1.435	1.475	5.0E-11	2.5E-08	1.2E-14	2.9	40455
		1020	1.0	0.805	1.52	1.329	1.382	5.0E-11	5.1E-08	2.5E-14	9.8	19580

Table D4-2: Coefficient of Consolidation (cv), Hydraulic Conductivity (k), and 1-D Modulus of Highly Compacted Bentonite (HCB) (Continued)

Test No.	Sample No.	Vertical Stress (kPa)	Vertical Stress (MPa)	Void Ratio, e	Dry Density (Mg/m ³)	EMDD (Mg/m ³)	EMDD-mid (Mg/m ³)	cv (m ² /sec)	mv (Pa ⁻¹)	k (m/s)	Volume strain (%)	1D-Modulus (kPa)
3	HCB3(06)											
		1020	1.0	0.701	1.61	1.425					0.0	
		1030	1.0	0.826	1.50	1.312	1.369	5.0E-11	7.3E-06	3.6E-12	7.3	136
		2070	2.1	0.827	1.50	1.311	1.311	5.9E-09	5.3E-10	3.1E-14	7.4	1899040
		3940	3.9	0.803	1.52	1.331	1.321	1.5E-09	7.0E-09	1.0E-13	6.0	142354
		8050	8.1	0.749	1.57	1.380	1.355	1.0E-09	7.3E-09	7.4E-14	2.8	137228
		3990	4.0	0.764	1.55	1.365	1.372	1.6E-09	2.1E-09	3.2E-14	3.7	473396
		1960	2.0	0.803	1.52	1.331	1.348	6.8E-10	1.1E-08	7.3E-14	6.0	91818
		1000	1.0	0.864	1.47	1.280	1.306	2.1E-10	3.5E-08	7.2E-14	9.6	28375
		3980	4.0	0.822	1.50	1.315	1.298	8.4E-10	7.6E-09	6.2E-14	7.1	132255
		7970	8.0	0.761	1.56	1.368	1.342	6.2E-10	8.4E-09	5.1E-14	3.5	119177
		15880	15.9	0.689	1.62	1.437	1.402	6.9E-10	5.2E-09	3.5E-14	-0.7	193465
4	HCB4(06)											
		8060	8.1	0.560	1.76	1.580					0.0	
		8220	8.2	0.651	1.66	1.477	1.528	2.5E-12	3.6E-07	8.9E-15	5.8	2743
		4170	4.2	0.724	1.59	1.403	1.440	1.0E-11	1.1E-08	1.1E-15	10.5	91597
		2040	2.0	0.782	1.54	1.350	1.377	2.0E-11	1.6E-08	3.1E-15	14.2	63312
		1080	1.1	0.842	1.49	1.298	1.324	2.0E-11	3.5E-08	6.9E-15	18.1	28512
		4140	4.1	0.803	1.52	1.331	1.314	5.8E-11	6.9E-09	3.9E-15	15.6	144526
		7950	8.0	0.753	1.56	1.375	1.353	4.3E-11	7.3E-09	3.1E-15	12.4	137389
		16000	16.0	0.693	1.62	1.433	1.404	4.8E-11	4.3E-09	2.0E-15	8.5	235194

Table D4-3: Coefficient of Consolidation (cv), Hydraulic Conductivity (k), and 1-D Modulus of Highly Compacted Bentonite (HCB) (Continued)

Test No.	Sample No.	Vertical Stress (kPa)	Vertical Stress (MPa)	Void Ratio, e	Dry Density (Mg/m ³)	EMDD (Mg/m ³)	EMDD-mid (Mg/m ³)	cv (m ² /sec)	mv (Pa ⁻¹)	k (m/s)	Volume strain (%)	1D-Modulus (kPa)
5	HCB5(06)											
		1030	1.0	0.898	1.44	1.254					0.0	
		960	1.0	1.238	1.22	1.038	1.146	2.8E-10	2.6E-06	6.9E-12	17.9	391
		1980	2.0	1.015	1.36	1.170	1.104	2.7E-10	9.8E-08	2.6E-13	6.2	10237
		4060	4.1	0.840	1.49	1.300	1.235	3.2E-10	4.2E-08	1.3E-13	-3.1	23950
		8110	8.1	0.690	1.62	1.436	1.368	4.3E-10	2.0E-08	8.4E-14	-11.0	49680
		15850	15.9	0.542	1.78	1.602	1.519	4.3E-10	1.1E-08	4.7E-14	-18.8	88382
		8120	8.1	0.588	1.73	1.547	1.574	5.6E-10	3.9E-09	2.1E-14	-16.3	259123
		4040	4.0	0.695	1.62	1.430	1.489	2.7E-10	1.7E-08	4.3E-14	-10.7	60552
		2020	2.0	0.796	1.53	1.336	1.383	2.4E-10	2.9E-08	7.0E-14	-5.4	33900
		1020	1.0	0.899	1.44	1.253	1.295	1.7E-10	5.7E-08	9.4E-14	0.1	17437
		1980	2.0	0.864	1.47	1.280	1.267	4.3E-10	1.9E-08	8.2E-14	-1.8	52087
		4010	4.0	0.774	1.54	1.356	1.318	3.5E-10	2.4E-08	8.2E-14	-6.5	42044
		8070	8.1	0.662	1.65	1.465	1.410	3.7E-10	1.6E-08	5.6E-14	-12.4	64308
		15780	15.8	0.534	1.79	1.613	1.539	4.1E-10	1.0E-08	4.0E-14	-19.2	100110

Table D4-4: Coefficient of Consolidation (cv), Hydraulic Conductivity (k), and 1-D Modulus of Highly Compacted Bentonite (HCB) (Continued)

Test No.	Sample No.	Vertical Stress (kPa)	Vertical Stress (MPa)	Void Ratio, e	Dry Density (Mg/m ³)	EMDD (Mg/m ³)	EMDD-mid (Mg/m ³)	cv (m ² /sec)	mv (Pa ⁻¹)	k (m/s)	Volume strain (%)	1D-Modulus (kPa)
6	HCB6(06)											
		1010	1.0	0.859	1.47	1.284					0.0	
		970	1.0	1.098	1.31	1.117					12.9	
		1990	2.0	1.060	1.33	1.141	1.129	2.2E-09	1.8E-08	3.8E-13	10.8	56315
		4100	4.1	0.970	1.39	1.201	1.171	9.1E-10	2.1E-08	1.8E-13	6.0	48296
		7940	7.9	0.865	1.47	1.279	1.240	8.0E-10	1.4E-08	1.1E-13	0.3	72046
		15820	15.8	0.772	1.55	1.358	1.319	8.9E-10	6.3E-09	5.5E-14	-4.7	158024
		7940	7.9	0.791	1.53	1.341	1.350	1.4E-09	1.4E-09	1.8E-14	-3.7	734914
		3990	4.0	0.831	1.50	1.308	1.325	7.1E-10	5.7E-09	3.9E-14	-1.5	176861
		1950	2.0	0.891	1.45	1.259	1.284	3.4E-10	1.6E-08	5.4E-14	1.7	62254
		1020	1.0	0.956	1.40	1.211	1.235	2.2E-10	3.7E-08	7.9E-14	5.2	27056
		1980	2.0	0.951	1.41	1.215	1.213	4.8E-10	2.7E-09	1.2E-14	4.9	375552
		4040	4.0	0.908	1.44	1.246	1.231	5.5E-10	1.1E-08	5.8E-14	2.6	93467
		7940	7.9	0.840	1.49	1.300	1.273	6.0E-10	9.1E-09	5.4E-14	-1.0	109429
		15940	15.9	0.774	1.54	1.356	1.328	8.0E-10	4.5E-09	3.5E-14	-4.6	223030

Table D4-5: Coefficient of Consolidation (cv), Hydraulic Conductivity (k), and 1-D Modulus of Highly Compacted Bentonite (HCB) (Continued)

Test No.	Sample No.	Vertical Stress (kPa)	Vertical Stress (MPa)	Void Ratio, e	Dry Density (Mg/m ³)	EMDD (Mg/m ³)	EMDD-mid (Mg/m ³)	cv (m ² /sec)	mv (Pa ⁻¹)	k (m/s)	Volume strain (%)	1D-Modulus (kPa)
7 HCB7 (07)												
		100	0.1	0.748	1.57	1.383					0.0	
		1021	1.0	0.761	1.56	1.371	1.377	8.5E-11	8.0E-09	6.7E-15	0.7	125365
		2003	2.0	0.745	1.57	1.386	1.379	6.4E-10	9.6E-09	6.0E-14	-0.2	104353
		3883	3.9	0.708	1.61	1.421	1.404	8.5E-10	1.1E-08	9.3E-14	-2.3	90036
		7942	7.9	0.655	1.66	1.475	1.448	8.1E-10	7.6E-09	6.1E-14	-5.3	130822
		15901	15.9	0.613	1.70	1.521	1.498	5.3E-10	3.2E-09	1.7E-14	-7.7	311688
		7922	7.9	0.640	1.67	1.492	1.506	6.2E-10	2.1E-09	1.3E-14	-6.2	479275
		4073	4.1	0.667	1.65	1.463	1.477	3.5E-10	4.3E-09	1.5E-14	-4.7	233036
		2000	2.0	0.693	1.62	1.436	1.449	4.7E-11	7.6E-09	3.6E-15	-3.2	130933
		1016	1.0	0.720	1.60	1.410	1.423	2.6E-10	1.6E-08	4.1E-14	-1.6	62567
		1982	2.0	0.709	1.61	1.420	1.415	1.1E-09	6.5E-09	6.9E-14	-2.2	154593
8 HCB8 (07)												
		100	0.1	0.685	1.63	1.444					0.0	
		992	1.0	0.690	1.62	1.439					0.3	
		1901	1.9	0.677	1.64	1.452	1.445	1.3E-09	8.4E-09	1.1E-13	-0.4	119734
		3967	4.0	0.632	1.68	1.500	1.476	1.6E-09	1.3E-08	2.1E-13	-3.2	75706
		7960	8.0	0.570	1.75	1.571	1.536	1.6E-09	9.5E-09	1.5E-13	-6.8	105015
		15920	15.9	0.519	1.81	1.634	1.603	9.2E-10	4.0E-09	3.6E-14	-9.8	248039
		7964	8.0	0.535	1.79	1.613	1.624	1.7E-09	1.3E-09	2.2E-14	-8.9	743512
		4019	4.0	0.558	1.76	1.586	1.600	9.2E-10	3.7E-09	3.3E-14	-7.5	270061
		2005	2.0	0.586	1.73	1.552	1.569	4.6E-10	8.8E-09	3.9E-14	-5.9	113238
		1004	1.0	0.587	1.73	1.550					-5.8	
		1993	2.0	0.589	1.73	1.548					-5.7	

Table D4-6: Coefficient of Consolidation (cv), Hydraulic Conductivity (k), and 1-D Modulus of Highly Compacted Bentonite (HCB) (Continued)

Test No.	Sample No.	Vertical Stress (kPa)	Vertical Stress (MPa)	Void Ratio, e	Dry Density (Mg/m ³)	EMDD (Mg/m ³)	EMDD-mid (Mg/m ³)	cv (m ² /sec)	mv (Pa ⁻¹)	k (m/s)	Volume strain (%)	1D-Modulus (kPa)
9	HCB9 (07)											
		139	0.1	0.606	1.71	1.529					0.0	
		3605	3.6	0.643	1.67	1.488	1.509				2.3	
		5007	5.0	0.645	1.67	1.486	1.487				2.5	
		8006	8.0	0.627	1.69	1.505	1.495	1.2E-09	3.6E-09	4.1E-14	1.3	275993
		15983	16.0	0.578	1.74	1.561	1.533	6.7E-10	3.8E-09	2.5E-14	-1.7	263668
		15974	16.0	0.549	1.77	1.596	1.579	9.1E-10	3.4E-08	3.1E-13	-3.5	29090
		8038	8.0	0.577	1.74	1.563	1.580	6.0E-10	2.2E-09	1.3E-14	-1.8	445977
		4004	4.0	0.653	1.66	1.477	1.520	2.3E-10	1.2E-08	2.7E-14	2.9	83446
		2007	2.0	0.736	1.58	1.395	1.436	2.1E-10	2.5E-08	5.3E-14	8.1	39879
		1011	1.0	0.805	1.52	1.332	1.363	1.7E-10	4.0E-08	6.7E-14	12.4	24945
10	HCB10 (07)											
		837	0.8	0.657	1.66	1.473					0.0	
		876	0.9	0.66	1.66	1.472	1.473				0.1	
		2576	2.6	0.670	1.64	1.460	1.466				0.8	
		4030	4.0	0.656	1.66	1.474	1.467	1.7E-09	5.6E-09	9.3E-14	0.0	179751
		7991	8.0	0.605	1.71	1.530	1.502	1.5E-09	7.8E-09	1.2E-13	-3.1	128479
		15959	16.0	0.548	1.77	1.598	1.564	1.0E-09	4.5E-09	4.5E-14	-6.6	221566
		8002	8.0	0.565	1.75	1.578	1.588	2.2E-09	1.4E-09	3.0E-14	-5.6	727198
		4117	4.1	0.586	1.73	1.552	1.565	7.2E-10	3.5E-09	2.5E-14	-4.3	286255
		1944	1.9	0.618	1.70	1.516	1.534	4.0E-10	9.3E-09	3.6E-14	-2.4	108040
		2016	2.0	0.685	1.63	1.445	1.480				1.7	
		2073	2.1	0.683	1.63	1.446	1.445	1.9E-09	1.8E-08	3.3E-13	1.6	55214
		899	0.9	0.702	1.61	1.428	1.437	1.3E-09	9.4E-09	1.2E-13	2.7	106028

Table D4-7: Coefficient of Consolidation (cv), Hydraulic Conductivity (k), and 1-D Modulus of Highly Compacted Bentonite (HCB) (Continued)

Test No.	Sample No.	Vertical Stress (kPa)	Vertical Stress (MPa)	Void Ratio, e	Dry Density (Mg/m ³)	EMDD (Mg/m ³)	EMDD-mid (Mg/m ³)	cv (m ² /sec)	mv (Pa ⁻¹)	k (m/s)	Volume strain (%)	1D-Modulus (kPa)
11 HCB11 (07)												
		650	0.6	0.645	1.67	1.486					0.0	
		1004	1.0	0.673	1.64	1.456	1.471				1.7	
		1986	2.0	0.668	1.65	1.461	1.459				1.4	
		3961	4.0	0.641	1.67	1.490	1.476	1.0E-09	8.2E-09	8.4E-14	-0.2	122475
		7773	7.8	0.592	1.72	1.545	1.517	9.6E-10	7.9E-09	7.5E-14	-3.2	126702
		15940	15.9	0.535	1.79	1.614	1.580	3.8E-10	4.4E-09	1.7E-14	-6.7	226781
12 HCB12(08)												
		1	0.0	0.687	1.63	1.442					0.0	
		123	0.1	0.688	1.63	1.441	1.442				0.1	
		880	0.9	0.622	1.69	1.511	1.476	1.1E-08	5.2E-08	5.4E-12	-3.8	19306
		1883	1.9	0.581	1.74	1.558	1.535	2.7E-09	2.5E-08	6.7E-13	-6.3	39590
		3957	4.0	0.528	1.80	1.623	1.591	2.2E-09	1.6E-08	3.5E-13	-9.4	61922
		7991	8.0	0.470	1.87	1.701	1.662	2.2E-09	9.4E-09	2.0E-13	-12.9	106232
		16333	16.3	0.400	1.96	1.805	1.753	1.1E-09	5.7E-09	6.1E-14	-17.0	175800
		7972	8.0	0.413	1.94	1.785	1.795	6.2E-10	1.1E-09	6.7E-15	-16.2	910400
		3934	3.9	0.430	1.92	1.760	1.772	1.3E-09	2.9E-09	3.7E-14	-15.2	343435
		1831	1.8	0.449	1.89	1.731	1.745	9.6E-10	6.4E-09	6.0E-14	-14.1	156491
		816	0.8	0.470	1.87	1.701	1.716	5.6E-10	1.4E-08	7.9E-14	-12.9	69474
		341	0.3	0.492	1.84	1.670	1.686	4.6E-10	3.2E-08	1.4E-13	-11.6	31719
		113	0.1	0.509	1.82	1.648	1.659	4.2E-10	4.9E-08	2.0E-13	-10.6	20353

Table D4-8: Coefficient of Consolidation (cv), Hydraulic Conductivity (k), and 1-D Modulus of Highly Compacted Bentonite (HCB) (Continued)

Test No.	Sample No.	Vertical Stress (kPa)	Vertical Stress (MPa)	Void Ratio, e	Dry Density (Mg/m ³)	EMDD (Mg/m ³)	EMDD-mid (Mg/m ³)	cv (m ² /sec)	mv (Pa ⁻¹)	k (m/s)	Volume strain (%)	1D-Modulus (kPa)
13 HCB13(08)												
		23	0.0	0.670	1.64	1.460					0.0	
		1054	1.1	0.660	1.65	1.470	1.465				-0.6	
		2093	2.1	0.638	1.68	1.493	1.482	3.6E-09	1.3E-08	4.5E-13	-1.9	79751
		4178	4.2	0.596	1.72	1.540	1.517	2.8E-09	1.2E-08	3.4E-13	-4.4	81336
		8448	8.4	0.538	1.78	1.610	1.575	1.3E-09	8.5E-09	1.1E-13	-7.9	117291
		16842	16.8	0.470	1.87	1.701	1.656	7.6E-10	5.3E-09	4.0E-14	-12.0	188906
		8446	8.4	0.485	1.85	1.680	1.691	1.5E-09	1.2E-09	1.8E-14	-11.1	800361
		4216	4.2	0.505	1.82	1.652	1.666	1.0E-09	3.2E-09	3.2E-14	-9.9	307920
		2104	2.1	0.533	1.79	1.616	1.634	6.9E-10	8.8E-09	5.9E-14	-8.2	114186
		1064	1.1	0.559	1.76	1.585	1.601	6.3E-10	1.6E-08	9.8E-14	-6.7	62979
		763	0.8	0.570	1.75	1.571	1.578	4.7E-10	2.5E-08	1.1E-13	-6.0	40503
		620	0.6	0.578	1.74	1.561	1.566	5.8E-10	3.5E-08	2.0E-13	-5.5	28533
		274	0.3	0.606	1.71	1.528	1.545	4.1E-10	5.2E-08	2.1E-13	-3.8	19229
14 HCB14(08)												
		2	0.0	0.633	1.68	1.499					0.0	
		107	0.1	0.720	1.60	1.410	1.455				5.3	
		848	0.8	0.716	1.60	1.413	1.411	3.6E-09	2.8E-09	1.0E-13	5.1	356386
		1900	1.9	0.680	1.63	1.450	1.431	1.8E-09	2.0E-08	3.7E-13	2.9	49327
		3921	3.9	0.630	1.68	1.502	1.476	1.5E-09	1.5E-08	2.2E-13	-0.2	68265
		8004	8.0	0.573	1.74	1.567	1.535	9.1E-10	8.5E-09	7.6E-14	-3.6	117376
		16158	16.2	0.528	1.80	1.622	1.595	6.9E-10	3.5E-09	2.4E-14	-6.4	286193

Table D4-9: Coefficient of Consolidation (cv), Hydraulic Conductivity (k), and 1-D Modulus of Highly Compacted Bentonite (HCB) (Concluded)

Test No.	Sample No.	Vertical Stress (kPa)	Vertical Stress (MPa)	Void Ratio, e	Dry Density (Mg/m ³)	EMDD (Mg/m ³)	EMDD-mid (Mg/m ³)	cv (m ² /sec)	mv (Pa ⁻¹)	k (m/s)	Volume strain (%)	1D-Modulus (kPa)
15	HCB14A (08)											
		111	0.1	0.667	1.65	1.463					0.0	
		347	0.3	0.679	1.63	1.450	1.456				0.7	
		783	0.8	0.669	1.64	1.460	1.455	1.4E-09	1.4E-08	1.9E-13	0.1	74062
		1815	1.8	0.644	1.67	1.487	1.474	1.2E-09	1.5E-08	1.7E-13	-1.4	68904
		3916	3.9	0.601	1.71	1.535	1.511	8.9E-10	1.3E-08	1.1E-13	-4.0	79760
		7963	8.0	0.549	1.77	1.597	1.566	8.0E-10	8.1E-09	6.4E-14	-7.1	123903
		16162	16.2	0.485	1.85	1.680	1.639	6.8E-10	5.0E-09	3.3E-14	-10.9	198709
		8010	8.0	0.503	1.83	1.656	1.668	8.7E-10	1.5E-09	1.3E-14	-9.9	665745
		3893	3.9	0.532	1.79	1.618	1.637	6.7E-10	4.7E-09	3.1E-14	-8.1	210745
		1848	1.8	0.562	1.76	1.580	1.599	3.2E-10	9.7E-09	3.1E-14	-6.3	103486
		842	0.8	0.585	1.73	1.553	1.567	6.6E-10	1.4E-08	9.3E-14	-4.9	69633
16	HCB15 (08)											
		165	0.2	0.674	1.64	1.455					0.0	
		1020	1.0	0.636	1.68	1.495	1.475				-2.3	
		2192	2.2	0.619	1.70	1.515	1.505	1.2E-10	9.1E-09	1.0E-14	-3.3	110146
		4183	4.2	0.558	1.76	1.585	1.550	1.9E-09	1.9E-08	3.4E-13	-6.9	53365
		8373	8.4	0.483	1.85	1.683	1.634	1.2E-09	1.2E-08	1.4E-13	-11.4	86398
		16758	16.8	0.409	1.95	1.791	1.737	6.4E-10	6.0E-09	3.8E-14	-15.8	167938
		4162	4.2	0.432	1.92	1.755	1.773	6.8E-10	5.0E-09	3.3E-14	-14.4	198799
		2104	2.1	0.466	1.87	1.706	1.731	5.0E-10	1.1E-08	5.6E-14	-12.4	87811
		1034	1.0	0.490	1.84	1.673	1.690	5.6E-10	1.5E-08	8.4E-14	-11.0	65104
		737	0.7	0.499	1.83	1.661	1.667	7.1E-11	2.0E-08	1.4E-14	-10.5	49079
		618	0.6	0.508	1.82	1.649	1.655	4.0E-10	5.2E-08	2.0E-13	-9.9	19407

**Table D5-1: Coefficient of Consolidation (cv), Hydraulic Conductivity (k), and 1-D Modulus of Dense Backfill (DBF)
(Continued)**

Test No.	Sample No.	Vertical Stress (kPa)	Vertical Stress (MPa)	Void Ratio, e	Dry Density (Mg/m ³)	EMDD (Mg/m ³)	EMDD-mid (Mg/m ³)	cv (m ² /sec)	mv (Pa ⁻¹)	k (m/s)	Volume strain (%)	1D-Modulus (kPa)
1	DBF1(06)											
		1	0.001	0.317	2.129	0.460					0.0	
		1	0.001	0.590	1.763	0.241	0.351	6.46E-09	5.89E-07	3.73E-11	20.8	1699
		251	0.251	0.357	2.066	0.406	0.323	8.54E-09	1.55E-07	1.30E-11	3.0	6433
		491	0.491	0.306	2.146	0.477	0.441	2.85E-08	9.38E-08	2.62E-11	-0.8	10665
		977	0.977	0.247	2.249	0.600	0.538	1.31E-08	2.96E-08	3.80E-12	-5.3	33797
		1949	1.949	0.211	2.316	0.710	0.655	2.18E-08	1.55E-08	3.31E-12	-8.0	64622
		3902	3.902	0.174	2.388	0.874	0.792	9.53E-08	1.65E-09	1.55E-12	-10.8	604616
		977	0.977	0.180	2.376	0.844	0.859	9.53E-09	1.54E-08	1.44E-12	-10.4	64728
		247	0.247	0.193	2.350	0.781	0.812				-9.4	
2	DBF2(06)											
		1	0.001	0.310	2.141	0.471					0.0	
		84	0.084	0.310	2.141	0.471	0.471	2.07E-08	1.11E-07	2.25E-11	0.0	9045
		246	0.246	0.286	2.180	0.512	0.492	2.71E-08	8.65E-08	2.30E-11	-1.8	11562
		492	0.492	0.259	2.227	0.570	0.541	1.81E-08	5.78E-08	1.03E-11	-3.9	17300
		978	0.978	0.223	2.291	0.667	0.618	4.82E-08	3.30E-08	1.56E-11	-6.6	30258
		1956	1.956	0.184	2.368	0.823	0.745	3.00E-08	1.27E-08	3.73E-12	-9.6	78845
		3899	3.899	0.155	2.428	0.996	0.910	2.50E-07	1.78E-09	4.36E-12	-11.8	562200
		975	0.975	0.161	2.415	0.955	0.975	1.50E-08	1.15E-08	1.69E-12	-11.4	86768
		242	0.242	0.171	2.395	0.894	0.925				-10.6	

**Table D5-2: Coefficient of Consolidation (cv), Hydraulic Conductivity (k), and 1-D Modulus of Dense Backfill (DBF)
(Continued)**

Test No.	Sample No.	Vertical Stress (kPa)	Vertical Stress (MPa)	Void Ratio, e	Dry Density (Mg/m ³)	EMDD (Mg/m ³)	EMDD-mid (Mg/m ³)	cv (m ² /sec)	mv (Pa ⁻¹)	k (m/s)	Volume strain (%)	1D-Modulus (kPa)
3	DBF3(06)											
		1	0.001	0.314	2.133	0.464					0.0	
		1	0.001	0.328	2.112	0.444	0.454	1.39E-07	1.37E-07	1.86E-10	1.0	7308
		247	0.247	0.283	2.185	0.518	0.481	1.63E-07	4.58E-08	7.31E-11	-2.4	21824
		489	0.489	0.269	2.210	0.547	0.533	2.32E-07	3.61E-08	8.22E-11	-3.4	27709
		977	0.977	0.246	2.249	0.600	0.574	3.93E-07	2.07E-08	7.97E-11	-5.1	48389
		1949	1.949	0.221	2.295	0.673	0.637	7.69E-07	1.23E-08	9.31E-11	-7.1	81045
		3902	3.902	0.192	2.352	0.786	0.730	1.18E-07	1.01E-09	1.18E-12	-9.3	985229
		977	0.977	0.195	2.345	0.771	0.778	7.69E-08	6.67E-09	5.03E-12	-9.0	149923
		247	0.247	0.201	2.334	0.746					-8.6	
4	DBF4(06)											
		1	0.001	0.314	2.133	0.463	0.463	8.37E-08	6.51E-08	5.35E-11	0.0	15353
		247	0.247	0.277	2.190	0.523	0.493	9.78E-08	4.23E-08	4.06E-11	-2.9	23636
		488	0.488	0.257	2.224	0.566	0.545	1.19E-07	2.53E-08	2.95E-11	-4.4	39496
		975	0.975	0.231	2.271	0.633	0.600	1.35E-07	1.43E-08	1.89E-11	-6.3	70128
		1957	1.957	0.200	2.329	0.736	0.685	2.00E-07	1.91E-09	3.74E-12	-8.7	524477
		3899	3.899	0.167	2.395	0.894	0.815	2.66E-07	1.01E-08	2.63E-11	-11.2	99343
		975	0.975	0.174	2.382	0.858	0.876	7.99E-08	6.36E-07	4.99E-10	-10.7	1573
		242	0.242	0.182	2.364	0.815					-10.1	

**Table D5-3: Coefficient of Consolidation (cv), Hydraulic Conductivity (k), and 1-D Modulus of Dense Backfill (DBF)
(Continued)**

Test No.	Sample No.	Vertical Stress (kPa)	Vertical Stress (MPa)	Void Ratio, e	Dry Density (Mg/m ³)	EMDD (Mg/m ³)	EMDD-mid (Mg/m ³)	cv (m ² /sec)	mv (Pa ⁻¹)	k (m/s)	Volume strain (%)	1D-Modulus (kPa)
5	DBF5(06)											
		1	0.001	0.336	2.098	0.432	0.432	1.16E-08	5.68E-08	6.48E-12	0.0	17591
		998	0.998	0.261	2.224	0.565	0.498	2.59E-08	2.87E-08	7.31E-12	-5.7	34843
		2000	2.000	0.224	2.289	0.663	0.614	3.78E-08	1.38E-08	5.13E-12	-8.4	72340
		3998	3.998	0.191	2.355	0.792	0.727	9.46E-08	1.14E-09	1.06E-12	-10.9	873575
		2000	2.000	0.193	2.349	0.779	0.786	7.50E-08	4.32E-09	3.18E-12	-10.7	231539
		998	0.998	0.199	2.339	0.757	0.768	3.01E-08	4.21E-09	1.24E-12	-10.3	237508
		502	0.502	0.201	2.334	0.747	0.752	1.88E-07	3.53E-09	6.51E-12	-10.1	283548
		998	0.998	0.199	2.338	0.756	0.751	2.14E-07	3.26E-09	6.86E-12	-10.3	306564
		2000	2.000	0.195	2.346	0.772	0.764	1.49E-07	3.27E-09	4.79E-12	-10.6	305854
		3998	3.998	0.187	2.361	0.807					-11.2	
6	DBF6(06)											
		1	0.001	0.322	2.120	0.452	0.452	1.40E-07	4.23E-08	5.79E-11	0.0	23664
		1002	1.002	0.266	2.214	0.553	0.502	2.57E-07	2.15E-08	5.42E-11	-4.2	46583
		1999	1.999	0.239	2.231	0.575	0.564	5.04E-07	1.16E-08	5.71E-11	-6.3	86566
		4002	4.002	0.210	2.284	0.654	0.615				-8.4	
		1999	1.999	0.211	2.284	0.654	0.654	3.99E-08	4.88E-10	1.91E-13	-8.4	2050688
		1002	1.002	0.211	2.283	0.652	0.653				-8.4	
		499	0.499	0.211	2.283	0.652	0.652				-8.4	
		1002	1.002	0.210	2.285	0.655	0.653	7.96E-07	2.18E-09	1.71E-11	-8.5	457756
		1999	1.999	0.208	2.290	0.663	0.659	5.29E-07	2.52E-09	1.31E-11	-8.7	397343
		4002	4.002	0.201	2.301	0.684					-9.1	

**Table D5-4: Coefficient of Consolidation (cv), Hydraulic Conductivity (k), and 1-D Modulus of Dense Backfill (DBF)
(Continued)**

Test No.	Sample No.	Vertical Stress (kPa)	Vertical Stress (MPa)	Void Ratio, e	Dry Density (Mg/m ³)	EMDD (Mg/m ³)	EMDD-mid (Mg/m ³)	cv (m ² /sec)	mv (Pa ⁻¹)	k (m/s)	Volume strain (%)	1D-Modulus (kPa)
7	DBF1(08)											
		78	0.078	0.291	2.091	0.426					0.0	
		78	0.078	0.285	2.101	0.435					-0.5	
		1003	1.003	0.256	2.150	0.480	0.458	1.05E-07	2.46E-08	2.53E-11	-2.7	40637
		2008	2.008	0.233	2.190	0.524	0.502	1.00E-06	1.83E-08	1.79E-10	-4.5	54780
		3938	3.938	0.207	2.237	0.584	0.554	4.83E-07	1.09E-08	5.18E-11	-6.5	91500
		2008	2.008	0.208	2.236	0.581	0.582	9.25E-10	4.26E-10	3.86E-15	-6.5	2349495
		1003	1.003	0.209	2.234	0.579	0.580	9.27E-10	7.53E-10	6.85E-15	-6.4	1327317
		500	0.500	0.211	2.229	0.572	0.576	3.71E-10	4.18E-09	1.52E-14	-6.2	239098
		1003	1.003	0.211	2.230	0.573	0.573	7.46E-09	5.01E-10	3.66E-14	-6.2	1996674
		2008	2.008	0.208	2.235	0.580	0.577	9.32E-08	2.40E-09	2.19E-12	-6.4	416592
		3938	3.938	0.201	2.248	0.599	0.590	1.85E-08	3.02E-09	5.49E-13	-7.0	331130
8	DBF2(08)											
		74	0.074	0.281	2.108	0.441					0.0	
		74	0.074	0.272	2.123	0.454	0.447	8.47E-10	3.74E-08	3.11E-13	-0.7	26713
		1014	1.014	0.227	2.200	0.536	0.495	1.39E-08	3.74E-08	5.11E-12	-4.2	26713
		2143	2.143	0.199	2.251	0.604	0.570	1.85E-08	2.01E-08	3.65E-12	-6.4	49752
		3930	3.930	0.174	2.300	0.682	0.643	2.06E-08	1.18E-08	2.40E-12	-8.4	84486
		1955	1.955	0.174	2.299	0.681	0.681	2.54E-08	1.52E-10	3.80E-14	-8.3	6568046
		1014	1.014	0.176	2.296	0.674	0.677	5.93E-08	1.76E-09	1.02E-12	-8.2	568833
		497	0.497	0.178	2.291	0.666	0.670	5.95E-09	3.73E-09	2.18E-13	-8.0	268110
		1014	1.014	0.177	2.295	0.672	0.669	8.96E-09	2.77E-09	2.44E-13	-8.1	360843
		1955	1.955	0.174	2.299	0.680	0.676	5.96E-08	2.03E-09	1.19E-12	-8.3	493193

**Table D5-5: Coefficient of Consolidation (cv), Hydraulic Conductivity (k), and 1-D Modulus of Dense Backfill (DBF)
(Continued)**

Test No.	Sample No.	Vertical Stress (kPa)	Vertical Stress (MPa)	Void Ratio, e	Dry Density (Mg/m ³)	EMDD (Mg/m ³)	EMDD-mid (Mg/m ³)	cv (m ² /sec)	mv (Pa ⁻¹)	k (m/s)	Volume strain (%)	1D-Modulus (kPa)
9	DBF3(08)	78	0.078	0.292	2.090	0.425					0.0	
		78	0.078	0.289	2.095	0.430	0.427	3.03E-09	2.53E-08	7.50E-13	-0.3	39591
		1003	1.003	0.259	2.145	0.476	0.453	1.05E-07	2.53E-08	2.61E-11	-2.6	39591
		2008	2.008	0.233	2.190	0.523	0.499	2.01E-07	2.02E-08	3.99E-11	-4.6	49468
		3938	3.938	0.197	2.256	0.610	0.567	9.65E-08	1.52E-08	1.44E-11	-7.4	65845
		2008	2.008	0.200	2.251	0.602	0.606		1.17E-09		-7.2	856826
		1003	1.003	0.201	2.247	0.598	0.600	1.22E-08	1.48E-09	1.76E-13	-7.0	677578
		500	0.500	0.203	2.245	0.594	0.596	9.16E-08	2.19E-09	1.97E-12	-6.9	456739
		200	0.200	0.207	2.236	0.582	0.588	1.22E-09	1.26E-08	1.52E-13	-6.6	79164
		78	0.078	0.214	2.225	0.567	0.575	1.23E-08	4.25E-08	5.14E-12	-6.1	23515
		1003	1.003	0.204	2.243	0.592	0.579	6.23E-08	8.84E-09	5.40E-12	-6.8	113084
		2008	2.008	0.192	2.265	0.624	0.608	4.54E-07	9.50E-09	4.23E-11	-7.7	105285
		3938	3.938	0.184	2.280	0.647	0.635	3.61E-08	3.34E-09	1.18E-12	-8.3	299531
10	DBF4(08)	74	0.074	0.283	2.105	0.438					0.0	
		74	0.074	0.276	2.116	0.448	0.443	1.06E-09	3.43E-08	3.56E-13	-0.5	29159
		1014	1.014	0.235	2.187	0.520	0.484	2.10E-08	3.43E-08	7.05E-12	-3.7	29159
		1955	1.955	0.212	2.227	0.569	0.545	1.96E-08	1.93E-08	3.72E-12	-5.5	51798
		3930	3.930	0.178	2.291	0.667	0.618	2.70E-08	1.43E-08	3.78E-12	-8.1	70147
		1955	1.955	0.182	2.284	0.654	0.660		1.69E-09		-7.8	590820
		1014	1.014	0.184	2.280	0.648	0.651	2.25E-08	1.64E-09	3.61E-13	-7.7	611614
		497	0.497	0.186	2.277	0.642	0.645	2.01E-08	2.93E-09	5.76E-13	-7.6	341650
		201	0.201	0.192	2.265	0.624	0.633	1.21E-08	1.76E-08	2.08E-12	-7.1	56799
		74	0.074	0.196	2.257	0.611	0.618	3.66E-09	2.92E-08	1.05E-12	-6.7	34252
		1014	1.014	0.188	2.272	0.635	0.623	7.37E-08	7.38E-09	5.34E-12	-7.4	135464
		1955	1.955	0.184	2.281	0.650	0.643	1.82E-07	4.14E-09	7.37E-12	-7.7	241838
		3930	3.930	0.176	2.296	0.675	0.663	2.25E-08	3.33E-09	7.36E-13	-8.3	300574

**Table D5-6: Coefficient of Consolidation (cv), Hydraulic Conductivity (k), and 1-D Modulus of Dense Backfill (DBF)
(Continued)**

Test No.	Sample No.	Vertical Stress (kPa)	Vertical Stress (MPa)	Void Ratio, e	Dry Density (Mg/m ³)	EMDD (Mg/m ³)	EMDD-mid (Mg/m ³)	cv (m ² /sec)	mv (Pa ⁻¹)	k (m/s)	Volume strain (%)	1D-Modulus (kPa)
11	DBF5(08)											
		74	0.074	0.290	2.093	0.428					0.0	
		1003	1.003	0.264	2.136	0.466	0.447	7.06E-08	1.60E-08	1.11E-11	-2.0	62434
		2008	2.008	0.244	2.171	0.502	0.484	3.70E-08	1.60E-08	5.81E-12	-3.6	62434
		3938	3.938	0.212	2.228	0.571	0.537	1.31E-07	1.34E-08	1.73E-11	-6.1	74681
		2008	2.008	0.214	2.223	0.565	0.568	1.25E-09	1.17E-09	1.43E-14	-5.8	852807
		1003	1.003	0.217	2.219	0.559	0.562	3.76E-09	1.93E-09	7.12E-14	-5.7	517195
		500	0.500	0.219	2.214	0.553	0.556	1.26E-09	4.27E-09	5.27E-14	-5.5	233945
12	DBF6(08)											
		74	0.074	0.291	2.092	0.427					0.0	
		1014	1.014	0.220	2.212	0.551	0.489				-5.4	
		1955	1.955	0.205	2.240	0.588	0.569	1.06E-08	1.33E-08	1.38E-12	-6.6	75297
		3930	3.930	0.185	2.278	0.644	0.616	1.89E-08	8.36E-09	1.55E-12	-8.2	119654
		1955	1.955	0.188	2.273	0.636	0.640	3.08E-08	1.12E-09	3.38E-13	-8.0	894585
		1014	1.014	0.190	2.269	0.629	0.633		2.00E-09		-7.8	499706
		497	0.497	0.192	2.265	0.624	0.627	8.97E-08	2.89E-09	2.54E-12	-7.7	346161

**Table D5-7: Coefficient of Consolidation (cv), Hydraulic Conductivity (k), and 1-D Modulus of Dense Backfill (DBF)
(Concluded)**

Test No.	Sample No.	Vertical Stress (kPa)	Vertical Stress (MPa)	Void Ratio, e	Dry Density (Mg/m ³)	EMDD (Mg/m ³)	EMDD-mid (Mg/m ³)	cv (m ² /sec)	mv (Pa ⁻¹)	k (m/s)	Volume strain (%)	1D-Modulus (kPa)
13	DBFS1(08)	18	0.018	0.286	2.100	0.433					0.0	
		68	0.068	0.273	2.121	0.452	0.443	1.52E-09	9.01E-08	1.35E-12	-1.0	11094
		117	0.117	0.268	2.129	0.460	0.456	2.10E-09	5.71E-08	1.18E-12	-1.4	17525
		216	0.216	0.261	2.140	0.471	0.465	9.17E-09	3.72E-08	3.35E-12	-1.9	26869
		415	0.415	0.251	2.159	0.489	0.480	1.19E-08	2.04E-08	2.38E-12	-2.7	49055
		811	0.811	0.237	2.183	0.516	0.502	8.26E-09	5.14E-08	4.17E-12	-3.8	19439
		1603	1.603	0.219	2.215	0.554	0.535	2.23E-08	4.45E-09	9.73E-13	-5.2	224941
		811	0.811	0.220	2.213	0.552	0.553	1.69E-08	7.00E-10	1.16E-13	-5.1	1427745
		415	0.415	0.220	2.214	0.553	0.552	7.94E-09	6.80E-10	5.30E-14	-5.2	1470224
		216	0.216	0.220	2.213	0.551	0.552	7.35E-09	6.80E-10	2.68E-13	-5.1	1470224
		117	0.117	0.221	2.212	0.550	0.550	2.42E-09	3.61E-09	6.03E-12	-5.1	277227
		68	0.068	0.222	2.210	0.548	0.549	8.02E-09	9.20E-09	7.24E-13	-5.0	108718
14	DBFS2(08)	18	0.018	0.285	2.101	0.435					0.0	
		66	0.066	0.284	2.103	0.437	0.436	6.01E-08	2.32E-08	1.37E-11	-0.1	43038
		114	0.114	0.280	2.109	0.442	0.439	2.85E-08	3.38E-08	9.46E-12	-0.4	29582
		210	0.210	0.274	2.119	0.450	0.446	2.24E-08	2.09E-08	4.60E-12	-0.8	47804
		403	0.403	0.269	2.128	0.459	0.455	3.49E-08	9.26E-09	3.17E-12	-1.3	108032
		787	0.787	0.261	2.142	0.472	0.465	1.34E-08	6.47E-09	8.50E-13	-1.9	154654
		1557	1.557	0.251	2.159	0.489	0.481	1.62E-08	2.82E-09	4.48E-13	-2.7	354898
		787	0.787	0.254	2.154	0.484	0.487	3.17E-09	4.06E-10	1.26E-14	-2.5	2461933
		403	0.403	0.256	2.150	0.481	0.483	7.31E-09	7.39E-10	5.30E-14	-2.3	1353716
		210	0.210	0.257	2.147	0.478	0.479	1.77E-08	2.53E-09	4.40E-13	-2.2	395275
		114	0.114	0.259	2.144	0.475	0.476	6.92E-09	7.73E-09	5.25E-13	-2.0	129341
		66	0.066	0.261	2.142	0.472	0.474	1.34E-08	1.30E-08	1.71E-12	-1.9	77051

**Table D6-1: Coefficient of Consolidation (cv), Hydraulic Conductivity (k), and 1-D Modulus of Light Backfill (LBF)
(Continued)**

Test No.	Sample No.	Vertical Stress (kPa)	Vertical Stress (MPa)	Void Ratio, e	Dry Density (Mg/m ³)	EMDD (Mg/m ³)	EMDD-mid (Mg/m ³)	cv (m ² /sec)	mv (Pa ⁻¹)	k (m/s)	Volume strain (%)	1D-Modulus (kPa)
1	HB2(06)	55	0.055	1.264	1.193	0.647	0.647	NA			0.0	
		81	0.081	1.270	1.189	0.644	0.646	NA			0.3	
		161	0.161	1.218	1.217	0.665	0.655	NA	2.8E-07	6.46E-12	-2.0	3521
		332	0.332	1.109	1.280	0.714	0.690	NA	2.9E-07	2.44E-12	-6.8	3460
		663	0.663	0.942	1.390	0.804	0.759	NA	2.4E-07	2.53E-12	-14.2	4184
		1326	1.326	0.774	1.522	0.921	0.863	NA	1.3E-07	1.54E-12	-21.6	7634
		2651	2.651	0.619	1.667	1.063	0.992	NA	6.6E-08	3.41E-13	-28.5	15152
2	HB3(06)	55	0.055	1.216	1.218	0.666					0.0	
		81	0.081	1.417	1.117	0.592					9.1	
		55	0.055	1.621	1.030	0.532					18.3	
		111	0.111	1.539	1.063	0.554	0.543	NA	5.7E-07	5.17E-12	14.6	1764
		221	0.221	1.334	1.157	0.621	0.588	NA	7.3E-07	9.24E-12	5.3	1370
		332	0.332	1.164	1.248	0.689	0.655	NA	6.6E-07	3.05E-12	-2.3	1511
		667	0.667	0.885	1.432	0.840	0.765	NA	3.8E-07	1.81E-12	-14.9	2625
		1326	1.326	0.672	1.615	1.010	0.925	NA	1.7E-07	8.94E-13	-24.5	5848
		668	0.668	0.700	1.589	0.985	0.997	NA	2.5E-08	5.52E-13	-23.3	40000
		336	0.336	0.773	1.522	0.921	0.953	NA	1.3E-07	4.47E-13	-20.0	7634
		166	0.166	0.944	1.389	0.803	0.862	NA	5.7E-07	7.92E-13	-12.3	1770
		55	0.055	1.334	1.157	0.621					5.3	

**Table D6-2: Coefficient of Consolidation (cv), Hydraulic Conductivity (k), and 1-D Modulus of Light Backfill (LBF)
(Continued)**

Test No.	Sample No.	Vertical Stress (kPa)	Vertical Stress (MPa)	Void Ratio, e	Dry Density (Mg/m ³)	EMDD (Mg/m ³)	EMDD-mid (Mg/m ³)	cv (m ² /sec)	mv (Pa ⁻¹)	k (m/s)	Volume strain (%)	1D-Modulus (kPa)
3	HB4(06)	55	0.055	1.149	1.257	0.696					0.0	
		81	0.081	1.626	1.028	0.530					22.2	
		166	0.166	1.103	1.284	0.717	0.624	NA	2.8E-07	4.79E-12	-2.1	3636
		332	0.332	0.989	1.357	0.776	0.747	NA	3.2E-07	2.02E-12	-7.4	3086
		665	0.665	0.811	1.491	0.893	0.834	NA	2.7E-07	8.49E-13	-15.7	3704
		1328	1.328	0.645	1.642	1.037	0.965	NA	1.4E-07	2.48E-13	-23.5	7246
		2654	2.654	0.510	1.788	1.193	1.115	NA	6.2E-08	1.06E-13	-29.7	16129
		1328	1.328	0.535	1.759	1.161	1.177	NA	1.3E-08	1.78E-13	-28.6	76923
		666	0.666	0.556	1.735	1.134					-27.6	
4	HB6(06)	55	0.055	1.313	1.167	0.628					0.0	
		39	0.039	1.446	1.104	0.583					5.8	
		56	0.056	1.438	1.107	0.585					5.4	
		166	0.166	1.242	1.204	0.656	0.620	NA	7.3E-07	5.42E-12	-3.1	1372
		332	0.332	1.021	1.336	0.759	0.707	NA	5.9E-07	4.05E-12	-12.6	1684
		664	0.664	0.790	1.509	0.909	0.834	NA	3.5E-07	1.96E-12	-22.6	2899
		1326	1.326	0.589	1.699	1.096	1.002	NA	1.7E-07	2.32E-12	-31.3	5917
		2652	2.652	0.440	1.875	1.294	1.195	NA	7.1E-08	2.55E-13	-37.7	14085
		3987	3.987	0.374	1.964	1.406	1.350	NA	3.4E-08	3.45E-13	-40.6	29412
		1326	1.326	0.436	1.880	1.300	1.353	NA	1.7E-08	1.39E-13	-37.9	58824
		668	0.668	0.497	1.803	1.210	1.255	NA	6.5E-08	9.55E-14	-35.3	15385
		336	0.336	0.583	1.706	1.103	1.157	NA	1.7E-07	2.13E-13	-31.6	5780
		167	0.167	0.722	1.568	0.964	1.034	NA	5.2E-07	4.13E-13	-25.6	1923
		57	0.057	1.074	1.302	0.732					-10.3	

**Table D6-3: Coefficient of Consolidation (cv), Hydraulic Conductivity (k), and 1-D Modulus of Light Backfill (LBF)
(Continued)**

Test No.	Sample No.	Vertical Stress (kPa)	Vertical Stress (MPa)	Void Ratio, e	Dry Density (Mg/m ³)	EMDD (Mg/m ³)	EMDD-mid (Mg/m ³)	cv (m ² /sec)	mv (Pa ⁻¹)	k (m/s)	Volume strain (%)	1D-Modulus (kPa)
5	HB7(06)											
		2	0.002	1.056	1.313	0.740					0.0	
		2	0.002	1.077	1.300	0.730					1.0	
		2	0.002	1.080	1.298	0.728					1.2	
		2	0.002	1.082	1.297	0.728					1.3	
		2	0.002	1.088	1.293	0.724					1.6	
		2	0.002	1.093	1.290	0.722					1.8	
		2	0.002	1.303	1.173	0.633					12.0	
		1	0.001	1.461	1.097	0.578					19.7	
		57	0.057	1.436	1.108	0.586	0.582	NA	3.4E-07	2.83E-11	18.5	2924
		167	0.167	1.203	1.225	0.672	0.629	NA	8.7E-07	7.98E-12	7.1	1155
		332	0.332	0.998	1.351	0.771	0.721	NA	5.7E-07	5.27E-12	-2.8	1770
		664	0.664	0.774	1.522	0.921	0.846	NA	3.4E-07	7.26E-12	-13.7	2950
		1326	1.326	0.576	1.714	1.112	1.016	NA	1.7E-07	9.18E-13	-23.3	5917
		2652	2.652	0.433	1.885	1.306	1.209	NA	6.8E-08	4.6E-12	-30.3	14706
		3986	3.986	0.366	1.976	1.421	1.364	NA	3.5E-08	6.06E-13	-33.6	28571
		2652	2.652	0.379	1.957	1.397					-32.9	
		1326	1.326	0.420	1.901	1.326					-30.9	
		664	0.664	0.482	1.822	1.232					-27.9	

**Table D6-4: Coefficient of Consolidation (cv), Hydraulic Conductivity (k), and 1-D Modulus of Light Backfill (LBF)
(Continued)**

Test No.	Sample No.	Vertical Stress (kPa)	Vertical Stress (MPa)	Void Ratio, e	Dry Density (Mg/m ³)	EMDD (Mg/m ³)	EMDD-mid (Mg/m ³)	cv (m ² /sec)	mv (Pa ⁻¹)	k (m/s)	Volume strain (%)	1D-Modulus (kPa)
6	HB8(06)											
		55	0.055	1.061	1.310	0.738					0.0	
		81	0.081	1.152	1.255	0.695					4.4	
		106	0.106	1.153	1.254	0.694					4.5	
		55	0.055	1.294	1.177	0.636					11.3	
		81	0.081	1.294	1.177	0.636					11.3	
		166	0.166	1.199	1.228	0.674	0.655	NA	4.9E-07	6.52E-12	6.7	2041
		332	0.332	0.999	1.351	0.771	0.723	NA	5.5E-07	6.14E-12	-3.0	1821
		664	0.664	0.774	1.522	0.921	0.846	NA	3.4E-07	1.08E-11	-13.9	2959
		1326	1.326	0.601	1.686	1.082	1.002	NA	1.5E-07	1.26E-12	-22.3	6803
		2652	2.652	0.477	1.828	1.239	1.160	NA	5.8E-08	4.34E-13	-28.3	17241
		1326	1.326	0.501	1.799	1.205	1.222	NA	1.2E-08	2.95E-13	-27.2	83333
		663	0.663	0.545	1.747	1.147	1.176	NA	4.5E-08	6.38E-14	-25.0	22222
7	HB9(06)											
		55	0.055	1.103	1.284	0.717					0.0	
		81	0.081	1.138	1.263	0.701					1.7	
		106	0.106	1.196	1.229	0.675					4.4	
		55	0.055	1.566	1.052	0.547					22.0	
		165	0.165	1.490	1.084	0.569	0.558	NA	2.7E-07	5.74E-11	18.4	3717
		331	0.331	1.288	1.180	0.638	0.603	NA	4.9E-07	1.38E-11	8.8	2037
		663	0.663	1.018	1.338	0.761	0.699	NA	3.6E-07	3.95E-12	-4.0	2817
		1336	1.336	0.792	1.507	0.907	0.834	NA	1.7E-07	1.43E-12	-14.8	5988
		2659	2.659	0.643	1.643	1.038	0.973	NA	6.3E-08	4.7E-13	-21.9	15873
		1336	1.336	0.663	1.623	1.018	1.028	NA	9.0E-09	1.42E-13	-20.9	111111
		663	0.663	0.712	1.577	0.973	0.996	NA	4.3E-08	3.87E-13	-18.6	23256
		331	0.331	0.800	1.500	0.901	0.937	NA	1.6E-07	4.56E-13	-14.4	6452
		165	0.165	0.983	1.361	0.780	0.840	NA	6.2E-07	3.75E-13	-5.7	1626
		55	0.055	1.457	1.099	0.579					16.8	

**Table D6-5: Coefficient of Consolidation (cv), Hydraulic Conductivity (k), and 1-D Modulus of Light Backfill (LBF)
(Continued)**

Test No.	Sample No.	Vertical Stress (kPa)	Vertical Stress (MPa)	Void Ratio, e	Dry Density (Mg/m ³)	EMDD (Mg/m ³)	EMDD-mid (Mg/m ³)	cv (m ² /sec)	mv (Pa ⁻¹)	k (m/s)	Volume strain (%)	1D-Modulus (kPa)
8	HB11(06)	0	0.000	1.081	1.297	0.728					0.0	
		25	0.025	0.996	1.353	0.773	0.750	NA	1.6E-06	8.16E-10	-4.1	614
		55	0.055	0.933	1.397	0.810	0.792	NA	1.0E-06	2.65E-10	-7.1	956
		166	0.166	0.773	1.523	0.922	0.866	NA	7.5E-07	6.33E-10	-14.8	1332
		332	0.332	0.651	1.636	1.031	0.977	NA	4.1E-07	2.16E-10	-20.7	2421
		664	0.664	0.536	1.758	1.159	1.095	NA	2.1E-07	1.38E-10	-26.2	4762
		1326	1.326	0.431	1.886	1.308	1.234	NA	1.0E-07	6.16E-12	-31.2	9709
		2661	2.661	0.334	2.024	1.485	1.397	NA	5.1E-08	5.51E-13	-35.9	19608
		3990	3.990	0.285	2.101	1.594	1.540	NA	2.8E-08	3.62E-13	-38.3	35714
		2661	2.661	0.297	2.081	1.565	1.580	NA	7.0E-09	5.58E-13	-37.7	142857
		1326	1.326	0.324	2.039	1.506	1.536	NA	1.5E-08	2.62E-13	-36.4	66667
		664	0.664	0.354	1.994	1.445	1.476	NA	3.4E-08	3.41E-13	-34.9	29412
		332	0.332	0.389	1.944	1.380	1.412	NA	7.7E-08	4.05E-13	-33.3	12987
		166	0.166	0.418	1.904	1.330					-31.9	
		55	0.055	0.466	1.841	1.254					-29.6	

**Table D6-6: Coefficient of Consolidation (cv), Hydraulic Conductivity (k), and 1-D Modulus of Light Backfill (LBF)
(Continued)**

Test No.	Sample No.	Vertical Stress (kPa)	Vertical Stress (MPa)	Void Ratio, e	Dry Density (Mg/m ³)	EMDD (Mg/m ³)	EMDD-mid (Mg/m ³)	cv (m ² /sec)	mv (Pa ⁻¹)	k (m/s)	Volume strain (%)	1D-Modulus (kPa)
9	HB12(06)	0	0.000	1.116	1.276	0.711					0.0	
		25	0.025	1.029	1.331	0.755	0.733	NA	1.6E-06	8.32E-10	-4.1	614
		55	0.055	0.959	1.378	0.794	0.774	NA	1.2E-06	1.07E-09	-7.4	869
		166	0.166	0.773	1.523	0.922	0.858	NA	8.6E-07	5.98E-10	-16.2	1161
		336	0.336	0.637	1.650	1.045	0.984	NA	4.5E-07	2.14E-11	-22.6	2217
		676	0.676	0.506	1.793	1.199	1.122	NA	2.3E-07	8.08E-12	-28.8	4274
		1340	1.340	0.400	1.929	1.361	1.280	NA	1.1E-07	1.25E-11	-33.8	9434
		2675	2.675	0.305	2.069	1.548	1.454	NA	5.1E-08	1.29E-12	-38.3	19608
		1340	1.340	0.326	2.037	1.503	1.526	NA	1.2E-08	5.81E-13	-37.3	83333
		676	0.676	0.354	1.994	1.445	1.474	NA	3.3E-08	3.68E-13	-36.0	30303
		336	0.336	0.386	1.948	1.385	1.415	NA	6.9E-08	3.58E-13	-34.5	14493
		167	0.167	0.418	1.904	1.330					-33.0	
		57	0.057	0.464	1.844	1.257					-30.8	
10	HB13(06)	1	0.001	1.137	1.264	0.702					0.0	
		25	0.025	1.067	1.306	0.735	0.718	NA	1.3E-06	2.95E-09	-3.3	747
		55	0.055	1.002	1.349	0.770	0.752	NA	1.1E-06	7.08E-10	-6.3	943
		166	0.166	0.834	1.472	0.875	0.823	NA	7.6E-07	3.1E-10	-14.2	1318
		332	0.332	0.721	1.569	0.965	0.920	NA	3.7E-07	3.12E-11	-19.5	2703
		663	0.663	0.608	1.679	1.075	1.020	NA	2.0E-07	1.17E-11	-24.8	5051
		1327	1.327	0.509	1.789	1.194	1.135	NA	9.3E-08	2.45E-12	-29.4	10753
		2650	2.650	0.412	1.913	1.341	1.267	NA	4.9E-08	1.27E-12	-33.9	20408
		1327	1.327	0.428	1.890	1.313	1.327	NA	9.0E-09	1.78E-13	-33.2	111111
		663	0.663	0.454	1.857	1.273	1.293	NA	2.7E-08	3.05E-13	-32.0	37037
		332	0.332	0.484	1.819	1.228	1.250	NA	6.3E-08	5.01E-13	-30.6	15873
		166	0.166	0.518	1.779	1.183					-29.0	
		55	0.055	0.575	1.714	1.112					-26.3	

**Table D6-7: Coefficient of Consolidation (cv), Hydraulic Conductivity (k), and 1-D Modulus of Light Backfill (LBF)
(Continued)**

Test No.	Sample No.	Vertical Stress (kPa)	Vertical Stress (MPa)	Void Ratio, e	Dry Density (Mg/m ³)	EMDD (Mg/m ³)	EMDD-mid (Mg/m ³)	cv (m ² /sec)	mv (Pa ⁻¹)	k (m/s)	Volume strain (%)	1D-Modulus (kPa)
11	HB14(06)											
		11	0.011	1.022	1.335	0.758					0.0	
		1	0.001	1.032	1.329	0.753					0.5	
		25	0.025	1.005	1.346	0.767	0.760	NA	5.4E-07	7.23E-10	-0.8	1855
		57	0.057	0.941	1.391	0.805	0.786	NA	1.0E-06	1.07E-09	-4.0	986
		167	0.167	0.726	1.564	0.961	0.883	NA	1.0E-06	3.73E-10	-14.6	998
		336	0.336	0.582	1.707	1.104	1.032	NA	5.0E-07	7.9E-11	-21.8	2020
		668	0.668	0.457	1.853	1.268	1.186	NA	2.4E-07	9.03E-12	-27.9	4184
		1343	1.343	0.355	1.992	1.442	1.355	NA	1.0E-07	2.33E-12	-33.0	9709
		2673	2.673	0.259	2.144	1.658	1.550	NA	5.3E-08	5.25E-13	-37.7	18868
		4000	4.000	0.206	2.239	1.808	1.733	NA	3.2E-08	7.31E-12	-40.4	31250
		2673	2.673	0.220	2.214	1.767	1.788	NA	9.0E-09	8.3E-13	-39.7	111111
		1343	1.343	0.247	2.164	1.688	1.728	NA	1.7E-08	2.91E-13	-38.3	58824
		668	0.668	0.282	2.107	1.603	1.646	NA	4.1E-08	2.57E-13	-36.6	24390
		336	0.336	0.317	2.050	1.521	1.562	NA	8.3E-08	2.45E-13	-34.9	12048
		167	0.167	0.348	2.003	1.457					-33.3	
		57	0.057	0.400	1.928	1.360					-30.8	

**Table D6-8: Coefficient of Consolidation (cv), Hydraulic Conductivity (k), and 1-D Modulus of Light Backfill (LBF)
(Continued)**

Test No.	Sample No.	Vertical Stress (kPa)	Vertical Stress (MPa)	Void Ratio, e	Dry Density (Mg/m ³)	EMDD (Mg/m ³)	EMDD-mid (Mg/m ³)	cv (m ² /sec)	mv (Pa ⁻¹)	k (m/s)	Volume strain (%)	1D-Modulus (kPa)
12	HB15(06)											
		1	0.001	1.082	1.297	0.728					0.0	
		25	0.025	1.020	1.337	0.760	0.744	NA	1.2E-06	4.72E-09	-3.0	805
		55	0.055	0.959	1.378	0.794	0.777	NA	1.0E-06	1.24E-09	-5.9	995
		166	0.166	0.798	1.502	0.903	0.848	NA	7.4E-07	1.31E-08	-13.6	1346
		332	0.332	0.692	1.595	0.990	0.947	NA	3.5E-07	5.51E-10	-18.7	2825
		664	0.664	0.569	1.721	1.119	1.055	NA	2.2E-07	5.27E-11	-24.6	4545
		1327	1.327	0.481	1.823	1.233	1.176	NA	8.4E-08	2.35E-12	-28.9	11905
		2656	2.656	0.392	1.939	1.374	1.303	NA	4.5E-08	1.96E-12	-33.1	22222
		3985	3.985	0.338	2.017	1.476	1.425	NA	2.9E-08	3.35E-12	-35.7	34483
		2656	2.656	0.340	2.015	1.473	1.475	NA	1.0E-09		-35.6	1000000
		1327	1.327	0.366	1.976	1.421	1.447	NA	1.5E-08	2.5E-13	-34.4	66667
		668	0.668	0.398	1.932	1.365	1.393	NA	3.5E-08	3.3E-13	-32.9	28571
		336	0.336	0.433	1.885	1.306	1.336	NA	7.5E-08	3.5E-13	-31.2	13333
		166	0.166	0.464	1.844	1.257					-29.7	
		55	0.055	0.515	1.782	1.186					-27.2	

**Table D6-9: Coefficient of Consolidation (cv), Hydraulic Conductivity (k), and 1-D Modulus of Light Backfill (LBF)
(Continued)**

Test No.	Sample No.	Vertical Stress (kPa)	Vertical Stress (MPa)	Void Ratio, e	Dry Density (Mg/m ³)	EMDD (Mg/m ³)	EMDD-mid (Mg/m ³)	cv (m ² /sec)	mv (Pa ⁻¹)	k (m/s)	Volume strain (%)	1D-Modulus (kPa)
13	HB16(06)	0	0.000	0.904	1.418	0.828					0.0	
		25	0.025	0.872	1.443	0.850	0.839	NA	6.8E-07	5.0E-10	-1.7	1468
		55	0.055	0.840	1.468	0.872	0.861	NA	5.7E-07	1.1E-10	-3.4	1754
		166	0.166	0.755	1.538	0.936	0.904	NA	4.2E-07	6.2E-10	-7.8	2410
		332	0.332	0.690	1.597	0.992	0.964	NA	2.2E-07	1.0E-10	-11.2	4464
		663	0.663	0.572	1.718	1.116	1.054	NA	2.1E-07	2.7E-11	-17.4	4739
		1327	1.327	0.462	1.847	1.261	1.188	NA	1.1E-07	2.4E-11	-23.2	9434
		2650	2.650	0.347	2.005	1.460	1.360	NA	5.9E-08	5.5E-12	-29.3	16949
		1327	1.327	0.360	1.986	1.434	1.447	NA	7.0E-09	2.2E-13	-28.6	142857
		663	0.663	0.378	1.959	1.399	1.417	NA	2.0E-08	6.1E-13	-27.6	50000
		332	0.332	0.400	1.929	1.361	1.380	NA	4.7E-08	4.1E-13	-26.5	21277
		166	0.166	0.416	1.907	1.333					-25.6	
		55	0.055	0.452	1.860	1.276					-23.7	
14	HB19(06)	1	0.001	1.129	1.268	0.705					0.0	
		25	0.025	1.057	1.313	0.740	0.723	NA	1.4E-06	9.2E-10	-3.4	718
		55	0.055	0.986	1.359	0.778	0.759	NA	1.1E-06	7.9E-10	-6.7	871
		166	0.166	0.787	1.511	0.911	0.844	NA	9.1E-07	6.9E-10	-16.1	1104
		332	0.332	0.656	1.631	1.026	0.968	NA	4.4E-07	1.1E-10	-22.2	2257
		663	0.663	0.540	1.753	1.154	1.090	NA	2.1E-07	2.2E-11	-27.7	4739
		1326	1.326	0.440	1.874	1.293	1.224	NA	9.7E-08	3.6E-12	-32.4	10309
		2660	2.660	0.348	2.003	1.457	1.375	NA	4.8E-08	8.9E-13	-36.7	20833
		1326	1.326	0.362	1.983	1.430	1.444	NA	8.0E-09	4.5E-13	-36.0	125000
		668	0.668	0.387	1.947	1.384	1.407	NA	2.8E-08	3.5E-13	-34.9	35714
		166	0.166	0.455	1.855	1.270	1.327	NA	9.9E-08	1.8E-12	-31.7	10101
		55	0.055	0.506	1.793	1.199					-29.3	

**Table D6-10: Coefficient of Consolidation (cv), Hydraulic Conductivity (k), and 1-D Modulus of Light Backfill (LBF)
(Continued)**

Test No.	Sample No.	Vertical Stress (kPa)	Vertical Stress (MPa)	Void Ratio, e	Dry Density (Mg/m ³)	EMDD (Mg/m ³)	EMDD-mid (Mg/m ³)	cv (m ² /sec)	mv (Pa ⁻¹)	k (m/s)	Volume strain (%)	1D-Modulus (kPa)
15 LBF_1(07)												
		1	0.001	1.131	1.268	0.705					0.0	
		1	0.001	1.308	1.171	0.631					8.3	
		55	0.055	1.086	1.295	0.726	0.678	4.09E-09	1.6E-06	6.6E-11	-2.1	613
		110	0.110	0.975	1.368	0.785	0.756	4.66E-09	8.8E-07	4.0E-11	-7.3	1141
		220	0.220	0.834	1.473	0.877	0.831	3.08E-09	5.9E-07	1.8E-11	-14.0	1706
		439	0.439	0.708	1.582	0.977	0.927	5.91E-09	2.8E-07	1.6E-11	-19.8	3592
		878	0.878	0.599	1.690	1.086	1.032	9.28E-09	1.3E-07	1.2E-11	-25.0	7756
		1702	1.702	0.512	1.787	1.192	1.139	6.84E-09	5.8E-08	3.9E-12	-29.1	17136
		878	0.878	0.525	1.772	1.174	1.183	5.59E-09	9.4E-09	5.2E-13	-28.4	106272
		439	0.439	0.542	1.752	1.153	1.164	1.99E-09	2.2E-08	4.3E-13	-27.7	45844
		220	0.220	0.558	1.734	1.134	1.143	9.05E-10	4.1E-08	3.7E-13	-26.9	24226
		110	0.110	0.578	1.712	1.110	1.122	4.63E-10	1.0E-07	4.7E-13	-26.0	9730
		55	0.055	0.591	1.699	1.095	1.103	2.84E-10	1.3E-07	3.6E-13	-25.4	7709
16 LBF_2(07)												
		1	0.001	1.127	1.270	0.707					0.0	
		1	0.001	1.217	1.219	0.667					4.2	
		55	0.055	0.985	1.361	0.780	0.723	3.07E-09	1.8E-06	5.4E-11	-6.7	561
		110	0.110	0.838	1.470	0.874	0.827	5.11E-09	1.2E-06	6.1E-11	-13.6	820
		221	0.221	0.696	1.593	0.989	0.931	7.28E-09	6.3E-07	4.5E-11	-20.3	1583
		441	0.441	0.549	1.744	1.144	1.066	2.21E-09	3.5E-07	7.6E-12	-27.2	2843
		882	0.882	0.430	1.889	1.312	1.228	3.10E-09	1.5E-07	4.7E-12	-32.8	6473
		1709	1.709	0.319	2.049	1.520	1.416	2.64E-09	8.3E-08	2.1E-12	-38.0	12071
		882	0.882	0.333	2.027	1.490	1.505	5.27E-09	1.1E-08	5.8E-13	-37.3	89290
		441	0.441	0.351	2.001	1.454	1.472	1.51E-09	2.7E-08	3.9E-13	-36.5	37582
		221	0.221	0.373	1.968	1.411	1.432	4.86E-10	6.5E-08	3.1E-13	-35.5	15413
		110	0.110	0.396	1.935	1.369	1.390	2.37E-10	1.4E-07	3.1E-13	-34.4	7407
		55	0.055	0.416	1.908	1.335	1.352	1.38E-10	2.3E-07	3.1E-13	-33.4	4407

**Table D6-11: Coefficient of Consolidation (cv), Hydraulic Conductivity (k), and 1-D Modulus of Light Backfill (LBF)
(Continued)**

Test No.	Sample No.	Vertical Stress (kPa)	Vertical Stress (MPa)	Void Ratio, e	Dry Density (Mg/m ³)	EMDD (Mg/m ³)	EMDD-mid (Mg/m ³)	cv (m ² /sec)	mv (Pa ⁻¹)	k (m/s)	Volume strain (%)	1D-Modulus (kPa)
17 LBF_3(07)												
		1	0.001	1.082	1.298	0.728					0.0	
		28	0.028	1.086	1.295	0.726					0.2	
		55	0.055	1.043	1.322	0.748	0.737	3.88E-10	7.0E-07	2.7E-12	-1.9	1434
		110	0.110	0.908	1.416	0.826	0.787	3.55E-09	1.1E-06	3.8E-11	-8.4	919
		220	0.220	0.784	1.515	0.914	0.870	1.03E-08	5.4E-07	5.4E-11	-14.3	1867
		440	0.440	0.651	1.636	1.031	0.973	7.67E-09	3.0E-07	2.3E-11	-20.7	3321
		879	0.879	0.550	1.743	1.143	1.087	9.32E-09	1.2E-07	1.1E-11	-25.6	8081
		1703	1.703	0.448	1.865	1.283	1.213	2.92E-09	7.0E-08	2.0E-12	-30.4	14292
		879	0.879	0.462	1.849	1.263	1.273	6.42E-10	9.5E-09	6.0E-14	-29.8	104981
		440	0.440	0.477	1.829	1.240	1.252	1.31E-09	2.1E-08	2.7E-13	-29.1	47204
		220	0.220	0.491	1.812	1.221	1.230	4.01E-10	3.7E-08	1.4E-13	-28.4	27151
		110	0.110	0.502	1.799	1.206	1.213	5.82E-10	5.8E-08	3.3E-13	-27.9	17349
		55	0.055	0.520	1.777	1.181	1.193	6.94E-11	2.0E-07	1.3E-13	-27.0	5051
18 LBF_4(07)												
		1	0.001	1.082	1.298	0.728					0.0	
		3	0.003	1.072	1.304	0.733					-0.5	
		55	0.055	0.998	1.353	0.773	0.753	3.43E-09	6.2E-07	2.1E-11	-4.0	1601
		110	0.110	0.864	1.450	0.856	0.814	7.73E-09	1.1E-06	8.4E-11	-10.5	904
		220	0.220	0.722	1.570	0.966	0.911	8.32E-09	6.3E-07	5.1E-11	-17.3	1599
		441	0.441	0.560	1.732	1.131	1.048	9.30E-09	3.8E-07	3.5E-11	-25.1	2625
		882	0.882	0.447	1.867	1.285	1.208	6.70E-09	1.5E-07	9.6E-12	-30.5	6848
		1709	1.709	0.332	2.028	1.491	1.388	4.00E-09	8.4E-08	3.3E-12	-36.0	11858
		882	0.882	0.346	2.008	1.464	1.478	7.43E-10	1.1E-08	7.7E-14	-35.4	94969
		441	0.441	0.362	1.984	1.431	1.448	1.27E-09	2.4E-08	3.0E-13	-34.6	40849
		220	0.220	0.380	1.958	1.398	1.415	1.95E-10	5.2E-08	9.9E-14	-33.7	19352
		110	0.110	0.394	1.939	1.373	1.386	3.99E-10	7.9E-08	3.1E-13	-33.1	12716
		55	0.055	0.415	1.909	1.336	1.355	1.36E-10	2.5E-07	3.3E-13	-32.0	4041

**Table D6-12: Coefficient of Consolidation (cv), Hydraulic Conductivity (k), and 1-D Modulus of Light Backfill (LBF)
(Continued)**

Test No.	Sample No.	Vertical Stress (kPa)	Vertical Stress (MPa)	Void Ratio, e	Dry Density (Mg/m ³)	EMDD (Mg/m ³)	EMDD-mid (Mg/m ³)	cv (m ² /sec)	mv (Pa ⁻¹)	k (m/s)	Volume strain (%)	1D-Modulus (kPa)
19 LBF_5B(07)												
	1	0.001	1.129	1.269	0.706						0.0	
	1	0.001	1.292	1.179	0.637						7.7	
	55	0.055	0.894	1.427	0.836	0.736		1.01E-08	3.0E-06	2.9E-10	-11.0	338
	110	0.110	0.755	1.540	0.937	0.886		6.84E-09	1.2E-06	8.1E-11	-17.6	833
	220	0.220	0.620	1.668	1.064	1.001		7.52E-09	6.3E-07	4.6E-11	-23.9	1594
	439	0.439	0.491	1.813	1.221	1.142		5.59E-09	3.2E-07	1.8E-11	-30.0	3112
	878	0.878	0.388	1.947	1.384	1.302		2.55E-09	1.4E-07	3.4E-12	-34.8	7276
	1701	1.701	0.286	2.101	1.593	1.488		1.65E-09	7.7E-08	1.3E-12	-39.6	12953
	878	0.878	0.302	2.075	1.557	1.575		2.06E-09	1.3E-08	2.6E-13	-38.8	79039
	439	0.439	0.323	2.042	1.510	1.534		2.12E-09	3.2E-08	6.7E-13	-37.8	30962
	220	0.220	0.349	2.003	1.458	1.484		3.30E-10	7.5E-08	2.4E-13	-36.6	13297
	110	0.110	0.371	1.971	1.415	1.436		4.27E-10	1.3E-07	5.4E-13	-35.6	7737
	55	0.055	0.399	1.932	1.364	1.390		7.09E-11	3.2E-07	2.2E-13	-34.3	3093
20 LBF_6(07)												
	1	0.001	1.112	1.279	0.714						0.0	
	14	0.014	1.121	1.274	0.710						0.4	
	1	0.001	1.159	1.251	0.692	0.701		4.19E-09	1.3E-06	5.3E-11	2.2	769
	55	0.055	0.990	1.358	0.777	0.735		7.17E-09	1.3E-06	9.3E-11	-5.8	755
	110	0.110	0.849	1.461	0.866	0.822		6.71E-09	1.2E-06	7.7E-11	-12.5	861
	221	0.221	0.676	1.612	1.007	0.937		5.04E-09	7.6E-07	3.8E-11	-20.7	1312
	442	0.442	0.542	1.752	1.153	1.080		2.86E-09	3.2E-07	9.0E-12	-27.0	3104
	883	0.883	0.426	1.895	1.318	1.236		1.47E-09	1.5E-07	2.2E-12	-32.5	6644
	1711	1.711	0.322	2.045	1.514	1.416		3.44E-09	7.7E-08	2.6E-12	-37.4	12928
	883	0.883	0.337	2.021	1.481	1.497		1.18E-09	1.2E-08	1.4E-13	-36.7	80791
	442	0.442	0.361	1.985	1.433	1.457		3.68E-10	3.6E-08	1.3E-13	-35.6	28158
	221	0.221	0.387	1.948	1.385	1.409		2.54E-10	7.5E-08	1.9E-13	-34.3	13369
	110	0.110	0.412	1.914	1.342	1.363		9.91E-11	1.4E-07	1.4E-13	-33.2	7099

**Table D6-13: Coefficient of Consolidation (cv), Hydraulic Conductivity (k), and 1-D Modulus of Light Backfill (LBF)
(Continued)**

Test No.	Sample No.	Vertical Stress (kPa)	Vertical Stress (MPa)	Void Ratio, e	Dry Density (Mg/m ³)	EMDD (Mg/m ³)	EMDD-mid (Mg/m ³)	cv (m ² /sec)	mv (Pa ⁻¹)	k (m/s)	Volume strain (%)	1D-Modulus (kPa)
21	LBF_1(08)											
		1	0.001	1.210	1.223	0.670					0.0	
		10	0.010	1.203	1.226	0.673					-0.3	
		55	0.055	0.956	1.382	0.797	0.735	7.74E-09	2.3E-06	1.7E-10	-11.5	436
		110	0.110	0.842	1.467	0.871	0.834	8.06E-09	9.6E-07	7.6E-11	-16.7	1047
		220	0.220	0.716	1.575	0.971	0.921	5.66E-09	5.6E-07	3.1E-11	-22.4	1800
		440	0.440	0.602	1.687	1.083	1.027	4.93E-09	2.7E-07	1.3E-11	-27.5	3730
		881	0.881	0.495	1.808	1.215	1.149	1.07E-08	1.3E-07	1.4E-11	-32.4	7463
		1761	1.761	0.389	1.945	1.381	1.298	6.20E-09	7.0E-08	4.3E-12	-37.1	14233
		881	0.881	0.403	1.926	1.358	1.370	3.49E-10	9.6E-09	3.3E-14	-36.5	104324
		440	0.440	0.415	1.910	1.337	1.347	1.01E-09	1.7E-08	1.7E-13	-36.0	57918
		220	0.220	0.428	1.892	1.314	1.326	1.03E-09	3.8E-08	3.8E-13	-35.4	26501
		110	0.110	0.442	1.873	1.292	1.303	4.92E-10	7.7E-08	3.7E-13	-34.7	12911
		55	0.055	0.463	1.847	1.261	1.277	6.29E-11	2.2E-07	1.4E-13	-33.8	4482
		1	0.001	0.520	1.778	1.182	1.221	7.96E-11	6.3E-07	4.9E-13	-31.2	1594

**Table D6-14: Coefficient of Consolidation (cv), Hydraulic Conductivity (k), and 1-D Modulus of Light Backfill (LBF)
(Continued)**

Test No.	Sample No.	Vertical Stress (kPa)	Vertical Stress (MPa)	Void Ratio, e	Dry Density (Mg/m ³)	EMDD (Mg/m ³)	EMDD-mid (Mg/m ³)	cv (m ² /sec)	mv (Pa ⁻¹)	k (m/s)	Volume strain (%)	1D-Modulus (kPa)
22	LBF_2(08)											
		1	0.001	1.140	1.262	0.700					0.0	
		14	0.014	1.137	1.264	0.702					-0.2	
		55	0.055	0.967	1.374	0.791	0.746	5.70E-09	1.8E-06	9.9E-11	-8.1	565
		110	0.110	0.811	1.492	0.893	0.842	9.06E-09	1.3E-06	1.2E-10	-15.4	769
		220	0.220	0.651	1.637	1.032	0.963	8.70E-09	7.3E-07	6.2E-11	-22.9	1377
		440	0.440	0.508	1.792	1.198	1.115	6.33E-09	3.5E-07	2.2E-11	-29.6	2849
		880	0.880	0.371	1.971	1.414	1.306	1.40E-09	1.8E-07	2.5E-12	-35.9	5500
		1760	1.760	0.260	2.145	1.659	1.537	5.02E-09	8.0E-08	4.0E-12	-41.1	12429
		880	0.880	0.272	2.124	1.628	1.644	8.14E-10	9.7E-09	7.7E-14	-40.6	103496
		440	0.440	0.284	2.104	1.599	1.613	9.48E-10	1.8E-08	1.7E-13	-40.0	54296
		220	0.220	0.298	2.081	1.565	1.582	7.53E-10	4.4E-08	3.2E-13	-39.3	22769
		110	0.110	0.312	2.059	1.534	1.550	4.95E-10	8.3E-08	4.0E-13	-38.7	12069
		55	0.055	0.332	2.028	1.491	1.513	8.88E-11	2.4E-07	2.1E-13	-37.8	4116
		1	0.001	0.391	1.942	1.377	1.434	3.77E-11	7.1E-07	2.6E-13	-35.0	1401

**Table D6-15: Coefficient of Consolidation (cv), Hydraulic Conductivity (k), and 1-D Modulus of Light Backfill (LBF)
(Continued)**

Test No.	Sample No.	Vertical Stress (kPa)	Vertical Stress (MPa)	Void Ratio, e	Dry Density (Mg/m ³)	EMDD (Mg/m ³)	EMDD-mid (Mg/m ³)	cv (m ² /sec)	mv (Pa ⁻¹)	k (m/s)	Volume strain (%)	1D-Modulus (kPa)
23	LBF_3(08)											
		1	0.001	1.214	1.220	0.668					0.0	
		11	0.011	1.223	1.216	0.665					0.4	
		55	0.055	1.021	1.337	0.760	0.712	1.23E-08	1.9E-06	2.3E-10	-8.7	533
		110	0.110	0.945	1.389	0.803	0.782	3.76E-09	6.2E-07	2.3E-11	-12.2	1620
		220	0.220	0.787	1.512	0.912	0.858	9.51E-09	6.7E-07	6.2E-11	-19.3	1499
		440	0.440	0.649	1.639	1.034	0.973	5.64E-09	3.1E-07	1.7E-11	-25.5	3187
		881	0.881	0.555	1.738	1.137	1.085	2.45E-09	1.2E-07	2.8E-12	-29.8	8689
		1762	1.762	0.456	1.855	1.271	1.204	1.45E-09	6.4E-08	9.0E-13	-34.2	15729
		881	0.881	0.470	1.839	1.251	1.261	2.05E-09	9.1E-09	1.8E-13	-33.6	110180
		440	0.440	0.489	1.814	1.223	1.237	2.33E-09	2.7E-08	6.1E-13	-32.7	37213
		220	0.220	0.514	1.785	1.189	1.206	6.16E-10	6.5E-08	3.9E-13	-31.6	15311
		110	0.110	0.540	1.754	1.155	1.172	2.97E-10	1.4E-07	4.1E-13	-30.4	7136
		55	0.055	0.597	1.692	1.088	1.122	1.18E-10	5.9E-07	6.8E-13	-27.9	1690
		1	0.001	1.005	1.348	0.769	0.928	2.07E-11	4.2E-06	8.5E-13	-9.4	239

**Table D6-16: Coefficient of Consolidation (cv), Hydraulic Conductivity (k), and 1-D Modulus of Light Backfill (LBF)
(Continued)**

Test No.	Sample No.	Vertical Stress (kPa)	Vertical Stress (MPa)	Void Ratio, e	Dry Density (Mg/m ³)	EMDD (Mg/m ³)	EMDD-mid (Mg/m ³)	cv (m ² /sec)	mv (Pa ⁻¹)	k (m/s)	Volume strain (%)	1D-Modulus (kPa)
24	LBF_4(08)											
		1	0.001	1.128	1.270	0.706					0.0	
		6	0.006	1.129	1.269	0.705					0.1	
		55	0.055	0.842	1.467	0.871	0.788	7.59E-09	2.5E-06	1.9E-10	-13.4	397
		110	0.110	0.733	1.559	0.956	0.913	6.15E-09	9.7E-07	5.9E-11	-18.6	1028
		219	0.219	0.605	1.684	1.080	1.018	8.93E-09	6.0E-07	5.3E-11	-24.6	1656
		438	0.438	0.490	1.814	1.222	1.151	9.21E-09	2.9E-07	2.6E-11	-30.0	3447
		877	0.877	0.383	1.953	1.391	1.307	6.62E-09	1.4E-07	9.3E-12	-35.0	7008
		1753	1.753	0.291	2.093	1.583	1.487	3.44E-09	6.7E-08	2.2E-12	-39.4	15017
		877	0.877	0.303	2.073	1.554	1.569	2.16E-09	9.6E-09	2.0E-13	-38.8	104172
		438	0.438	0.319	2.049	1.520	1.537	2.36E-09	2.3E-08	5.4E-13	-38.0	43180
		219	0.219	0.335	2.025	1.486	1.503	8.46E-10	4.8E-08	4.0E-13	-37.3	20908
		110	0.110	0.353	1.997	1.449	1.467	2.48E-10	1.1E-07	2.7E-13	-36.4	9085
		55	0.055	0.378	1.962	1.402	1.426	1.20E-10	2.8E-07	3.3E-13	-35.3	3512
		1	0.001	0.535	1.760	1.162	1.282	1.02E-10	1.9E-06	1.9E-12	-27.9	540

**Table D6-17: Coefficient of Consolidation (cv), Hydraulic Conductivity (k), and 1-D Modulus of Light Backfill (LBF)
(Continued)**

Test No.	Sample No.	Vertical Stress (kPa)	Vertical Stress (MPa)	Void Ratio, e	Dry Density (Mg/m ³)	EMDD (Mg/m ³)	EMDD-mid (Mg/m ³)	cv (m ² /sec)	mv (Pa ⁻¹)	k (m/s)	Volume strain (%)	1D-Modulus (kPa)
25	LBF_5(08)											
		1	0.001	1.159	1.251	0.692					0.0	
		14	0.014	1.175	1.242	0.685					0.7	
		55	0.055	1.051	1.317	0.744	0.714	8.75E-09	1.3E-06	1.1E-10	-5.0	792
		110	0.110	0.905	1.418	0.828	0.786	7.67E-09	1.2E-06	8.8E-11	-11.8	851
		220	0.220	0.759	1.536	0.934	0.881	4.38E-09	6.3E-07	2.7E-11	-18.6	1588
		441	0.441	0.618	1.670	1.065	1.000	2.24E-09	3.2E-07	7.1E-12	-25.1	3087
		882	0.882	0.499	1.802	1.209	1.137	1.59E-09	1.5E-07	2.3E-12	-30.6	6756
		1764	1.764	0.386	1.949	1.386	1.297	1.36E-09	7.5E-08	1.0E-12	-35.8	13307
		882	0.882	0.406	1.922	1.352	1.369	1.91E-09	1.4E-08	2.6E-13	-34.9	73406
		441	0.441	0.433	1.886	1.308	1.330	9.87E-10	3.8E-08	3.7E-13	-33.6	26203
		220	0.220	0.467	1.842	1.255	1.281	5.15E-10	9.5E-08	4.8E-13	-32.1	10574
		110	0.110	0.502	1.799	1.206	1.231	2.40E-10	1.9E-07	4.4E-13	-30.5	5308
		55	0.055	0.536	1.759	1.160	1.183	1.51E-10	3.7E-07	5.5E-13	-28.9	2703
		1	0.001	0.719	1.572	0.968	1.064	1.73E-10	1.9E-06	3.3E-12	-20.4	514

**Table D6-18: Coefficient of Consolidation (cv), Hydraulic Conductivity (k), and 1-D Modulus of Light Backfill (LBF)
(Concluded)**

Test No.	Sample No.	Vertical Stress (kPa)	Vertical Stress (MPa)	Void Ratio, e	Dry Density (Mg/m ³)	EMDD (Mg/m ³)	EMDD-mid (Mg/m ³)	cv (m ² /sec)	mv (Pa ⁻¹)	k (m/s)	Volume strain (%)	1D-Modulus (kPa)
26	LBF_6(08)											
		1	0.001	1.116	1.277	0.712					0.0	
		10	0.010	1.139	1.263	0.701					1.1	
		55	0.055	1.020	1.338	0.761	0.731	9.38E-09	1.1E-06	1.1E-10	-4.5	872
		110	0.110	0.894	1.426	0.835	0.798	1.49E-08	1.0E-06	1.5E-10	-10.5	974
		219	0.219	0.763	1.533	0.931	0.883	7.25E-09	5.7E-07	4.1E-11	-16.7	1754
		439	0.439	0.642	1.645	1.041	0.986	3.77E-09	2.8E-07	1.0E-11	-22.4	3575
		878	0.878	0.533	1.762	1.164	1.103	2.46E-09	1.3E-07	3.2E-12	-27.5	7436
		1756	1.756	0.433	1.885	1.307	1.235	1.43E-09	6.5E-08	9.2E-13	-32.2	15306
		878	0.878	0.449	1.864	1.282	1.294	2.70E-09	1.1E-08	2.9E-13	-31.5	90165
		439	0.439	0.474	1.833	1.244	1.263	1.39E-09	3.5E-08	4.7E-13	-30.3	28982
		219	0.219	0.505	1.795	1.201	1.222	4.81E-10	8.4E-08	4.0E-13	-28.8	11920
		110	0.110	0.535	1.760	1.162	1.181	3.01E-10	1.6E-07	4.7E-13	-27.4	6330
		55	0.055	0.564	1.728	1.126	1.144	1.87E-10	3.0E-07	5.6E-13	-26.1	3279
		1	0.001	0.771	1.526	0.924	1.025	1.55E-10	2.2E-06	3.3E-12	-16.3	459